
**Inaugural-Dissertation zur Erlangung der Doktorwürde der
Tierärztlichen Fakultät der Ludwig-Maximilians-Universität
München**

**Analysis of expression patterns
of heat shock proteins
HSPA1, HSPA5 and HSPH4
in the course of epileptogenesis**

von..... Marta Nowakowska

aus..... Łask

München 2020

**Aus dem Veterinärwissenschaftlichen Departement der
Tierärztlichen Fakultät
der Ludwig-Maximilians-Universität München**

Lehrstuhl für Pharmakologie, Toxikologie und Pharmazie

Arbeit angefertigt unter der Leitung von:

Univ.-Prof. Dr. Heidrun Potschka

Mitbetreuung durch:

Dr. Fabio Gualtieri, PhD

Dr. Eva-Lotta von Rüden, PhD

**Gedruckt mit Genehmigung der Tierärztlichen Fakultät
der Ludwig-Maximilians-Universität München**

Dekan:

Univ.-Prof. Dr. Reinhard K. Straubinger, Ph.D.

Berichterstatter:

Univ.-Prof. Dr. Heidrun Potschka

Korreferent/en:

Univ.-Prof. Dr. Dr. h. c. Hans-Joachim Gabius

Univ.-Prof. Dr. Asisa K. Volz

Univ.-Prof. Dr. Cornelia A. Deeg

Univ.-Prof. Dr. Eckhard Wolf

Tag der Promotion: 25. Juli 2020

There are two kinds of scientific progress: the methodical experimentation and categorisation which gradually extend the boundaries of knowledge, and the revolutionary leap of genius which redefines and transcends those boundaries. Acknowledging our debt to the former, we yearn, nonetheless, for the latter.

Academician Prokhor

Zakharov, "Address to the Faculty"

Sid Meier's Alpha Centauri

For Science

LIST OF CONTENTS

I.	INTRODUCTION	1
II.	LITERATURE OVERVIEW	4
1.	Epilepsy	4
1.1.	Definition and classification of the disease	4
1.2.	Epidemiology of epilepsy.....	8
1.2.1.	Issues with current therapy methods in veterinary medicine	10
2.	Epileptogenesis	13
2.1.	Animals models of epileptogenesis	13
2.1.1.	SE-BLA model of epileptogenesis	14
2.2.	Alterations in brain in the course of epileptogenesis	15
2.2.1.	Pathological anatomy of epileptogenesis.....	15
2.2.2.	Histopathology and pathophysiology of epileptogenesis	21
3.	Role of neuroinflammation in epileptogenesis	28
3.1.	Toll-like receptor signalling in epilepsy	31
3.2.	Endogenous ligands of TLR4	36
4.	Heat shock proteins and their relation to epilepsy	40
4.1.	Heat shock protein family description	40

4.2.	Role of HSPA1 in the cell and in TLR signalling	42
4.3.	Heat shock proteins in the endoplasmic reticulum	49
III.	SCOPE OF THE DISSERTATION	55
IV.	MATERIALS AND METHODS.....	56
1.	Animals.....	56
1.1.	Rat electrical status epilepticus model.....	56
1.2.	Canine clinical model	59
2.	Tissue processing.....	62
3.	Immunostaining	64
4.	Image analysis	73
4.1.	Stereological cell counting.....	73
4.2.	Colocalisation analysis	82
4.2.1.	HSPA1	82
4.2.2.	HSPA5 and HSPH4.....	85
4.3.	Optical density.....	86
5.	Statistics	88
V.	RESULTS	89
1.	HSPA1 expression in the rat model of epileptogenesis.....	89
1.1.	HSPA1 expression levels in the course of	

epileptogenesis	90
1.2. Profiling of HSPA1 expression in various cell types	94
2. HSPA5 and HSPH4 expression in epilepsy	101
2.1. Rat model of epileptogenesis	101
2.2. HSPA5 and HSPH4 profiling in various cell populations.....	106
2.3. HSPA5 and HSPH4 expression profiles in dogs	111
VI. DISCUSSION.....	115
1. HSPA1.....	115
2. HSPA5 and HSPH4.....	122
VII. CONCLUSIONS	131
VIII. SUMMARY	132
IX. ZUSAMMENFASSUNG	135
X. LIST OF REFERENCES.....	138
XI. ADDENDUM.....	163
1. Software and devices	163
2. Solutions and substances.....	166
3. Protocols for immunohistochemistry.....	172

XII. ACKNOWLEDGEMENT 180

LIST OF ABBREVIATIONS

ABC	Avidin-biotin complex
ADP	Adenosine diphosphate
AEDs	Anti-epileptic drugs
AMP	Adenosine monophosphate
ANOVA	Analysis of variance
AP	Antero-posterior
AT	Area tempestas
ATF6	Activating transcription factor 6
ATP	Adenosine triphosphate
BLA	Basolateral amygdala
BSA	Bovine serum albumin
CA(1-3)	Cornu Ammonis (1-3)
CD	Cluster of differentiation
CE	Coefficient of error
COX-2	Cyclooxygenase-2
CV	Coefficient of variation
Cy2	Cyanine dye 2
Cy3	Cyanine dye 3
DAMPs	Damage-associated molecular patterns
DG	Dentate gyrus
DNA	Deoxyribonucleic acid
DNAJ	40 kDa heat shock protein

DV	Dorso-ventral
EEG	Electroencephalography
Ent	Entorhinal cortex
ER	Endoplasmic reticulum
GABA	γ -aminobutyric acid
GFAP	Glial fibrillary acidic protein
HIER	Heat-induced epitope retrieval
Hil	Hilus of the dentate gyrus
HMGB1	High mobility group box 1
HSF-1	Heat shock factor 1
HSP	Heat shock protein
IHC	Immunohistochemistry
IL	Interleukin
IL-1R	Interleukin-1 receptor
ILAE	International League Against Epilepsy
IP3R	Inositol trisphosphate receptor
IRAK	Interleukin-1 receptor-associated kinase
IRE1	Inositol-requiring enzyme 1
IRF3	Interferon regulatory factor 3
Kir 4.1	Inwardly rectifying potassium 4.1 channel
LPS	Lipopolysaccharide
MAMs	Mitochondria associated membranes
MAPK	Mitogen-activated protein kinases

miRNA	microRNA
ML	Medio-lateral
mTOR	Mammalian target of rapamycin
MyD88	Myeloid differentiation primary response 88
N	Sample size
NBD	Nucleotide-binding domain
NF- κ B	Nuclear factor kappa-light-chain-enhancer of activated B cells
NGS	Normal goat serum
NMDA	N-Methyl-D-aspartic acid
p	P value, probability value
PAMPs	Pathogen-associated molecular patterns
PBS(T)	Phosphate buffered saline (with 0.05% Tween 20)
PERK	Protein kinase R-like ER kinase
PHC	Parahippocampal cortex
Pir(1-3)	Piriform cortex (layer 1-3)
PRh	Perirhinal cortex
RNA	Ribonucleic acid
SBD	Substrate-binding domain
SE	Status epilepticus
SEM	Standard error of the mean
SRS	Systematic random sampling
SRSs	Spontaneous recurrent seizures

SVZ	Subventricular zone
TBS(T)	Tris-buffered saline (with 0.05% Tween 20)
TGF- β	Transforming growth factor β
TIR	Toll/interleukin-1 receptor
TIRAP	TIR domain containing adaptor protein
TLE	Temporal lobe epilepsy
TLR(4)	Toll-like receptor (4)
TNF	Tumour necrosis factor
TRAM	TRIF related adaptor molecule
TRIF	TIR domain containing adapter-inducing interferon β
UPR	Unfolded protein response

I. INTRODUCTION

Epilepsy is one of the most common neurological disorders of dogs and cats as well as one of the conditions with the highest burden in human medicine. The disease, known since the ancient times, has served for a long time as an insight into the pathophysiology of the brain function, since behavioural consequences of a seizure depend on where in the brain it originates (KANDEL et al., 2000).

The nature of seizures has been fascinating the human species since antiquity. It had been for a long time believed to be of occult (either divine or demonic) origin, even though the relationship between head injuries and seizure activity was clear even to ancient Greeks (GROSS, 1992; KANDEL et al., 2000). Historical records describe predominantly generalised convulsive seizures, with partial seizures probably misdiagnosed or overlooked (KANDEL et al., 2000).

The Renaissance and the epoch of Enlightenment have brought a more rational view of the nature of the disease. The rise of *post mortem* examinations allowed physicians, with honourable mentions of Paracelsus, Le Pois and Sylvain, to better understand the connection between pathologies of the nervous system (such as collection of blood or pus in the brain tissue) with the occurrence of seizures (GROSS, 1992; PANTELIADIS et al., 2017). Epilepsy has been separated from other convulsive conditions (such as hysteria), focal seizures have been recognised and designated as “petit mal”, while convulsive, generalised attacks were specified as “grand mal” (GROSS, 1992). In the modern era, distinct work and observations

were made by John Hughlings Jackson in the 19th century, who described epilepsy as caused by paroxysmal, excessive discharge of neurons within a localised area that could affect other regions of the brain (GROSS, 1992). Also in the 19th century, first successful surgical interventions were performed by Victor Horsley, who resected an epileptic focus (KANDEL et al., 2000) and also performed first surgeries using a famed stereotactic frame (JENSEN et al., 1996). Stereotactic interventions were intensely developed later on in the Soviet Union (KANDEL, 1990). Finally, the development of anticonvulsive medications such as barbiturates as well as improvement of the diagnostic tools (mostly concerning the invention of electroencephalography) in the 1920s and 1930s has brought the epileptology to the current state of medical knowledge (GROSS, 1992; KANDEL et al., 2000).

Currently, epileptic seizures are known to originate in hyperexcitable neuronal networks. Moreover, it is recognised that an occurrence of an epileptic seizure in a neuronal circuit often increases the likelihood of manifestation of subsequent seizures emerging from the same circuit. This results from the series of modifications and dysregulatory changes called epileptogenesis. The subject of this thesis is to understand if and to which extent the epileptogenic process influences activation of specific stress-related proteins.

Heat shock proteins are members of a family of molecules discovered in 1962 by an Italian geneticist Ferruccio Ritossa (DE MAIO et al., 2012) and serve several important functions in the cell. They play a pivotal role in activation of the inflammatory cascade (VABULAS et al.,

2002b; PANDOLFI et al., 2016), which is one of factors contributing to initiation and further development of epileptogenic modifications (VEZZANI et al., 2002; PITKANEN, 2010; RAVIZZA et al., 2011). Better understanding of changes that heat shock proteins undergo subsequently to the insult initiating epileptogenesis may be of use in context of development of treatment strategies targeting these proteins and the metabolic pathways in which they are involved.

II. LITERATURE OVERVIEW

1. Epilepsy

1.1. Definition and classification of the disease

According to the definition of the International League Against Epilepsy (ILAE), “epilepsy is a disorder of the brain characterised by an enduring predisposition to generate epileptic seizures, and by the neurobiological, cognitive, psychological, and social consequences of this condition” (ILAE, 2014). This definition of epilepsy requires an occurrence of at least one epileptic seizure, and from the practical, clinical point of view, an additional high risk of manifestation of another epileptic incident, or having at least two unprovoked epileptic seizures >24 h apart (FISHER et al., 2014; BERENDT et al., 2015). An epileptic seizure is understood as a transient manifestation of signs or symptoms resulting from excessive synchronous, usually self-limiting epileptic activity of neurons in the brain. They may be objective (loss of awareness, stiffening or jerking) or subjective (a rising sensation from the abdomen to the chest, a smell of burned rubber or déjà vu in humans), as well as motor, autonomic (e.g. dilated pupils, hypersalivation, vomiting) or behavioural (e.g. anxiousness, restlessness, unexplainable fear reactions, abnormal attention seeking etc.) (FISHER et al., 2014; BERENDT et al., 2015; DEVINSKY et al., 2018).

ILAE classifies seizures into ones of focal, generalised or unknown onset, with further subcategorisation into motor or non-motor (autonomic or behavioural) seizures and the description of the awareness level for the focal type. Focal onset results from abnormal neuronal activity arising in a single or multiple localised brain regions or in one hemisphere, generalised seizures arise from anomalous activity of neurons spread over both hemispheres: Allocation of seizures to the unknown type is recommended when available clinical and laboratory data cannot fully identify the onset as a focal or a generalised class. An epileptic seizure may also start in a localised area in the brain and spread afterwards, finally involving both hemispheres – this kind of incident is called a focal epileptic seizure evolving to become generalised or a focal seizure with secondary generalisation (BERENDT et al., 2015; FISHER et al., 2017; DEVINSKY et al., 2018). Current veterinary terminology regarding epileptic seizures is summarised in Table 1.

Terminology	Clarification
Focal epileptic seizure	An epileptic seizure with clinical signs indicating activity, which starts in a localised area in the brain. It presents with focal motor, autonomic or behavioural signs alone or in combination.
Generalised epileptic seizure	An epileptic seizure with clinical signs indicating activity involving both cerebral hemispheres from the start. In dogs and cats, the seizure presents predominantly as immediate tonic-clonic convulsions and loss of consciousness. Salivation, urination and/or defecation often also occur during convulsions. May also (but rarely) present as atonic or myoclonic seizures.

<p>Focal epileptic seizure evolving to become generalised (focal seizure with secondary generalisation)</p>	<p>An epileptic seizure, which starts in a localised area in the brain and spreads subsequently to involve both hemispheres. In dogs and cats, the seizure starts with localised motor, autonomic and/or behavioural signs rapidly followed by convulsions. Salivation, urination and/or defecation often also occur during convulsions.</p>
---	--

Table 1. Veterinary terminology referring to epileptic seizures (modified from BERENDT et al. (2015)).

An epileptic seizure in veterinary medicine terms is usually classified as an ictus (seizure activity *per se*) followed by a postictal phase (restoration of the normal brain functionality, clinically demonstrating as vocalisation, compulsive locomotion, ataxia, excessive thirst and hunger, immediate need to urinate and defecate). In some animals, a prodrome might be present – a preictal phase involving changes occurring hours to days before a seizure and indicating an upcoming incident. Human patients may experience long periods of emotional fluctuations; in dogs the prodromal signs usually demonstrate as restlessness, anxiousness, aggression or attention-seeking patterns (BERENDT et al., 2015)

Aetiological classification of the disease in veterinary medicine has been suggested by the international veterinary epilepsy task force consensus and currently consists of an idiopathic and structural group. Idiopathic type involves cases where no structural cerebral pathology is suspected. It can either have a proven (genetic epilepsy) or a suspected genetic background (suspected genetic epilepsy), or an unknown underlying cause with no indication of structural epilepsy (idiopathic epilepsy). Structural epilepsy, also known as symptomatic epilepsy, is a type of the disease caused by identified cerebral pathology. Former cryptogenic epilepsy (where involvement of structural brain pathology is possible or probable, nevertheless it remains obscure) is currently classified as epilepsy of unknown cause (idiopathic epilepsy) (BERENDT et al., 2015).

1.2. Epidemiology of epilepsy

Epilepsy is one of the most important neurological diseases in both human and veterinary medicine. It is also one of the oldest recognised disorders in the world, with written records dating back to 4000 BCE. It is estimated that around 65 million people worldwide suffer from epilepsy (DEVINSKY et al., 2018; VEZZANI et al., 2019), affecting 4 to 10 people per 1000, while the proportion increases to 7-15 per 1000 in low- and middle-income countries (ORGANISATION, 2019). Global burden of disease, a metric used commonly by World Health Organisation (encompassing mortality, morbidity, injuries and other risk factors related to the disease etc.), reaches 0.6% in case of epilepsy (ORGANISATION, 2019) and shows a significant decrease from 1990 to 2016 worldwide (COLLABOLATORS, 2019). Despite

that fact, epilepsy is still an important cause of disability and mortality as well as general decline in life quality for human patients. Thus, reducing the burden of the disease is one of priorities in treatment development. Additionally, epilepsy often correlates with other neurological and psychiatric comorbidities, such as cognitive deficits, anxiety, depression or autism spectrum disorders (VEZZANI et al., 2019).

Epilepsy poses a serious problem also in veterinary practice. With a prevalence ranging from 0.55 to 5.7 percent of the canine population, it is the most frequent neurological disorder described in dogs (LOSCHER et al., 1985; BERENDT et al., 2002; KEARSLEY-FLEET et al., 2013; BERENDT et al., 2015; HAMAMOTO et al., 2016; URIARTE & MAESTRO SAIZ, 2016). Prevalence in certain breeds is higher than in the whole canine population, e.g. in Danish Labrador retrievers it reaches 3.1%, whereas prevalence of 1% is described for the general population (BERENDT et al., 2002). Some risk factors associated with epilepsy of unknown origin include sex and breed, with male dogs having significantly higher odds of developing the disease than females (KEARSLEY-FLEET et al., 2013). German shepherd dogs and border terriers show also high correlation between breed and epilepsy of unknown origin. Pugs, boxers, basset hounds and border terriers have shown a higher risk of seizure events as compared to Labrador retrievers with odds ratio reaching from 1.74 to 1.96 (ERLEN et al., 2018). Purebred dogs were however not found to be at overall higher risk of the disease than crossbred ones (KEARSLEY-FLEET et al., 2013). The available literature regarding feline epileptic patients remains scarce in comparison to data

presented in dogs. However, epileptic seizures pose a common neurological manifestation also in cats, with estimated prevalence ranging between 0.5 to 3.5% (CHARALAMBOUS et al., 2018).

1.2.1. Issues with current therapy methods in veterinary medicine

Pharmacoresistance towards anti-epileptic drugs (AEDs) is a substantial problem in veterinary medicine, both in clinics and in drug research and development. Drug resistant epilepsy is defined in human medicine as “a failure of adequate trials of two appropriately chosen and used antiepileptic drug schedules (whether as monotherapies or in combination) to achieve sustained seizure freedom” (KWAN et al., 2010). It is estimated that around one third of canine population is pharmacoresistant to standard therapeutic measures (PACKER et al., 2014). Data regarding drug resistance in cats is much more limited – the problem is however known in clinical praxis and in research (BARNES HELLER, 2018). Also a significant proportion of human patients (more than 40%, SHARMA et al. (2015)) do not respond to any of two to three first line AEDs, despite administration in an optimally tailored and monitored regimen. Pharmacoresistance seems to correlate with certain features of the disease, such as high seizure frequency, febrile seizures prior to treatment or early onset of seizures (REMY & BECK, 2006).

The search for alternative treatment targets in epilepsy is of invaluable importance, especially considering disadvantages of standard therapy. For example, benzodiazepines are one of most common antiepileptic, anxiolytic and sedative hypnotic drugs (ENGEL &

PEDLEY, 2008). Their effect results from modulation of γ -aminobutyric acid(GABA)-evoked currents by activating the benzodiazepine recognition site of GABA_A receptors. However, drugs acting on GABA receptors are known for their loss efficacy over time (tolerance), development of dependence and a potential for drug abuse (LOSCHER et al., 2004). GABA_A receptor subunit composition can change over prolonged seizure activity resulting in drug tolerance. Moreover, the result of activation of the GABA_A receptor depends on the state of chloride channels and, as a consequence, on chloride homeostasis— changes in expression of chloride ionophores may lead to chloride efflux, resulting in gradual depolarisation instead of hyperpolarisation of neurons and, by that, leading to excessive excitation (POTSCHKA, 2013). In that case, application of GABA agonists would increase neuronal excitability instead of decreasing it.

In human tissue from patients with drug-resistant epilepsy and in rodent models of chronic epilepsy, several alterations of sodium channel function and expression have been observed. Among identified changes, downregulation of accessory subunits, altered alpha subunit expression and induction of neonatal forms of the channel are known to play a role in granule cells of dentate gyrus as well as pyramidal cells of Cornu Ammonis 1 (CA1) and Cornu Ammonis 3 (CA3) regions of the hippocampus (REMY & BECK, 2006).

An additional difficulty in therapy of canine patients by means of the most common antiepileptic drugs emerges from the fact that the majority of them is either eliminated by dogs more rapidly in comparison to humans, or toxicity of the drug remains high in its

effective doses (SCHWARTZ-PORSCHKE et al., 1985; LOSCHER et al., 2004). Half-life sufficient to keep a drug concentration in blood effective is present only in few AEDs, i.e. phenobarbital, primidone and potassium bromide (FREY & LOSCHER, 1985; POTSCHKA et al., 2013). Among medications suitable to be applied in treatment of canine patients, the most effective in idiopathic epilepsy cases proved to be: phenobarbital (administered orally), imepitoin and potassium bromide in monotherapy, as well as levetiracetam and zonisamide as adjunct AEDs, according to one systematic review of veterinary clinical studies (CHARALAMBOUS et al., 2014). The authors however stated that a large part of studied articles was of doubtful quality, describing non-randomised trials with small group sizes and showing a relatively high risk of bias.

Treatment in feline patients differs substantially from methodology used in canines due to divergent safety profiles in the two species. There are many therapy guidelines available for epileptic dogs, taking into consideration efficacy of different AEDs in this species – such guidelines are lacking however in feline neurology (CHARALAMBOUS et al., 2018). There is no consensus among veterinary practitioners about the exact time point, when the antiepileptic treatment should be started – it is suggested not to begin the therapy after a single seizure, but after a few seizure occurrences (PAKOZDY et al., 2014).

2. Epileptogenesis

Epileptogenesis is a multifactorial process of development and extension of tissue capable of generating spontaneous seizures, which results in emergence of an epileptic condition in the first place and/or in progression of already established epilepsy. It can either result from an external or internal event (epileptogenic insult) or arise from genetic background of the disease (PITKANEN, 2010; DEVINSKY et al., 2018). The cause may however remain unknown in many patients. In temporal lobe epilepsy (TLE) the process begins before the first spontaneous seizure and leads to functional alterations of a normal brain network toward a higher seizure susceptibility. The process as well as frequency and severity of unprovoked incidents can progress over weeks in animal models and for years in humans, in the end resulting in increased probability of neuronal networks in altered brain tissue to generate spontaneous recurrent seizures (SRSs) (PITKANEN et al., 2015).

2.1. Animals models of epileptogenesis

In vivo animal models are common in the research field of epileptology. They play a pivotal role in understanding mechanisms underlying ictogenesis (generation of seizures) and epileptogenesis (with many of them being common for both processes, e.g. neuroinflammation (VEZZANI et al., 2019)), as well as in development of anti-epileptic drugs, representing an important link in the chain of progress from bench to bedside (LOSCHER, 2011). Essentially, animal models used in epilepsy research can be classified either as

models of epileptic seizures, or as models of epilepsy (LOSCHER, 2011). Rodent models of acquired focal epilepsy mostly tend to base on brain insults such as status epilepticus (SE), traumatic brain injury, stroke, infections and neoplasms (DEVINSKY et al., 2018). Post-status epilepticus models of temporal lobe epilepsy are often considered as possessing the greatest parallels to development and progression of the disease in humans (LOSCHER, 2011). Various forms of SE used in epileptogenesis research include: injections of chemoconvulsants, such as pilocarpine or kainic acid, and direct electrical stimulation of brain regions involved in generating seizures, e.g. hippocampus or basolateral amygdala (BLA). Depending on the model, video electroencephalography (EEG) monitoring after insult may reveal no SRSs up to two weeks after status epilepticus (“latency period”). Afterwards, initial recurrent seizures tend to be non-convulsive, with following convulsive, short (tens of seconds) SRSs (BERTRAM & CORNETT, 1993; PITKANEN et al., 2015). Frequency of unprovoked seizures generally increases with time after insult, and they often occur in clusters (WILLIAMS et al., 2009).

2.1.1. SE-BLA model of epileptogenesis

In the project underlying this dissertation, brains were collected from animals used in another study (WALKER et al., 2016), in which the electrical SE-BLA model was implemented. Continuous electrical stimulation of BLA proved to provoke a focal, self-sustained status epilepticus in rats (MCINTYRE et al., 1982). Based on that finding, a protocol leading to a self-conserving SE with subsequent appearance of SRSs has been established (BRANDT et al., 2003; BRANDT et al., 2004). In this model, rats undergo 25-minute electrical stimulation via

electrode implanted into BLA, which is interrupted after 4h by a diazepam injection. This induces one of three behavioural types of self-sustained SE:

- continuous focal, non-convulsive seizures (type 1)
- continuous focal, not convulsive SE, repeatedly interrupted by occasional generalised seizures (type 2)
- continuous generalised, convulsive SE (type 3).

Overall, around 80% of rats develop SRSs afterwards, reaching however only up to 33% of spontaneous seizures in animals undergoing type 1 SE and more than 90% in the type 2 and type 3 (BRANDT et al., 2003). These proportions remain stable, regardless of the strain and gender of rats.

2.2. Alterations in brain in the course of epileptogenesis

Epileptogenesis involves many changes in the brain, on both structural and morphological level. Additionally, certain genetic and epigenetic modifications engaged in epileptogenetic processes had been identified in animal models and were validated in human patients. All of the changes imply a constant interplay between pathogenic and compensatory mechanisms, affecting in the end the outcome of epileptogenesis and clinical manifestation of epilepsy.

2.2.1. Pathological anatomy of epileptogenesis

To understand pathological changes of the brain anatomy underlying the epileptogenic process, one should also consider physiological

composition of areas involved in seizure generation and propagation. The most relevant regions encompass the hippocampal formation, comprising of the hippocampus and the parahippocampal cortex.

Hippocampus in humans is an elongated structure resembling macroscopically a seahorse (hence the name), located deep within the medial temporal lobe of the brain. In rodents, the hippocampus is a relatively big structure, placed underneath the neocortex. In rats, the region is elongated and C-shaped, extending from septal nuclei at the rostro-dorso-medial end to the temporal lobe at the caudo-ventro-lateral end (DESHMUKH & KNIERIM, 2012). The longitudinal hippocampal axis is thus referred to as the septotemporal axis, while the orthogonal one is called the transverse axis.

In the hippocampus, three separate regions can be distinguished: dentate gyrus (DG), cornu ammonis (CA) and subiculum. In DG, principal neurons form a granular cell layer, usually U- or V-shaped as seen in coronal sections, with dendrites extending into the molecular layer, located superficially to the granular cell layer. Traditionally, the dorsal part of the granular cell layer is referred to as the upper blade, while the ventral one – the lower blade. Between the upper and lower blades one can distinguish the polymorphic cell layer, also known as the hilus of the dentate gyrus. In the hilus, mossy fibers (axons of the principal neurons of the DG) provide their collaterals to form connections with glutamergic neurons (mossy cells) and inhibitory interneurons. Mossy cells also project back to the granular layer.

In CA regions, bodies of pyramidal neurons form a distinctive, well-defined layer (stratum pyramidale). In coronal sections, stratum

pyramidale of CA3 begins between the blades of the DG, near to the hilar region, and progresses temporally, finally forming an arch-like structure and proceeding gently into CA2, followed by CA1 in the medial direction. Cells of the pyramidal layer of CA3 are bigger and more dispersed than in CA1, with CA2 cells showing morphology transitional between the neighbouring regions. A layer located superficially to the stratum pyramidale, called stratum oriens, contains mainly cell bodies of inhibitory basket cells and dendrites of pyramidal neurons. Stratum radiatum, underlying the pyramidal layer, as well as neighbouring stratum lacunosum-moleculare and stratum lucidum (thin layer located solely in CA3) contain predominantly fibers and synapses as well as scarce cell bodies of interneurons. Functionally, CA regions can be divided into proximal (located closer to the DG) and distal parts (located closer to the subiculum).

The entorhinal cortex (Ent) is located in the rostral parahippocampal gyrus and serves as a junction between the hippocampus and sensory cortices. In humans, it comprises Brodmann areas 28 and 34 (VISMER et al., 2015). It consists of six layers, with cell-rich outer (V and VI) and inner (II and III) layers separated by a layer with scarce cells (IV). Neurons from layers II and III send major inputs to the DG and the subiculum, while layers V and VI receive the feedback from CA1 and subiculum (DESHMUKH & KNIERIM, 2012). Ent is subdivided into two major parts, the rostro-lateral and the caudo-medial entorhinal cortex, which differ in their architecture and functions. Lateral Ent is organised in patches of neurons surrounded by bundles of fibers, while the histology of the medial Ent resembles neocortex, with clearly distinguishable laminae and columnar

organisation of neurons and fibers (VISMER et al., 2015). Cells located laterally in the lateral Ent and dorso-caudally in the medial Ent project to septal parts of the hippocampus, while those located medially in the lateral Ent and rostro-ventrally in the medial Ent connect predominantly with its temporal levels (DESHMUKH & KNIERIM, 2012). Ent receives input also from the piriform cortex (consisting of around 33% of the total afferents into the Ent) as well as from temporal and frontal cortices. The major output of the entorhinal cortex reaches the piriform cortex and the hippocampus (VISMER et al., 2015).

The perirhinal cortex (PRh) is located in the parahippocampal gyrus and it borders with the entorhinal cortex ventro-laterally. In humans, it stretches along the collateral sulcus in the ventro-medial part of the temporal lobe, comprising Brodmann areas 35 and 36 (VISMER et al., 2015). It is involved in complex visual memory functions, such as object recognition and spatial orientation. In human patients with temporal lobe epilepsy, it is associated with a phenomenon of *déjà vu*, experienced often at the onset of seizures (MARTIN et al., 2012). PRh receives its major input from Ent as well as from the piriform cortex, from bordering association areas as well as from other cortical and limbic areas, and it projects back to the same regions (VISMER et al., 2015). Due to its interconnectivity and its strategic location in the temporal lobe, it serves as the main interface of sensory inputs between the neocortex and the hippocampal formation, relaying signals in both directions (WITTER & GROENEWEGEN, 1986).

The piriform cortex (Pir) is a part of olfactory system, serving mostly

as a processor of olfactory signals and coding memories. It expands over the ventro-lateral surface of the forebrain and constitutes of three cellular layers, presenting cytoarchitectonics typical for the paleocortex (SQUIRE, 2009). The superficial plexiform layer I (Pir1) consists of two sublamina: layer Ia, including axons of mitral and tufted cells of the olfactory bulb, and layer Ib, located deeper, consisting of associative axons from Pir and other cortical areas. Layer II (Pir2), located deeper in reference to Pir1, contains cell bodies of most of principal neurons of the piriform cortex. Layer III (Pir3) comprises of fibres and cell bodies of some pyramidal and multipolar cells (SQUIRE, 2009; VISMER et al., 2015). Endopiriform nucleus is a structure adjacent to the layer III of the piriform cortex, comprising mostly multipolar cells and sharing many properties with the rest of the region, such as excitatory discharges, hyperexcitability and fast signal propagation (VISMER et al., 2015).

The piriform cortex projects directly to Ent, PRh and to the amygdala, there are however significant differences in the connectivity between the rostral and caudal portion of Pir. Local GABAergic circuitry is more prominent in the caudal subregion, gradually decreasing in the rostral direction, becoming the least prominent in the area tempestas (AT) (VISMER et al., 2015). This ventro-rostral portion of Pir constitutes a histologically and functionally distinct region, highly responsive to chemoconvulsants. AT shows a lower density of GABAergic axons as well as decreased number of interneurons as compared with the rest of the piriform cortex. A unilateral injection of picomole amounts of GABA receptors antagonists or glutamate receptor agonists into this locus can trigger generalised seizures (PIREDDA & GALE, 1985).

Connectivity of the hippocampal formation in relation to epileptogenesis

A transverse section of the hippocampus shows the classical hippocampal connectivity of the “trisynaptic loop”. This pathway has originally been described by Santiago Ramón y Cajal (RAMÓN Y CAJAL, 1995). It serves as a basic model of hippocampal circuitry. Briefly, neurons of the layer II of the entorhinal cortex (Ent) provide the major input from the cortex to the hippocampus, with the most pronounced pathway reaching the dentate gyrus (DG) region, forming the first synapse of the loop with dendrites in the molecular layer of the DG. The DG projects axons to the cornu ammonis 3 region (CA3) via the mossy fibers pathway (second synapse), and finally, CA3 projections reach cornu ammonis 1 (CA1) via the Schaffer collateral pathway (third synapse). Finally, CA1 projects back to the Ent, finishing the circuit (DESHMUKH & KNIERIM, 2012). Proximal CA3 neurons send more projections to distal CA1 cells and distal CA3 neurons preferably connect to the proximal part of the CA1 (DESHMUKH & KNIERIM, 2012).

A basic theorem in epileptology states that abnormal neuronal activity in particularly vulnerable circuits can cause modifications leading to permanently enhanced neuronal excitability (OSWALD STEWARD, 2001). Pyramidal cells, principal neurons of regions described above, appear as complex spiking cells in extracellular recordings, meaning they are able to generate a burst of action potentials separated by short interspike intervals (DESHMUKH & KNIERIM, 2012). Such bursting may be a mechanism leading to an increase of downstream

excitability by summing the excitatory postsynaptic potentials (EPSPs) in subsequent neurons. Repeated high frequency excitation of neighbouring cells is also a basis of long-term potentiation (LTP), underlying the mechanisms of hippocampal plasticity (DESHMUKH & KNIERIM, 2012). Repeated intense synaptic activation leads however to abnormally increased neuronal excitability, recruitment of more neurons into the circuitry and finally, to construction of a primary focus able to exhibit independent and spontaneous epileptiform discharges (OSWALD STEWARD, 2001). Thus, epileptogenesis heavily relies on synaptic plasticity in the described limbic and cortical regions, and may be induced on all levels of this circuitry, particularly prone to generating and propagating ictal discharges.

2.2.2. Histopathology and pathophysiology of epileptogenesis

Alterations of neuronal cells

One of the most common and characteristic histological changes in the temporal lobe epilepsy includes hippocampal sclerosis with neuronal cell loss (predominantly in the pyramidal layer of the Cornu Ammonis region) and growth of granule cell axons (mossy fibre sprouting). The axonal outgrowth occurs predominantly into the inner molecular layer and the polymorphic layer (hilus) of the dentate gyrus. Mossy fibres serve *de novo* excitatory positive feedback loops with granule cells, contributing to increased excitability in neuronal circuits. Mossy fibre sprouting is however not necessary for the process of epileptogenesis and blocking the sprouting does not imply reduction of seizure occurrence (SANTHAKUMAR et al., 2005; BUCKMASTER,

2014). Alternative hypotheses suggest that some deviant mossy fibres may innervate inhibitory basket cells in the granular cell layer (SLOVITER et al., 2006) or that dentate granule cell become GABAergic after repeated seizures (MODY, 2002), supporting the role of the new outgrowing axons in the recurrent inhibitory circuits. Mossy fibre sprouting is driven by different stimuli, among which degeneration of excitatory granular cells and loss of inhibitory GABAergic and neuropeptidergic interneurons in the hilus seem the most likely. Additionally, the axonal outgrowth of mossy cells can be promoted by multiple factors, e.g. exposure to neuromodulin, brain-derived neurotrophic factor, proteins of the extracellular matrix and mammalian target of rapamycin (mTOR) (DEVINSKY et al., 2018). In fact, rapamycin, an mTOR inhibitor, suppresses mossy fibre sprouting without influencing seizure frequency in a mouse model of TLE (BUCKMASTER & LEW, 2011). It is probable that cells of different age are being influenced by different mediators, making them more or less responsive to them and in the end, leading to variable contributions to the process of reconstructing neuronal circuits after the insult (DANZER, 2017).

Neurogenesis, persistent in adult mammals, especially in the subgranular zone of the hippocampal dentate gyrus and the subventricular zone (SVZ) of the forebrain lateral ventricles, is also heavily influenced by epileptic brain activity and can contribute to the process of epileptogenesis as a whole (PARENT & KRON, 2012). In the rat pilocarpine model of mesial temporal lobe epilepsy, neurogenesis is increased even 5-10 fold within weeks following status epilepticus both in the SVZ and in the subgranular zone of the

dentate gyrus (PARENT & KRON, 2012). Approximately 3-4 weeks after SE, proliferation rates return back to the baseline levels and they decrease below the baseline in the chronic phase of the TLE. Many novel cells tend to migrate into the hilus or the molecular layer instead into the granule cell layer of the dentate gyrus, creating a pool of ectopic granular cells (PARENT & KRON, 2012). Histopathologically it can be demonstrated as granular cell dispersion, usually defined as granule cell layer thicker than 10 cells (THOM, 2014).

Alterations in glial cells

Many morphological changes occurring in glial cells are also attributed to epileptogenesis. Abnormal glia, glial scars and tumours are frequent findings in epileptic foci in human patients and in experimental epilepsy models (DEVINSKY et al., 2013). Glia can promote epileptogenesis by changes in the milieu of epileptic foci promoting hyperexcitability (reactive astrogliosis) and inflammation (microglia activation).

Reactive astrogliosis occurs in the epileptic focus, consisting of proliferation as well as morphological and functional changes of those glial cells. Astrocytes regulate the flow of K^+ and water molecules between cells and extracellular space in the brain, supervising the changes in volume of the extracellular matrix. Shrinking the extracellular space promotes excitability by increasing concentrations of extracellular potassium ions and conceivably by intensifying ephaptic (non-synaptic) contact between neurons (DEVINSKY et al., 2013). In epilepsy, aquaporin 4 channels present on the astrocytes undergo redistribution and enhance water entry into the neuropil, while

lessening water transport into capillaries. At the same time, expression of inwardly rectifying potassium (Kir) 4.1 channel is decreased, leading to higher local extracellular K⁺ concentrations, and predisposing to hyperexcitability (DEVINSKY et al., 2013; DEVINSKY et al., 2018). Reactive astrocytes show also some changes in their enzymatic composition: increased activity of adenosine kinase (regulating levels of adenosine by its conversion into 5'-adenosine monophosphate) was demonstrated, lowering in the consequence concentrations of inhibitory adenosine, while glutamine synthetase, converting glutamate to glutamine (used later in synthesis of GABA), demonstrates decreased activity, disrupting the balance of glutamate and GABA in neurons. Additionally, in some TLE patients, reduced expression of astroglial glutamate transporters was observed (SARAC et al., 2009). Thus, impaired glutamate intake may contribute to neuronal excitability in epilepsy. Furthermore, excessive release of gliotransmitters in activated astrocytes and downregulation of gap junction connexins should be considered while assessing a role of astrocytosis in promoting seizure activity (DEVINSKY et al., 2018).

Microglia are immunologically competent cells present in the central nervous system. They actively scan the brain and spinal cord, interact with neurons and modulate neuro- and gliotransmission (EYO et al., 2017). Their activation is detected very early (within 5-10 minutes) following acute neuronal hyperactivity triggered by activation of N-methyl-D-aspartate (NMDA) receptors *in vivo* (EYO et al., 2014). Microglia can be activated by many types of molecules: neurotransmitters (released by living hyperactive cells or damaged cells), damage-associated molecule pattern particles (DAMPs), e.g.

adenosine triphosphate (ATP) or high mobility group box 1 (HMGB1); pathogen-associated molecular pattern molecules (PAMPs), e.g. lipopolysaccharide (LPS); molecules originating from blood (EYO et al., 2014; DEVINSKY et al., 2018). The role of microglia is implied in epilepsy-associated neurodegeneration as well as in abnormal neurogenesis following the status epilepticus (EYO et al., 2017). Bidirectional communication between microglia and neurons is tightened by neuronal release of the chemokine fractalkine, activating microglial CXC-chemokine receptor 1, affecting neurogenesis, neuronal survival and synaptic plasticity (EYO et al., 2017; DEVINSKY et al., 2018). Activated glial cells, both microglia and astroglia, release DAMPs, cytokines, e.g. interleukin-1 β (IL-1 β) or tumour necrosis factor (TNF), and chemokines, contributing to epileptogenesis by promoting neuronal hyperexcitability (VEZZANI et al., 2011a). Studies using minocycline, a potent microglia inhibitor, have shown a protective effect against seizures in rodent SE models and in human patients, suggesting a pro-convulsive role of activated microglia (EYO et al., 2017). Similarly, expression of markers of M1-polarised cells (expressing pro-inflammatory cytokines and driving infiltration of cells) is commonly upregulated in an acute post-SE phase, which may signal their role in epileptogenesis. However, one should not forget the importance of M2-polarised population of microglia, acting in restorative and neuroprotective manner, promoting phagocytosis of debris and expression of enzymes associated with cellular integrity and scaffolding, as well as anti-inflammatory cytokines, e.g. interleukin-4 and interleukin-10 (BENSON et al., 2015). Henceforth, microglia can have both pathogenic and reparative functions, and

would require selective inhibition or modulation of their state in case of pharmacological intervention.

Cytokines and chemokines released from activated glial cells can be the cause of blood vessel inflammation, leading to dysfunction of the blood-brain barrier (BBB). BBB dysfunction is a common finding in acquired and structural epilepsies in animal models and in patients and it is associated with development of the disease in rodent models (DEVINSKY et al., 2018). Increased permeability of the BBB leads to extravasation of many blood components, such as albumin and macrophages, contributing to local inflammation (VAN VLIET et al., 2016; BANKSTAHL et al., 2018). Extravasated serum albumin activates a transforming growth factor beta (TGF- β) receptor and mediates activation of a signalling cascade leading to upregulation of transcription of inflammatory genes in glia and, in consequence, to local inflammation. It also results in decreased expression of Kir 4.1 potassium channels and glutamate transporters present in astroglial cells, facilitating neuronal hyperexcitability by modifying ionic and neurotransmitter composition of the extracellular matrix (DEVINSKY et al., 2013). Overexpression of TGF- β has been also demonstrated to reinforce neurogenesis (MATHIEU et al., 2010).

Besides, epileptogenesis involves several genetic and epigenetic modifications. Changes in gene expression, both turn-in and turn-off, may underlie evolving pathology, such as gliosis, neuroinflammation, ion channel and neurotransmitter receptors expression or processes plasticity (HENSHALL & KOBOW, 2015). Some of transcriptional pathways involved in cell cycle and cell death like the Janus kinase or

signal transducers and activators of transcriptions are activated during epileptogenesis and their inhibition lowers severity of epileptic seizures in a rat model (DEVINSKY et al., 2018). Epigenetic mechanisms active in the course of the epileptogenic process include:

- alterations of DNA methylation (hypomethylation occurring in the acute post-insult phase and hypermethylation present in the chronic phase),
- histone acetylation and phosphorylation (e.g. valproate, being an inhibitor of histone deacetylase, leads to reduction of abnormal neurogenesis in the dentate gyrus)
- microRNA expression (injection of synthetic mimic of miRNA-146a impairs signal transduction of IL-1 β receptor/Toll-like receptor 4 neuroinflammatory pathway, strongly inhibiting epileptogenesis) (HENSHALL & KOBOW, 2015; IORI et al., 2017; DEVINSKY et al., 2018).

Other molecular mechanisms promoting epileptogenesis involve deficiency of neuropeptides, neurosteroids, sphingosine 1-phosphate receptors and erythropoietin, which are speculated to contribute to neuronal hyperexcitability (DEVINSKY et al., 2018).

3. Role of neuroinflammation in epileptogenesis

Inflammation is a dynamic process comprising of production and release of pro-inflammatory mediators as well as anti-inflammatory molecules in response to harmful stimuli or immune stimulation. The inflammatory response is a defence mechanism that evolved to protect higher organisms from infection and injury. Inflammatory molecules are generated by specialised, immunocompetent cells, either residing in tissue or circulating with blood. Mechanisms of both innate and adaptive immunity are involved in activation of inflammation. The innate immune system is characterised by a non-specific and prompt response, involving leukocytes (granulocytes, natural killer cells), myelomonocytic cells (monocytes, macrophages and microglia) and dendritic cells. The adaptive immunity gets triggered in response to innate immunity activation, and recognises specific non-self-antigens. Lymphocytes B and T get stimulated by dendritic cells, macrophages and microglia in order to commence a humoral (antibody production) or cellular immune response (VEZZANI et al., 2011b).

Due to presence of the blood-brain barrier and lack of lymphatic drainage in traditional terms, the central nervous system is conventionally viewed as an immunologically privileged structure. Immune privilege is a concept concerning protection of certain vital organs, like the brain or the eye, from destructive influences of inflammation directed against pathogens (HONG & VAN KAER, 1999). However, both innate and adaptive immune responses are

effectively mobilised in the brain. Microglia, astrocytes and neurons as well as endothelial cells and extravasating circulating immunocompetent cells are able to produce molecules of inflammatory cascades. Inflammatory response can be evoked both in infectious and sterile conditions, the latter being induced in response to tissue injury or exposed self-antigens (VEZZANI et al., 2011b; VEZZANI et al., 2015; VEZZANI et al., 2016).

There is an extensive clinical evidence that pathological conditions of the immune system may promote seizures and epilepsy (VEZZANI et al., 2019). Autoimmune disorders, such as systemic lupus, multiple sclerosis and paraneoplastic syndromes can be a cause of recurrent seizures (VEZZANI et al., 2011b). Fever, being one of the main symptoms of inflammation, which exacerbates pro-inflammatory responses, can commonly induce seizures, especially in children (DUBE et al., 2007). Increased neuronal activity can evoke an inflammatory response also in absence of other pro-inflammatory stimuli – it is then referred to as neurogenic inflammation. Firstly described for peripheral nervous system, it is also known to be activated by neuronal hyperexcitability during seizures in the central nervous system (VEZZANI et al., 2019). In rodent models, status epilepticus triggers an immediate increase of pro-inflammatory cytokines in brain regions involved in seizure generation and propagation, predominantly described in activated astrocytes and microglia (VEZZANI et al., 2011b).

Cytokines and other molecules synthesised as the consequence of pro-inflammatory cascade activation in the CNS may affect excitability

of neurons as well as the degree of neurogenesis and neurodegeneration. Cyclooxygenase-2 (COX-2) is an enzyme catalysing the first step in the formation of prostanoids, involved in many of physiological and pathophysiological processes (ALEXANIAN & SOROKIN, 2017). It is expressed constitutively in hippocampal neurons and is activated shortly after a seizure. Several prostaglandins, the products of the cascade initiated by COX-2, play a role in long-time potentiation of the synapse of the perforant path (between axons from the entorhinal cortex and dendrites of granule cell layer of the dentate gyrus), which is a crucial connection for propagation of seizure activity in the brain (VEZZANI et al., 2013b). Selective COX-2 inhibition leads to significant reduction of membrane excitability in dendrites and in the cell soma, while application of prostaglandin E enhances firing frequency and excitatory postsynaptic potential amplitude in excitatory neurons in CA1 (CHEN & BAZAN, 2005; VEZZANI et al., 2013b). Administration of the non-steroidal anti-inflammatory drug celecoxib, a selective inhibitor of COX-2, to neonatal rats in kainic acid SE model, showed neuroprotective effects due to inhibition of the pro-inflammatory cascade (MORALES-SOSA et al., 2018). Selective COX-2 inhibitors applied after SE also proved to lower the number of proliferating cells in the dentate gyrus (VEZZANI et al., 2013b).

Glia-mediated neuroinflammation can serve as a promoter of ictal- and epileptogenesis, particularly if physiological servomechanisms fail to limit the process. Chronic uncontrolled glial activation leads to excessive release of pro-inflammatory mediators, damage to the blood-brain barrier and following extravasation of albumin and other

blood components, and to disturbances in ionic homeostasis and imbalance of neurotransmitters, which can affect seizure development. Chronically activated astrocytes form a glial scar, having both advantageous and detrimental impact on pathologically changed brain tissue. A scar can limit exposure of neurons to stress factors and restrict migration of activated immune cells. On the other hand, it impairs axonal regeneration and restoration of normal neuronal circuits (DEVINSKY et al., 2013).

3.1. Toll-like receptor signalling in epilepsy

Activated glial cells release inflammatory molecules acting either in autocrine or paracrine manner, inducing transcriptional and post-transcriptional signalling in themselves or in nearby cells. One of the most crucial pathways, involved in the initiation of tissue inflammation by activating cells of the innate immunity, is the interleukin-1 receptor/toll-like receptor (IL-1R/TLR) signalling track. The cascade is initiated by activation of members of a superfamily of 24 transmembrane receptors, all of which share a cytosolic toll/interleukin-1 receptor (TIR) domain (VEZZANI et al., 2011a). The superfamily consists of the IL-1R family and the TLR family, the latter being in the scope of this dissertation.

Toll-like receptors (TLRs) are a key component of the innate immune system. The group consists of eleven [in humans; thirteen in mice (YU et al., 2010)] evolutionarily conserved proteins belonging to the pattern recognition receptors family. The receptors are responsible for recognition of both pathogen-associated and damage-associated

molecular pattern molecules (PAMPs and DAMPs), meaning they recognise highly conserved motifs in pathogens and in non-infectious endogenous compounds (JANSSENS & BEYAERT, 2003; VAURE & LIU, 2014). TLRs are located in a membrane as well as in some intracellular compartments like endoplasmic reticulum (ER) and lysosomes of innate immune cells (e.g. dendritic cells and macrophages) and in non-immunocompetent cells (e.g. fibroblasts and epithelial cells). They are glycoproteins with an extracellular leucine-rich repeat domain, which is involved in antigen recognition, and an intracellular TIR-like domain, a protein-protein interaction module, necessary for signal transduction (JANSSENS & BEYAERT, 2003; KAWASAKI & KAWAI, 2014; VAURE & LIU, 2014).

Toll-like receptor 4 (TLR4) is located on the cell surface. It specifically recognises lipopolysaccharide (LPS), an antigen found in an outer layer of Gram-negative bacteria, as well as several other exogenous PAMPs (e.g. lipoteichoic acids of Gram-positive bacteria). Additionally, it binds also endogenous DAMPs, such as heat shock proteins and S100 proteins, normally expressed in the cytoplasm and cell organelles, but released into the extracellular matrix during tissue injury and thus available for binding with receptors on the cell surface (VAURE & LIU, 2014).

TLR4 in rats shows 61% of amino acid similarity with a human receptor in the extracellular domain, 68% similarity in the transmembrane domain, and 92% in the proximal and 38% in the distal cytoplasmic region. Canine TLR4 shows 70-77% overall similarity to human nucleotide and amino acid sequences, being also highly similar to

other mammalian TLR4 sequences (VAURE & LIU, 2014). It shows a relatively high conservation of the receptor's structure, especially in the intracellular domain. Nevertheless, the spectrum of agonists and antagonists of TLR4 varies significantly across species, resulting in diverse functionality and expression pattern of the same receptor. In the human central nervous system, TLR4 is expressed predominantly by astrocytes and microglia, while in rats it was observed solely in microglial cells (VAURE & LIU, 2014).

After binding to a ligand (Fig. 1), TLR4 undergoes dimerisation leading to induction of one of the two major pathways described for that receptor: TIR adapter protein – myeloid differentiation factor 88 (TIRAP – MyD88) cascade, in which IL-1R associated kinases 4, 1 and 2 (IRAK4, IRAK1, IRAK2) are released from MyD88. IRAK4 is activated initially and regulates release of nuclear factor κ B (NF- κ B) and mitogen-activated protein kinases (MAPK). Following activation of IRAK1 and IRAK2 amplifies the signal from NF- κ B and MAPK. The MyD88-dependent pathway signalling leads to induction of transcription of many genes and the consequent synthesis of pro-inflammatory molecules (JANSSENS & BEYAERT, 2003; KAWAI & AKIRA, 2010; VEZZANI et al., 2011a; KAWASAKI & KAWAI, 2014). TLR4 can also signal using a MyD88-independent pathway involving TIR-domain-containing adapter-inducing interferon- β (TRIF). The signal from TLR4 to TRIF is transduced by TRIF-related adaptor molecule (TRAM) and it results in activation of interferon regulatory factor 3 (IRF-3), supervising synthesis of interferons α and β (KAWAI & AKIRA, 2010; VEZZANI et al., 2011a; KAWASAKI & KAWAI, 2014).

Several negative regulators of TLR signalling have been identified. They act on multiple levels in the cascade initiated by TLR activation and involve ubiquitin ligases and deubiquitinases, transcriptional regulators, molecules controlling mRNA stability as well as miRNA (KAWAI & AKIRA, 2010). The negative regulation of TLR-evoked pathways is important for suppressing inflammation and harmful consequences of chronic inflammatory processes for the tissue.

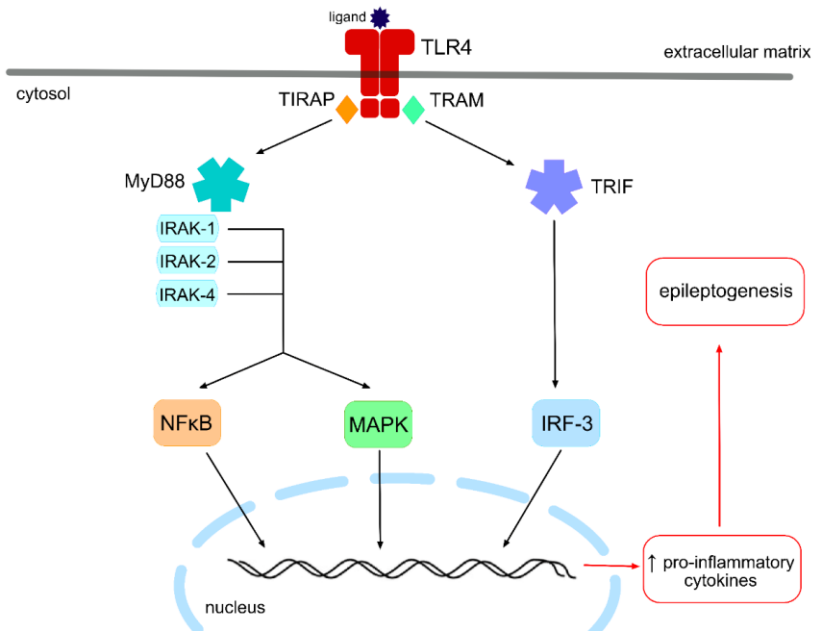


Figure 1. Pro-inflammatory TLR4 signalling. TLR4, located on the cell surface, initiates signalling to the two major downstream adaptor proteins, MyD88 and TRIF. TIRAP mediates the signal from TLR4 to MyD88, and TRAM transfers the signal from TLR4 to TRIF. The subsequent signalling cascades lead to the upregulation of transcription of genes encoding pro-inflammatory cytokines and to exacerbation of the inflammatory process.

Balanced production of inflammatory molecules supports key roles of the immune system like combating infections or controlling tumour cell growth. Nevertheless, overstimulation of TLR4 can lead to severe pathologies, including sepsis, autoimmune diseases as well as acute and chronic neurological disorders, also epilepsy (MAROSO et al., 2010; MAROSO et al., 2011; VEZZANI et al., 2011a; ZHANG et al., 2013b). Reciprocally, tissue injuries and seizures may cause upregulation of expression of TLR4, which is present on brain cells at low levels in physiological conditions (MAROSO et al., 2010; VEZZANI et al., 2013b). Single elements of TLR4-induced cascade are upregulated in neurons and glial cells in tissue from epileptic human patients and in mice models (WANG et al., 2018a).

Exogenous application of LPS into rat cerebral cortex increased excitability of local neurons by tripling evoked field potential amplitudes and producing focal epileptiform discharges. This activity commenced within 10 minutes after LPS administration and recurred every 1-2 minutes for 30 minutes of the recording time. These effects were prevented by pre-application of IL-1R inhibitors, which implicates a role of IL-1 β released from activated microglia and astrocytes, and supports a critical part of innate immunity mechanisms in ictogenesis (RODGERS et al., 2009). The activation of TLR4 by LPS also exerts long-term effects on neuronal excitability – LPS injection in rats within two post-natal weeks decreased seizure threshold in adult animals exposed to various pro-convulsive compounds in their adulthood (RIAZI et al., 2010). The effect extends also onto glial cells – TLR4 stimulation causes disruption of gap junctions, leading to uncoupling of astroglial cells, impaired K⁺ buffering and generation of

spontaneous seizures (BEDNER et al., 2015). Astrocytic TLR4 pathways prove to regulate postnatal development of excitatory synapses in hippocampus (SHEN et al., 2016). TLR4-deficient mice developed less severe epilepsy following SE (VEZZANI et al., 2013a). This evidence demonstrates that brain inflammation erupted in early stages of life can lead to long-term alterations in neuronal excitability, and trigger and/or promote epileptogenic modifications as the consequence.

Pharmacological or genetic interference with the IL-1R/TLR pathway before a seizure episode provides further evidence of its engagement in epileptogenesis and highlights the possibility of modulation of the outcome of the epileptogenic process. TLR4 knock out mice were protected from detrimental effects of LPS peripheral injection on astrocytes (BEDNER et al., 2015). Exogenous application of a synthetic mimic of miRNA-146a impaired IL-1R/TLR signal transduction and reduced neuronal excitability and acute seizures as well as diminished disease progression and decreased chronic spontaneous recurrent seizures in a mouse model of acquired epilepsy (IORI et al., 2017).

3.2. Endogenous ligands of TLR4

TLRs are responsible for PAMPs recognition, they respond however, in addition to microbial ligands, also to a number of endogenous molecules, which serve as potent activators of inflammatory responses. They are capable of activating not only the innate immune system, but also the adaptive immune response by induction of

costimulatory proteins present in antigen-presenting cells (TSAN & GAO, 2004). Damage-associated molecular patterns (also referred to as alarmins or danger signals) are molecules constitutively expressed in all cell compartments where they play a role in cell homeostasis. When present in the extracellular environment however, they act as ligands for pattern-recognition receptors, such as TLRs, leading to activation of pro-inflammatory processes. Since they proved to be released by cells undergoing necrosis, but not the apoptotic ones, they were originally associated solely with cell death. DAMPs can be however also secreted by stressed living cells or expressed constitutively in the extracellular matrix and cleaved as the result of injury or inflammation (SCAFFIDI et al., 2002; KAWAI & AKIRA, 2010; VENEREAU et al., 2015; PANDOLFI et al., 2016).

The group of DAMPs serving as ligands for TLR4 includes:

- polysaccharides and degradation products of proteoglycan (biglycan, CD138, soluble hyaluronan, heparin sulphate),
- phospholipids (OxPAPC),
- small organic molecules (monosodium urate crystals),
- proteins and peptides (α -crystallin A chain, β -defensin 2, endoplasmic reticulum chaperones, fibrinogen, fibronectin, HMGB1, many members of the heat shock protein superfamily, resistin, S100 proteins, surfactant protein A and tenascin-C) (TSAN & GAO, 2004; PARK et al., 2006; KAWAI & AKIRA, 2010; KAWASAKI & KAWAI, 2014).

High mobility group box 1 (HMGB1) protein is among the best-characterised DAMPs. It is a highly conserved and abundant DNA

chaperone. It interacts with DNA and histones to transiently and reversibly modify chromatin structure, facilitating nucleosome formation and regulating key nuclear processes, i.e. transcription, replication and DNA repair (MAGNA & PISETSKY, 2014; RAVIZZA et al., 2018). During inflammation, it is translocated from cells into the extracellular space and recognised by TLR4. HMGB1 plays an important role in acute pathological conditions (e.g. sepsis, shock), but also in several autoimmune and inflammatory disorders, such as rheumatoid arthritis, systemic lupus erythematosus, myositis, scleroderma and ankyloses spondylitis (MAGNA & PISETSKY, 2014). It also proved to be translocated from nucleus to cytoplasm in neuronal and glial cells at sites of local damage in animal models of acquired epilepsy within one hour from the seizure onset (MAROSO et al., 2010; RAVIZZA et al., 2018). HMGB1 release accelerates the seizure precipitation evoked by chemoconvulsants and exacerbates their number and severity. At the same time, antagonists of HMGB1 and TLR4 retard seizure onset and decrease recurrence of acute and chronic seizures (MAROSO et al., 2010). The activation of HMGB1-TLR4 signalling has also been demonstrated in human tissue from epileptic patients resected during surgery, indicating a role of this pathway in the disease in humans (MAROSO et al., 2010; RAVIZZA et al., 2018). Administration of therapeutic anti-HMGB1 monoclonal antibodies in mice models of both acute and chronic epilepsy attenuated severity of kindling- and kainic acid-induced seizures, but also reduced the number of spontaneous recurrent general and focal seizures. (SOBIESKI & CHRISTIAN, 2017; ZHAO et al., 2017). The example of HMGB1 clearly indicates a role of DAMP-related TLR

signalling in epileptogenesis. Therefore, examination of other TLR ligands and their influence on epileptogenic processes is of great interest concerning the search for possible targets for therapeutic intervention. Based on an extensive proteomics study (WALKER et al., 2016) as well as on their physiological and pathological relevance, three members of heat shock protein family, a group of TLR ligands, were selected for in-depth investigation during this study.

4. Heat shock proteins and their relation to epilepsy

4.1. Heat shock protein family description

Heat shock proteins (HSPs) constitute a class of potent TLR ligands (ASEA et al., 2002; TSAN & GAO, 2004; YU et al., 2010). HSPs comprise a heterogeneous group of molecules with highly conserved structure, expressed ubiquitously in cells of the body and present in all cell compartments (nucleus, cytosol, mitochondria, chloroplasts, endoplasmic reticulum). They appear in all domains of life: archaea, eubacteria and eukaryotes. Some of them are expressed constitutively in order to promote proper folding and assembling of proteins, while most of them are produced in response to cellular stress, including oxidative stress, hyperthermia, ischemic injury and neuronal excitability, which result in accumulation of denatured and misfolded proteins (BENARROCH, 2011). Polypeptides folded improperly tend to form aggregates, which is a prominent characteristic of several neurodegenerative diseases, like Alzheimer disease, Parkinson disease and Huntington disease (ASEA, 2008; BENARROCH, 2011; ASEA, 2016). HSPs provide a first line of defence against accumulation of misfolded proteins (serving as so-called chaperones) as well as execute other neuroprotective effects, e.g. inhibition of apoptosis, protection of cytoskeletal structures and immune modulation in stress conditions (BENARROCH, 2011).

Traditionally, HSPs are classified according to their molecular weight

in kilodaltons (kDa) into several major classes: HSP110, HSP90, HSP70, HSP60, HSP40 and small HSPs, with molecular weight smaller than 40 kDa (KAMPINGA et al., 2009; BENARROCH, 2011). This nomenclature however can often be confusing, since a lot of HSP family members do not include “heat shock” in their commonly used names. Moreover, the number of members of particular classes is gradually increasing (KAMPINGA et al., 2009). For the purpose of this monography, the modified nomenclature suggested in the guideline by KAMPINGA et al. (2009) will be implemented:

- Members of the heat shock protein family of 70 kDa molecular weight (usually referred to as HSP70) will be specified as **HSPA**, in particular:
 - Products of genes *HSPA1A* and *HSPA1B*, differing by two amino acids, are considered fully interchangeable proteins. In the suggested nomenclature they are referred to as HSPA1A/1B, in literature they are also known as HSP72, HSP70i and HSP70. For the purpose of clarity, this protein of interest will be referred to as **HSPA1**.
 - Product of *HSPA8* gene is a cognate of HSPA1 expressed constitutively and designated in literature as heat shock cognate 70 kDa (HSC70), HSP71 and HSP73. In this publication, the name **HSPA8** will be used.
 - Product of *HSPA5* gene is a heat shock protein localised in the endoplasmic reticulum. Other common names include 78 kDa glucose regulated

protein (GRP78) and binding immunoglobulin protein (BiP). It will be referred to as **HSPA5**.

- Members of the heat shock protein family of 110 kDa molecular weight (so-called HSP110), a group showing a high homology to HSPA, will be specified as **HSPH**:
 - Product of *HSPH4* gene, a compartment-specific chaperone located in the endoplasmic reticulum, is commonly referred to as hypoxia upregulated protein 1 (HYOU1), 170 kDa glucose-regulated protein (GRP170) or 150 kDa oxygen-regulated protein (ORP150). In this monography, the name **HSPH4** will be used.
- Members of the heat shock protein family of 90 kDa molecular weight (HSP90), will be referred to as **HSPC**.
- Members of the heat shock protein family of 40 kDa molecular weight (HSP40), will be referred to as **DNAJ**.
- Heat shock proteins of molecular weight smaller than 40 kDa will be referred to as **HSPB** or **small HSPs** (KAMPINGA et al., 2009; UNIPROT, 2019a, 2019b, 2019c).

4.2. Role of HSPA1 in the cell and in TLR signalling

According to the definition from 1986, HSPA (HSP70) family includes “proteins whose synthesis is stimulated by stress, and whose genes contain a marker nucleotide block—heat shock consensus element — CT-GAA-TTC-AG” (MALYSHEV, 2013). It includes at least thirteen isoforms, both constitutive and inducible, expressed in all cell

compartments as well outside of the cell (KAMPINGA et al., 2009; TURTURICI et al., 2011). In humans, they account for 2% of all protein mass under stress conditions (TURTURICI et al., 2011; ZUIDERWEG et al., 2013). HSPA8 and HSPA5 as well as mitochondrial HSPA9 are expressed abundantly under normal conditions. HSPA1 levels are however induced in response to different stress stimuli (TURTURICI et al., 2011). The synthesis of HSPA1 in a cell is controlled transcriptionally – the process of HSPA1 transcription is strongly induced immediately after heat shock, whereas the translation rate remains almost unchanged, meaning the protein synthesis rate depends predominantly on the transcription rate of the *HSPA1A/1B* gene (GERNER et al., 2002). Biological half-life of HSPA1 was estimated for 18.1 – 20 h in cell culture (GERNER et al., 2002).

The heat shock response is triggered by accumulation of unfolded and misfolded proteins (BENARROCH, 2011). In a physiological state, members of HSPC (HSP90) family bind to a transcription factor called heat shock factor-1 (HSF-1), keeping it inactive in the cytoplasm. In the presence of improperly folded or unfolded polypeptides, HSPs dissociate from HSF-1, enabling it to undergo trimerisation, followed by its translocation into the nucleus, where it binds to heat shock elements in HSP genes, activating the production of HSPA, DNAJ and HSPB proteins. The basic function of HSPs as chaperones is refolding misfolded proteins due to conformational changes and hydrolysis of adenosine triphosphate (ATP). However, if abnormal proteins cannot be repaired, HSPs target them for degradation by the ubiquitin-proteasome pathway or by lysosome-mediated autophagy (BENARROCH, 2011). The chaperone role of HSPs is of high

importance especially in neuronal cells, since they cannot dilute the concentration of protein aggregates through mitosis (TURTURICI et al., 2011).

HSPA family proteins are extremely highly conserved proteins (showing 68% homology between HSPA1 of *E. coli* and HSPA8 of humans (ZUIDERWEG et al., 2013)), therefore studying their properties in one organism poses a good approximation of their behaviour in the others. HSPA1 and its cognates are built in form of dimers, each of them containing three domains:

- N-terminal nucleotide-binding domain (NBD) of ca. 45 kDa, serving the purpose of binding and hydrolysing ATP
- C-terminal substrate-binding domain (SBD) of ca. 25 kDa, further subdivided into:
 - β -sandwich subdomain functionally serving as a binding scaffold that interacts with substrate proteins
 - α -helical, flexible subdomain, able to adopt an open or a closed conformation and acting as a lid, which has no direct contact with the substrate
- short (around 10-15 kDa) linker domain, a highly conserved and hydrophobic structure (TURTURICI et al., 2011; MALYSHEV, 2013; ZUIDERWEG et al., 2013; MORGNER et al., 2015; FERNANDEZ-FERNANDEZ & VALPUESTA, 2018).

HSPA1 requires specific monovalent and divalent metal ions (K^+ and Mg^{2+}) to perform its weak ATPase activity. It adopts three conformations, one bound to adenosine diphosphate (ADP), one

bound to ATP and one in the absence of a nucleotide (TURTURICI et al., 2011; ZUIDERWEG et al., 2013). In the presence of ATP, the lid subdomain of the SBD remains open, allowing substrates to bind (or products to dissociate). Nucleotide hydrolysis closes the lid and enhances substrate affinity (TURTURICI et al., 2011; ZUIDERWEG et al., 2013). However, HSPA1 is not tightly locked in one of the two conformations in the cycle – substrates are also able to bind to the SBD in the ADP-bound conformation. Similarly, in the presence of ATP, the lid may not remain fully open, suggesting several conformations present on different time scales in the presence of both nucleotides (GENEST et al., 2019). The communication between the domains runs bidirectionally, since interactions between the SBD and its substrates can increase the rate of ATP hydrolysis (TURTURICI et al., 2011).

In its role of the chaperone, HSPA1 requires: cochaperones, including members of DNAJ (HSP40) family, which deliver substrates to HSPA1 and stimulate ATP hydrolysis; nucleotide exchange factors, which increase the rate of nucleotide exchange of the NBD; HSPA1-interacting protein, which assists in retaining substrates (MALYSHEV, 2013). During protein folding, HSPA proteins cooperate with members of HSPC (HSP90) family to coordinate folding and maturation of client substrates. In protein disaggregation processes HSP are assisted by heat shock proteins of 100 kDa molecular weight and HSPH molecules (DRAGOVIC et al., 2006; FERNANDEZ-FERNANDEZ & VALPUESTA, 2018).

HSPA1 plays a crucial role in protein degradation. It facilitates

ubiquitination of its client proteins as well as their delivery to proteasome, but also assists in endosomal microautophagy and macroautophagy (FERNANDEZ-FERNANDEZ & VALPUESTA, 2018).

Protective function of several HSPs is expressed also in their role of regulators of apoptosis. HSPA1 acts as an inhibitor of apoptosis on three levels: premitochondrial, mitochondrial and postmitochondrial stage. At the first stage, HSPA1 inhibits stress-activated c-Jun N-terminal kinase, critical for upregulation of pro-apoptotic genes (DHANASEKARAN & REDDY, 2008). At the mitochondrial level, it inhibits the translocation of C-cell lymphoma 2-associated protein X to the mitochondrial outer membrane, therefore protecting it from its permeabilisation and release of cytochrome c (BENARROCH, 2011; RICHTER-LANDSBERG, 2011). Postmitochondrially, HSPA1 binds to apoptotic protease activating factor 1, preventing apoptosome formation and caspase 9 activation. Finally, by binding to another mitochondria-associated protein, apoptosis-inducing factor, HSPA1 inhibits caspase-dependent nuclear fragmentation (RICHTER-LANDSBERG, 2011).

HSPs are intracellular chaperones, they can, however, be expressed extracellularly, in the plasma membrane or in the extracellular space, where they have the capacity to activate the immune system (VEGA et al., 2008; BENARROCH, 2011). Initially they were believed to be released from necrotic cells. However, HSPs proved to be present in the extracellular matrix in the absence of cell death. Members of HSPA and HSPC families can be transported and released via exosomes or

in an endolysosomal-dependent pathway (VEGA et al., 2008). Extracellular HSPA1 is recognised by major histocompatibility complex class I molecules, triggering specific CD8+ T-cell responses (BENARROCH, 2011). It has been described as a DAMP, knowing to bind to human monocytes and activating pro-inflammatory cytokine cascades, such as induction of above-mentioned IL-1R/TLR signalling (ASEA et al., 2000; VABULAS et al., 2002a; TSAN & GAO, 2004; YU et al., 2010). The protein has shown immunomodulatory characteristics in interstitial spaces and tissue fluids (POCKLEY et al., 1998; MAMBULA & CALDERWOOD, 2006). Whether HSPA1 augments or suppresses inflammation seems to depend also on a type of activated receptor (FONG et al., 2015), leading to contradictory views on a function of a single protein. It has been also discussed that endotoxin contamination could be responsible for such particular outcomes regarding the role of secreted HSPA1 (GAO & TSAN, 2003).

HSPA1 seems to play a protective role in cells, prolonging their viability after exposure to several stress factors. Overexpression of inducible HSPA1 showed protective effects against sublethal heat stress in cultured hippocampal neurons (BEAUCAMP et al., 1998) and against hypoxia in chondrocyte cell culture (TSUCHIDA et al., 2014). Moreover, in the diseases of proteostasis (including Alzheimer, Parkinson and Huntington diseases), characterised by misfolding of normal cell proteins and their subsequent aggregation and accumulation in the form of inclusions, HSPs suppress neurodegeneration. Overexpression of different HSPs inhibits the aggregation of falsely folded proteins and protects against cell death

in models of Parkinson disease, Huntington disease and amyotrophic lateral sclerosis (BENARROCH, 2011). The induction of the overexpression of HSPA1 and associated chaperones, e.g. by using a compound able to upregulate HSP gene expression like celastrol, has neuroprotective effects *in vivo* in animal models of Alzheimer disease and Huntington disease. The role of HSPA1 in epilepsy models remains however uncertain. In the kainic acid rat model of SE, HSPA1 expression was upregulated in the early post-insult phase brain-wide in regions related to epileptogenicity (SANZ et al., 1997). Despite the expression of HSPA1, no neuroprotection was observed, showing severe neuronal loss and gliosis in the hippocampus as well as an increase of dying cells (YANG et al., 2008; TURTURICI et al., 2011). In this case, HSPA1 may only serve as an indicator of neuronal stress in the acute phase of epileptogenesis. In the kindling model, upregulation of *HSPA1A* gene proved to have a pro-epileptogenic effect, promoting ictogenesis in naïve animals (VON RUDEN et al., 2018). Conversely, a similar study conducted on *HSPA1A*-deficient mice supports a protective role of HSPA1 with an effect on microglia activation in hippocampus and on spread of seizure activity (VON RUDEN et al., 2019).

A putative neuroprotective role of extracellular HSPA1 in epilepsy has been suggested in several studies. EKIMOVA et al. (2010) demonstrated for the first time anticonvulsive properties of exogenous HSPA1. In this study, HSPA1 and HSPA8 (HSC70) injection exerted a seizure attenuating effect in a chemically induced SE model. Both proteins proved to be able to modulate GABAergic transmission and to penetrate into brain areas involved in generation and propagation

of generalised seizures (like cortex, hippocampus, and thalamus). Extracellular HSPA1 has also shown neuroprotective effects in different brain injury models (BENARROCH, 2011; KIM & YENARI, 2013; KIM et al., 2018), as well as in lethal oxidant lung injury, where activation of TLR4 signalling expressed potent cytoprotective properties (ZHANG et al., 2013a). This double-faced functionality of HSPA1 inside and outside of cells suggests possible scenarios in therapy development targeting HSPA1 expression.

4.3. Heat shock proteins in the endoplasmic reticulum

In eukaryotic cells, most proteins destined for secretion or membrane expression are synthesised in the endoplasmic reticulum (ER). Its physical segregation from the cytosol leads to a distinct folding milieu with proper protein machinery engaged in processes of folding, assembly, modification, quality control and recycling (BRAAKMAN & BULLEID, 2011). Correct protein folding and maturation is the role of compartment-specific chaperones. An imbalance between the load of proteins to be folded and the folding capacity of local chaperones leads to aggregation of misfolded proteins and a condition known as ER stress (PREISLER & RON, 2018). Several heat shock proteins are involved in the ER stress response, among which two of them, HSPA5 and HSPH4, are the topic of this monography.

HSPA5

In HSPA family, HSPA1 is present ubiquitously in the tissue. In the cell, it localises mostly in the cytosol, similarly to the constitutive form of the protein, HSPA8, which can be found in the cytosol as well as in

the nucleus. HSPA5 is a homologue form of HSPA8 present predominantly in the endoplasmic reticulum, it can be however found also on the cell surface, in the extracellular matrix, in the cytosol and in the mitochondria, where it plays various roles (VOS et al., 2008; NI et al., 2011).

Endoplasmic HSPA5 is essential for the normal functioning of the ER and is widely used as a marker of ER stress (NI et al., 2011). It is involved in translocating the newly synthesised polypeptides across the ER membrane, facilitating the folding and assembly of proteins, targeting misfolded proteins for ER-associated degradation, regulating calcium homeostasis, and serving as an ER stress sensor (WANG et al., 2009). It is also one of the main factors of the unfolded protein response (UPR), a set of dynamic adjustments within the ER aimed to protect protein homeostasis inside the compartment as a result of stress. The UPR depends on activation of transmembrane signal transducers: inositol-requiring enzyme 1 (IRE1), protein kinase R-like ER kinase (PERK) and activating transcription factor 6 (ATF6). Their activation evokes two main downstream effects: it limits the influx of proteins into the ER to lower the folding load and upregulates the expression of proteins involved in ER protein quality control to increase the folding capacity in the ER (PREISLER & RON, 2018). In the physiological conditions, HSPA5 is bound to the signal transducers, involving its typical substrate-like interactions (PREISLER & RON, 2018) Following the ER stress, HSPA5 is released from the signal transducers, which leads to the activation of the UPR signalling pathways (WANG et al., 2009). The response involves both rapid posttranslational regulation of active chaperones

in the ER and the slower induction of ER protein quality control genes. In the end, it promotes degradation of cytotoxic misfolded proteins and cell survival (WANG et al., 2009). However, if the stress is too long or too severe to cope with, the ER stress-induced apoptosis pathways can be activated (WANG et al., 2009).

HSPA5 has a relatively long half-life in cell culture (≥ 24 h) and in tissues (≥ 3 days) and is present at high basal concentrations in the ER. The prolonged ER stress conditions can increase the HSPA5 expression several fold (PREISLER & RON, 2018). In the ER, it can be present in an active or an inactive state, where the other one can be achieved either by posttranslational modification or by protein storage. The regulation involving posttranslational changes is based most prominently on binding of adenosine monophosphate (AMP) via a phosphodiester bond to HSPA5 (AMPylation), which locks the protein in a low-affinity state for substrates, therefore causing its functional inactivation. This process is especially prominent during the recovery period after the prolonged ER stress, since the HSPA5 half-life is relatively long. The chaperone can also be deposited into a dynamic inactive pool of proteins by its oligomerisation, which utilises the competitive binding of other HSPA5 proteins instead of substrates, consequently lowering non-productive interactions with proteins in conditions of low folding need. AMPylated HSPA5 is excluded from oligomers, since its substrate affinity is low (PREISLER & RON, 2018). Oligomerisation is a rapid process, facilitating HSPA5 availability on short timescale (seconds to minutes), while AMPylation operates in longer (minutes to hours) timeframes (PREISLER & RON, 2018). In total, the concentration of overall HSPA5 molecules in

the endoplasmic reticulum vastly exceeds the concentration of molecules able to engage substrates.

In other cell compartments, as well as outside the cell, HSPA5 has several additional functions. ER stress leads not only to increase of HSPA5 levels in the ER, but also promotes the relocalisation of the protein to the cell surface, where it acts as a receptor for pro-survival growth signalling, but also for viral internalisation (as in case of Borna disease virus or Japanese encephalitis virus) (NI et al., 2011; NAIN et al., 2017). HSPA5 is expressed on the cell surface of proliferating cells, making it a suitable target for novel anti-cancer therapy methods (NI et al., 2011). HSPA5 is present also in the cytoplasm, where it functions as a regulator of the UPR signalling – the cytosolic form is however a product of alternative splicing of *HSPA5* gene.

HSPA5 is often secreted into the extracellular space, both under the pathological and in physiological conditions. High HSPA5 levels were observed in tumour matrix (KERN et al., 2009) as well as in sera of patients with gastric cancer (TSUNEMI et al., 2010). Studies indicate an increased secretion of HSPA5 into the bronchoalveolar lavage fluid in chronic cigarette smokers (AKSOY et al., 2017). In addition, HSPA5 has been found in the oviductal fluid from healthy women in the periovulatory period, having the ability to regulate the binding of sperm to the zona pellucida during fertilisation (MARIN-BRIGGILER et al., 2010). These findings strongly suggest the role of the protein in modulation of many biologically crucial processes in both normal and pathologically changed tissue.

HSPH4

HSPH (HSP110) family is a part of HSP superfamily and is closely associated with HSPA proteins in its molecular form and function in the cell (LIN et al., 2001; DRAGOVIC et al., 2006). Substrates enter the HSPA complex in the configuration bound to ATP, when the substrate change rate is high and the affinity is low. ATP hydrolysis performed by cofactors, i.e. of DNAJ family, stabilises the affinity of HSPA protein to its substrate. As a result, nucleotide exchange factors are activated to transmute ADP with ATP, which is followed by a substrate release. One of those ATP exchange factors are, in mammalian cells, proteins belonging to HSPH family (DRAGOVIC et al., 2006; VOS et al., 2008). HSPH proteins are known to prevent aggregation by binding protein substrates and holding unfolded proteins in a folding-competent state, so they can act as both substrate loaders (similarly to DNAJ family members) and nucleotide exchange factors in the HSPA chaperoning complex (DRAGOVIC et al., 2006; VOS et al., 2008). The results of titration revealed that HSPH proteins are the most effective for folding at ratios equimolar to HSPA (DRAGOVIC et al., 2006).

Four known HSPH proteins are highly homologous to HSPA family members. The linker domain is however longer, with insertions of varying lengths, as well as the C-terminus is less conserved in the HSPH family (DRAGOVIC et al., 2006; VOS et al., 2008). Among four HSPH family members, HSPH4 (also known as 170 kDa glucose-regulated protein, Grp170, 150 kDa oxygen-regulated protein, ORP150, and Hypoxia Upregulated 1, HYOU1) is a chaperone located

in the endoplasmic reticulum. The plethora of its names reflects the conditions in which the protein gets induced – which include hypoxia, nutrient (especially glucose) deprivation as well as reducing agents, low pH and calcium depletion (WANG et al., 2014). In the ER, it fills a role of a nucleotide exchange factor for HSPA5, where it enhances substrate release in an ATP-dependent manner (DRAGOVIC et al., 2006).

Mutations in nucleotide exchange factor genes may cause several disorders. The mutation in *SIL1* gene, coding a protein associated with HSPA5, inactivates its nucleotide exchange function and potentially causes Marinesco-Sjörger syndrome, an autosomal recessive neurodegenerative disease in humans as well as ataxia phenotype in woozy mice, associated with selective Purkinje cell degeneration (DRAGOVIC et al., 2006). This suggests that correct function of nucleotide exchange factors is crucial for cellular homeostasis and their levels may vary depending on the cell type. The role played by ER stress over status epilepticus induced cell death is still debated. Some authors report that ER stress causes neuronal death (SOKKA et al., 2007; CHEN et al., 2013), while others sustain its role in pro-survival mechanisms (KITAO et al., 2001).

III. SCOPE OF THE DISSERTATION

So far, several studies described expression of HSPA1 in chemically induced SE rodent models, connecting excessive neuronal activity with induction of the protein (VASS et al., 1989; LIVELY & BROWN, 2011; RICHTER-LANDSBERG, 2011). No such investigations exist at the moment for ER heat shock proteins, HSPA5 and HSPH4. The aim of this study is to describe the expression profile of selected HSPs in the model of electrically induced SE, which already demonstrated alterations in expression of several DAMPs in the course of epileptogenesis (WALKER et al., 2016; KECK et al., 2018). By means of comprehensive proteome analysis, five heat shock proteins were found to be upregulated in the brain undergoing epileptogenesis, with a pronounced upregulation of HSPA1 in the hippocampus and in the parahippocampal cortex in the early post-insult phase and in the latency phase. HSPA5 and HSPH4 exhibited a slight upregulation in the acute post-SE phase and in the latency phase. The goal of this study was to quantitatively measure and qualitatively assess expression of proteins interest in different cell populations in hippocampal, parahippocampal and accessory regions relevant for epileptogenesis.

IV. MATERIALS AND METHODS

1. Animals

1.1. Rat electrical status epilepticus model

For purposes of this project, brain tissue samples were collected from animals used in the proteomics study by Andreas Walker as a part of his dissertation at the Institute of Pharmacology, Toxicology and Pharmacy of the Faculty of Veterinary Medicine of Ludwig-Maximilians-University in Munich (WALKER et al., 2016). Therefore, the description of all *in vivo* procedures relates to that study. Briefly, female Sprague Dawley rats (n = 47) were housed under controlled standard environment conditions. Females proved to show a lower mortality rate than males in the characterisation of the model (BRANDT et al., 2003), this being the reason to use only specimens of this sex.

Experimental procedures were carried out in accordance with the German Animal Welfare Act, the European Communities Council Directive of 22 September 2010 (2010/63/EU), approved by the Committees of the Government of Upper Bavaria (reference number: AZ 55.2-1-54-2532-94-11, AZ 55.2-1-54-2532-011-2015) and in compliance with the ARRIVE (Animal Research: Reporting of *In Vivo* Experiments) guidelines. During the experiment, every attempt was made to minimise pain or discomfort as well as to lower the number of

animals used.

For the purposes of this study, animals were assigned either to a SE or to a control group. Sampling of brain tissue was later performed at three different time points during epileptogenesis (Fig. 2):

- two days post-SE (early post-insult phase),
- ten days post-SE (latency phase)
- eight weeks post-SE (chronic phase with SRSs).

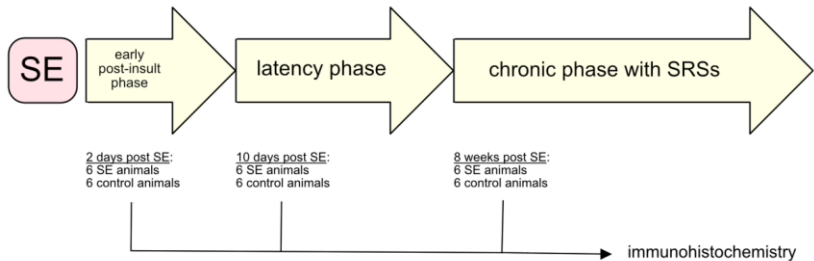


Figure 2. For the purpose of immunohistochemical staining, brain tissue samples were collected from electrically-stimulated rats as well as from control animals at three time points, corresponding to the early post-insult phase (2 days following SE), the latency phase (10 days following SE) and the chronic phase with spontaneous recurrent seizures (8 weeks following SE).

All of the animals underwent a stereotaxic surgery to implant an electrode into the right basolateral amygdala (BLA) performed under general anesthesia. The electrode served for both electrical stimulation and EEG recording. Following the electrode implantation, animals were left to recover for the period of six weeks. Afterwards,

self-sustained status epilepticus was evoked using the protocol established already at the institute (ONGERTH et al., 2014). A self-sustained SE was confirmed by EEG recording and it was interrupted by intraperitoneal administration of diazepam 4 hours after the start of the stimulation. Animals' behavioural seizure activity was scored for the entire duration of SE using the Racine scale (RACINE et al., 1972) in which five stages of seizure severity can be observed:

- stage 1: animal immobility and facial automatisms (eye closure, facial clonus),
- stage 2: head nodding and more severe facial and mouth clonus (mastication),
- stage 3: unilateral forelimb clonus,
- stage 4: rearing and bilateral forelimb clonus,
- stage 5: rearing and falling accompanied by generalised tonic–clonic seizures.

Furthermore, animals were grouped according to the types of status epilepticus described above (partial non-convulsive, partial non-convulsive with occasional generalisation or generalised convulsive SE). For subsequent experiments, only animals exhibiting generalised convulsive seizures were included, constituting 85% of the whole population (WALKER et al., 2016). Animals assigned to the group with sampling eight weeks after SE (corresponding to development of spontaneous recurrent seizures) underwent continuous video- and EEG-monitoring.

1.2. Canine clinical model

Canine brain tissue was collected from 48 dogs aged from two months to 15 years, which either had been undergoing treatment at the Small Animal Clinic of the University of Veterinary Medicine in Hanover, Germany, or had served previously as experimental animals in parasitology study at the Institute of Parasitology of the same university. Dogs were distributed into different groups, depending on whether seizure frequency or aetiology of the disease was taken into consideration:

1. Patient control group (CTR_{pat}) comprising owner kept dogs without clinically nor pathologically stated diseases of the central nervous system (n = 18, age range 2-180 months; mean 70.67 ± 12.58)
2. Experimental control group (CTR_{exp}) consisting of experimental dogs without neurological diseases, but infested with *Toxocara canis* and *Uncinaria stenocephala* or *Angiostrongylus vasorum* (n = 10, age range 4-12 months; mean 7.33 ± 3.94)
3. Epileptic animals:
 - a. Grouping according to the aetiology as defined by international veterinary task force (BERENDT et al., 2015):
 - i. Structural epilepsy caused by identified cerebral pathology (n = 12, age range 30-140 months; mean 81.17 ± 12.29)
 - ii. Idiopathic epilepsy group, subtype unknown cause and no identification of structural

epilepsy (n = 8, age range 2.5 - 157 months; mean 51.94 ± 18.82)

- b. Grouping according to the occurrence of seizures (BERENDT et al., 2015):
 - i. Seizure clusters, defined clinically as two or more incidents within a 24 h period (n = 9, age range 80 - 140 months; mean 68 ± 15.63)
 - ii. Status epilepticus, defined clinically as epileptic seizures of duration ≥ 5 min (n = 4, age range 36 - 120 months; mean 67.75 ± 20.15)

According to the information gathered in the anamnesis, all epileptic canine patients included in the study exhibited convulsive seizures, either focal or generalized. No report about atonic, myoclonic or absence type of seizures was present. The first seizure event before the last clinical presentation, followed by death or euthanasia, occurred within a time interval from one day up to eleven years. Onset of seizures before death and euthanasia varied between one hour and one week. The seizure frequency ranged from one episode a month to four seizures a day.

The neuropathological examination of dogs belonging to the group with structural epilepsy revealed four cases of meningoencephalitis, three of brain tumour (meningioma and glioblastoma), two of hydrocephalus, two of vacuolisation in the white matter, one of

encephalomalacia (possibly as a result of cerebral infarct) and one of toxoplasmosis. Animals from patient control group demonstrated cardiovascular pathological changes (eight animals), not neurologically related neoplasms (three patients) and other disorders: splenic and gastric torsion, pneumonia, foreign bodies in stomach.

All animal experiments using canines were conducted in accordance with the German Animal Welfare Law and were approved by the local authorities (Niedersächsisches Landesamt für Verbraucherschutz und Lebensmittelsicherheit (LAVES), Oldenburg, Germany, permission numbers: 33.9-42502-05-12A241, 33.19-42502-05-16A044). The owners of dogs included in this study signed an informed consent form.

2. Tissue processing

Rat brain samples were collected after the perfusion process. Animals' skulls were opened using surgical tools and brains were softly extracted with a spatula. Afterwards, they were placed in 4% paraformaldehyde solution (pH 7.4) for 24 hours at 4°C. Consecutively, samples were transferred to a 30% sucrose solution in 0,01 M phosphate buffered saline (PBS) for cryopreservation and left until tissue sank (24-72 hours, depending on the brain size). After reaching this stage, tissue was embedded in optimal cutting temperature compound and cut on a cryostat in 18 series, each consisting of ten to twelve 40 µm thick slices in coronal plane. For the analysis, only slices containing hippocampus, parahippocampal cortex and accessory regions (thalamus, amygdala, parietal cortex) were considered relevant, so only samples from bregma +1.56 to -9.00 (PAXINOS & WATSON, 2005) were saved. Slices were later embedded in a cryoprotective solution (30% glycerol, 30% ethylene glycol, 0,1M PBS) and stored at -80°C.

In canine patients, during *post-mortem* examinations, brains were inspected macroscopically, removed and fixed in 10% formalin for several days, then cut by in blocks by means of matrices, embedded in paraffin wax and cut transversally to 2 µm thick sections. Slices containing the hippocampus in a range from #1360 to #1660 of the canine brain atlas (WALLY WELKER, 2015) were mounted on positively charged microscope slides and stored at room temperature at the Department of Pathology of the University of Veterinary Medicine in Hanover, Germany.

Brain tissue from the archive of the Department of Pathology of the University of Veterinary Medicine in Hanover has been used in accordance to the ethical rules and in compliance with the recommendations of the University of Veterinary Medicine in Hanover, Germany.

3. Immunostaining

To perform both quantitative and qualitative analysis, proteins of interest (HSPA1, HSPA5, HSPH4) were stained by means of immunohistochemistry (IHC).

HSPA1 – single immunostaining

To perform HSPA1 quantification, rat brain samples were stained by means of 3,3'-diaminobenzidine colour reaction. Free-floating frozen sections were first washed thrice at room temperature in Tris-buffered saline (TBS) for 10 minutes each washing step. Then, to reverse chemical antigen modifications caused by formaldehyde fixation of the tissue, heat-induced epitope retrieval (HIER) process was performed at 80°C for 30 minutes using sodium citrate buffer (pH 6.0). Endogenous peroxidase activity was inhibited by incubating brain slices in 1% H₂O₂ in TBS during 30 minutes. Afterwards, a blocking step in 5% normal goat serum (NGS) diluted in TBS was performed to prevent any non-specific antibody binding. Consequently, overnight (16h) incubation of brain sections with anti-Hsp70/Hsp72 (anti-HSPA1) antibody was performed at 1:750 dilution at 4°C. All antibodies described in this publication used for staining of rat tissue were diluted in an antibody carrier (1% bovine serum albumin, 1% NGS, 0.3% Triton in TBS). Following the primary antibody incubation, the slices were washed three times in TBS and then incubated with biotinylated goat anti-mouse secondary antibody at dilution 1:1000 for 2 hours at room temperature. After three consecutive washes in TBS, incubation with horse radish peroxidase-coupled streptavidin was performed at 1:1400 dilution for one hour at room temperature,

followed by three more washing steps in TBS. Afterwards, a colour reaction was implemented, using 3,3'-diaminobenzidine tetra hydrochloride (DAB) converted by horse radish peroxidase into a brown product. DAB is water-soluble in its unoxidised form, it creates however precipitates after oxidisation, making localisation of proteins of interest visible. For this reaction, 0.05% DAB was used, with addition of 0.01% H₂O₂ and 0.01% nickel ammonium sulfate. Nickel is a known enhancer of DAB signal, yielding in intense, dark blue staining. Subsequently, stained sections were mounted on positively charged microscope glasses and cover-slipped with Entellan.

HSPA1 – multiple immunostaining

To determine the expression profile in main cell types involved in epileptogenesis and/or inflammation processes in the central nervous system, several double immunolabelling procedures of HSPA1 and cell markers were performed. Chosen biomarkers included: NeuN (Fox-3, Rbfox3, or Hexaribonucleotide Binding Protein-3), neuronal nuclear antigen commonly used to label neurons; GFAP (glial fibrillary acidic protein), to mark astrocytes and Iba1 (ionized calcium-binding adapter molecule 1), also known as AIF-1 (allograft inflammatory factor 1), expressed in macrophages and microglia.

For HSPA1 double immunostaining with markers for various cell populations of the brain, three different protocols were used. For the immunofluorescent labelling with NeuN, free-floating sections were firstly washed three times in TBS with 0.05% Tween (TBST) and underwent heat-induced epitope retrieval as described above. Later, slices were incubated with blocking solution (5% NGS and 2% bovine

serum albumin in TBS) at room temperature. Both primary antibodies were acquired from the same host (mouse), therefore they were applied to the sections sequentially to exclude the possibility of cross-binding of secondary antibodies, reactive against the same host. Briefly, samples were incubated with anti-Hsp70/Hsp72 antibody (clone description above) at 1:1500 dilution overnight (16 h) in a cold room (4°C). The following day, after three further washes in TBST, goat anti-mouse biotinylated secondary antibody was applied at 1:1000 dilution for 1 h at room temperature. Afterwards, sections were washed thrice in TBST and incubated with streptavidin coupled with a Cyanine Dye 3 (Cy3), to amplify the signal. Concentrations were selected to fulfil as many binding sites on the primary antibody as possible and lower the risk of cross-binding of the second secondary antibody. After finishing the construct for the first marker, slices were again washed in TBST and incubated overnight in a cold room (16 h, 4°C) with anti-NeuN antibody at dilution of 1:500. The next day, after further washing in TBST, slices were incubated with goat anti-mouse secondary antibody coupled with an Alexa Fluor 488 dye at 1:750 dilution for 1 h. Afterwards, sections were rinsed thrice in PBS and counterstaining of cell nuclei with Hoechst 33342 dye at 0.5 µg/mL concentration was performed for 5 minutes. Finally, stained slices were mounted on microscope glass and cover-slipped with immunofluorescence anti-fading medium.

For double immunolabelling of HSPA1 with GFAP, sections were processed with HIER and incubated in a blocking solution as described above. Since both primary antibodies were obtained from different host species (anti-HSPA1 – mouse, anti-GFAP – rabbit),

parallel staining method was chosen, meaning free floating slices were incubated with both antibodies at the same time (overnight – 16 h, at 4°C, anti-HSPA1 dilution: 1:1500; anti-GFAP dilution: 1:3000). The following day, three washes in TBST were performed. Afterwards, slices were incubated with goat anti-mouse secondary antibody coupled with a Cyanine Dye 2 (Cy2; 1:1000 dilution) and goat anti-rabbit secondary antibody linked to an Alexa Fluor 594 dye (1:1000 dilution) for 1 h at room temperature. Sections were then washed thrice in PBS, counterstained with Hoechst 33342 (0.5 µg/mL), mounted on a microscope glass and cover-slipped using immunofluorescence anti-fading mounting medium, analogically to the HSPA1/NeuN staining.

To show interactions between HSPA1 and TLR4 as well as with microglia, triple immunostaining was performed. For that purpose, free floating slices were processed with HIER as described above. Possible unspecific binding target sites were blocked using blocking solution containing 2% of bovine serum albumin and additional 0.1% cold fish skin gelatine to improve penetration of antibodies into the tissue (ZUKOR et al., 2010). Two out of three antibodies used were acquired from the same host species (anti-HSPA1 – mouse, anti-TLR4 – mouse), therefore they were applied to the sections in a sequential manner. Firstly, samples were incubated with anti-HSPA1 antibody at 1:1500 dilution overnight in a cold room (16 h, 4°C). Afterwards, following three washing steps in PBS with 0.05% Tween (PBST), a biotinylated goat anti-mouse secondary antibody was added at dilution of 1:1000 and one-hour long incubation at room temperature was executed. Sections were again rinsed in PBST and

incubated with streptavidin coupled with a Cy3 dye at 1:1500 dilution for 1 h at room temperature. After three consecutive washes in PBS, sections were incubated with anti-TLR4 antibody at 1:250 dilution and anti-Iba1 antibody at 1:10000 dilution overnight in a cold room (16 h, 4°C). Since both of the primary antibodies were obtained from different species (anti-Iba1 – rabbit), it was possible to add them in parallel without risking cross-binding. The day after, slices were washed in PBST three times and incubated with secondary antibodies: goat-anti mouse coupled with an Alexa Fluor 488 dye (1:500) and goat anti-rabbit linked to an Alexa Fluor 647 fluorochrome (1:500). Incubation took 1 h at room temperature and was followed by additional washing steps in PBS, counterstaining with Hoechst 33342 (0.5 µg/mL), mounting on microscope glasses and cover-slipping with immunofluorescence anti-fading mounting medium.

HSPA5 and HSPH4 – single staining in rats

For immunohistochemical labelling of HSPA5 and HSPH4 in rats, frozen free floating sections were processed with HIER as described above. Activity of endogenous peroxidase was inhibited by 20 min incubation in 3% H₂O₂ diluted in TBS. Afterwards, possible non-specific binding sites were blocked by a blocking solution (5% NGS, 2% bovine serum albumin) applied for 60 min. Sections were then incubated with either an anti-ORP150/HSP12A (anti-HSPH4; 1:750 dilution) or an anti-GRP78 BiP antibody (anti-HSPA5; 1:5000) overnight (16h) at 4°C. The day after, three washing steps in TBST were performed, following incubation with a biotinylated goat anti-rabbit secondary antibody (dilution: 1:1000 for anti-HSPH4; 1:1500 for

anti-HSPA5) during 1h at room temperature. Slices were then rinsed thrice in TBST and incubated for 60 min at room temperature using VECTASTAIN ABC-Peroxidase Kit (1:100). ABC is an abbreviation for avidin-biotin complex, implementation of which is one of methods of amplification of the target antigen signal in immunohistochemistry (Fig. 3).

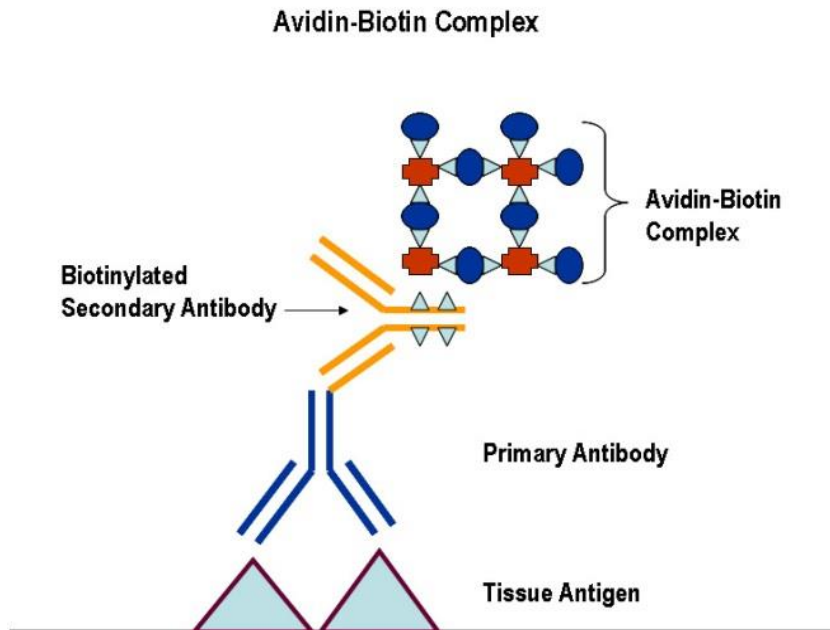


Figure 3. Illustration of avidin-biotin complex formation. Biotin-containing enzyme molecules rapidly and firmly bind to avidin, forming a complex net-like structure connected to the secondary antibody. The enzyme is later on involved in colour reaction with DAB. Modified from Dako Educational IHC Guidebook (CLIVE R. TAYLOR, 2006).

By allowing binding of biotin-containing enzyme molecules to avidin, a tetrameric glycoprotein, a complex net-like structure is formed, where avidin molecules are linked together by the biotinylated enzyme (in this case, peroxidase). A colour reaction was performed using 3,3'-diaminobenzidine tablets according to the instructions found in the datasheet. Slices stained for HSPH4 were additionally counterstained with a Hemalum solution acidic according to Mayer to ensure a better cell and brain region recognition under the microscope. Afterwards, sections were mounted on microscope glasses and cover-slipped using Entellan, as described in the case of HSPA1.

HSPA5 and HSPH4 – multiple staining

Analogically to HSPA1, to describe the expression profile of HSPA5 and HSPH4, double immunofluorescent labelling for neurons, astrocytes and microglia was performed. Six animals, three from control and three from SE groups, were randomly selected from the entire pool of animals for each time point (<http://randomizer.org>). Sections were initially rinsed thrice in PBST, followed by HIER as described above. Afterwards, a 1 h blocking step was performed at room temperature using PBS added with 2% BSA and 0.01% cold water fish skin gelatine in order to prevent unspecific bindings. Primary antibodies for the proteins of interest (anti-HSPA5, dilution 1:2500; anti-HSPH4, dilution 1:150) were incubated overnight in a cold room (4°C, 16 h) in combination with either antibodies aimed against NeuN (1:500), GFAP (1:1000) or Iba1 (1:1000). Following three PBST washes, sections were incubated with secondary antibodies. Alexa Fluor 594-conjugated goat anti-rabbit antibody (1:1000, 1 h, 24°C)

was used to label HSPA5, while biotinylated goat anti-rabbit (1:1000, 1 h, 24°C) together with Cy3-conjugated streptavidin (1:2000, 1 h, 24°C) was used to target HSPH4. Alexa Fluor 488-conjugated goat anti-mouse antibody was used to label both NeuN and GFAP (1:1000, 1 h, 24°C) while for Iba1 labelling Cy2-conjugated donkey anti-goat antibody (1:1000, 1.5 h, 24°C) was chosen. Since in all of the cases primary antibodies were gained from different host species, they could be incubated in parallel without risking cross-linking of secondary antibodies. Finally, after three following washing steps in PBS, slices were counterstained using Hoechst 33342 (0.5 mg/mL), mounted on microscope glasses and cover-slipped with Immunoselect Antifading Mounting Medium.

HSPA5 and HSPH4 – single staining in dogs

In canine tissue, HSPA5 and HSPH4 stainings were performed in paraffin-embedded whole-mount sections, therefore all incubation processes took place in humidity chambers. Slices were initially deparaffinised and rehydrated by means of ethanol and xylene gradients. Afterwards, sections were processed with HIER as described for rat tissue. Then, activity of endogenous peroxidase was inhibited with 3% H₂O₂ and non-specific binding sites were blocked using solution containing 0.25% casein in TBS. Subsequent incubation with primary antibodies (anti-HSPA5, dilution 1:50; anti-HSPH4, dilution 1:50), suspended in antibody carrier (0.25% casein in TBST) was performed overnight in a cold room (16h, 4°C). The day after, following the initial triple wash performed in glass cuvettes, incubation with a biotinylated goat anti-rabbit secondary antibody

(dilution 1:500) was performed for 1 h at room temperature. Afterwards, sections were rinsed thrice in TBST and incubated in VECTASTAIN ABC-Peroxidase Kit (dilution 1:100) for 1 h at room temperature. A colour reaction was developed using 3,3'-diaminobenzidine tablets dissolved according to manufacturer's instructions and counterstaining with Hemalum solution acidic according to Mayer was performed. Slices were then held for 15 minutes under running tap water to remove undesirable over-colouration and non-specific background staining caused by Hemalum solution. Finally, microscope glasses with brain sections were air dried in a fume hood overnight and cover-slipped the following day with Entellan.

In both, rat and canine samples, negative controls were processed in the same manner as experimental sections, with omission of primary antibody incubation.

4. Image analysis

4.1. Stereological cell counting

To determine an approximate number of positive cells in rat brains, stereological cell counting using the optical fractionator method was implemented. The method uses thick (in this case, 40 μm) sections to estimate a total population of cells in an organ through cell numbers collected by systematic random sampling (SRS). To achieve that, an unbiased grid of virtual counting spaces is created by a software. The spaces are distanced regularly in X, Y and Z directions and cover the whole region of interest. The software is able of estimation of the total number of objects based on the number of objects marked by an operator. It is also able to calculate the volume of the region of interest, using the Cavalieri principle (GUNDERSEN, 1986; GUNDERSEN & JENSEN, 1987; WEST et al., 1991; GARCIA-FINANA et al., 2003).

In this study, stereological cell counting was performed in rat brain sections distanced from each other by 720 μm . Three proteins of interest (HSPA1, HSPA5 and HSPH4) were analysed in following brain regions:

- Hippocampus:
 - Hilus of dentate gyrus (corresponding to the layer of polymorphic cells of dentate gyrus), bregma from -2.16 to -6.36 mm, *Hil*
 - Cornu Ammonis region 1 (pyramidal cell layer), bregma from -2.28 to -6.60 mm, *CA1*

- Cornu Ammonis region 3 (pyramidal cell layer), bregma from -1.72 to -6.12 mm, CA3
- Parahippocampal cortex:
 - Perirhinal cortex, bregma from -3.00 to -9.00 mm, *PRh*
 - Entorhinal cortex, lateral and medial, bregma from -3.12 to -9.00 mm, *Ent*
 - Piriform cortex, bregma from 1.56 to -4.92 mm, divided into:
 - Piriform cortex layer I, *Pir1*
 - Piriform cortex layer II, *Pir2*
 - Piriform cortex layer III, *Pir3*,

considering their different susceptibility to electrical stimulation (VAUGHAN & JACKSON, 2014; VISMER et al., 2015).

Additionally, in HSPA1 staining, several associated brain regions were analysed:

- Thalamus (encompassing all thalamic subregions), bregma from -3.12 to -7.08 mm, *Thal*
- Parietal association cortex (posterolateral and –medial parts), bregma from -3.00 to -6.12 mm, *Par*
- Amygdala, bregma from -1.58 to -4.44 mm, *Amy*

From each group (status epilepticus and control animals; 2 days, 10 days and 8 weeks after electrical stimulation), six randomly selected animals were fully analysed. Cell counting was performed in a blinded manner, with all the samples randomised (<http://randomizer.org>). The exact number of quantified sections varied in the range between 13

and 27 slices.

For stereological cell counting, an optical bright-field microscope equipped with a motorised stage and a colour CCD camera was used. Quantification was performed by means of Stereo Investigator software using the optical fractionator to assess the cell population and the Cavalieri's principle to calculate volumes of given brain regions. The region area was restricted at low magnification (5x/0.12 NA; Fig. 4), while cells were marked at high magnification (40x/0.65 NA).

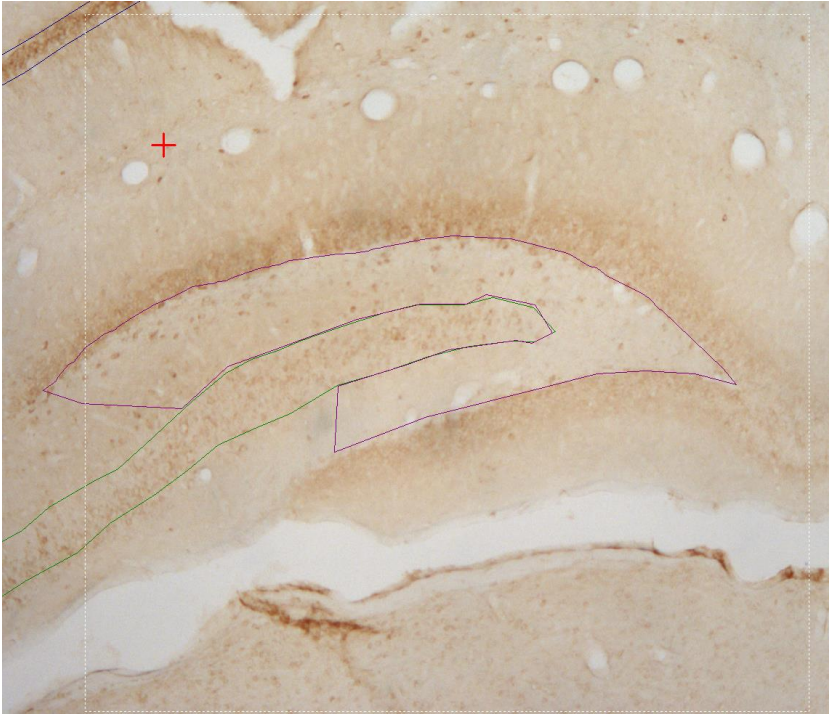


Figure 4. An exemplary image of region outlines performed at low (5x) magnification in Stereo Investigator software. Different colours of the contours indicate different regions of interest: purple - hilus of the dentate gyrus, green - Cornu Ammonis 3, blue - Cornu Ammonis 1.

The size of the SRS grid as well as of counting frames were set experimentally, for each region separately, before the actual analysis. Cells were marked for counting according to instructions in software manual (BIOSCIENCE, 2019a). Briefly, all cells being in focus and lying within the optical fractionator counting frame or lying outside and being in contact with its green lines, but not crossing red lines, were counted (Fig. 5)

Estimated positive cells population and measured volume were afterwards used to calculate cell density in respective brain regions:

$$\text{Cell density} = \frac{(\text{HSPA1 or HSPA5 or HSPH4}) \text{ positive cells}}{\text{Calculated volume}}$$

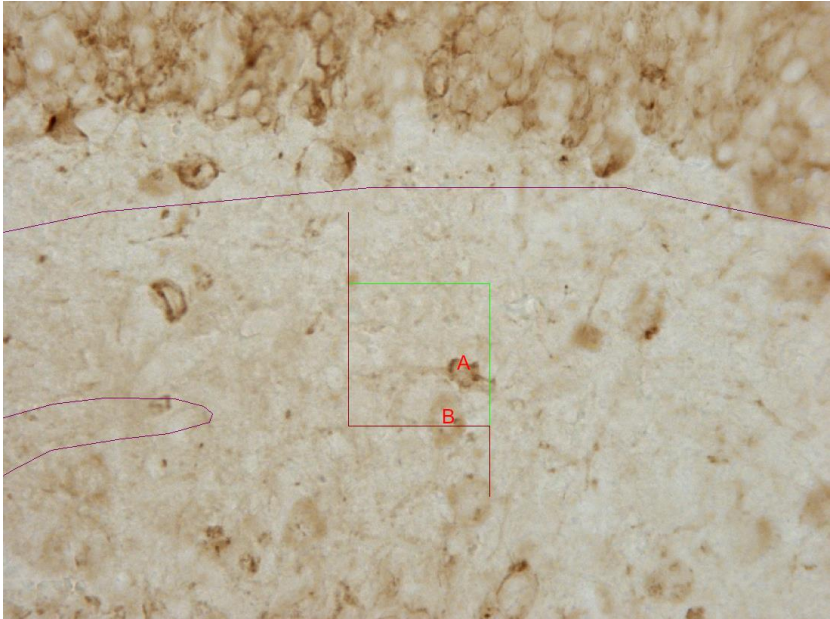


Figure 5. An exemplary image of the counting frame used by the optical fractionator. Positively stained cells were quantified at high (40x) magnification. Cells lying within the region of interest (indicated by the purple contour) were counted, when they appeared in the counting frame and/or when they came into contact with the green line while lying outside the frame, unless they were crossed by the red line. In this case, cell A would be calculated, whereas the cell B would not, even if it were in focus.

Quality of stereological quantitative analysis can be assessed by estimating a coefficient of error (CE). The value of CE is calculated by dividing the standard error of the mean of repeated measurements by the mean (BIOSCIENCE, 2019b). CE is returned by the software in two so called smoothing classes: for $m = 0$ and $m = 1$. It is generally accepted to employ CE for $m = 1$ in biological samples, since it assumes that the shape of analysed region does not contain any abrupt changes (GUNDERSEN & JENSEN, 1987; GUNDERSEN et al., 1999). Moreover, to further evaluate the study design, the coefficient of variation (CV) was calculated as the standard deviation divided by the mean. In this case, both intra-animal variability (CE) and inter-animal differences (CV) were assessed.

For evaluation of the study design, they were expressed as $[CE^2/CV^2]$ and values ≤ 0.5 were considered acceptable (GUNDERSEN, 1986; RAJKOWSKA et al., 2016). Tables 2-4 enclose the information regarding the quality of the quantification for HSPA1 (Table 2), HSPA5 (Table 3) and HSPH4 (Table 4).

	Hil	CA3	CA1	Ent	PRh	
Mean HSPA1 cells	4084.7	13172.6	8862.1	22089.6	17156.8	
SD	4330.3	24653.4	17356.8	32542.1	31456.6	
Mean CE (m=0)	0.456	0.400	0.398	0.398	0.447	
Mean CV	1.060	1.872	1.959	1.473	1.833	
CE²/CV²	0.185	0.046	0.041	0.073	0.059	
Frame size (μm²)	2025	2025	2025	2025	4225	
Grid size (μm²)	14400	19600	19600	32400	62500	
Average Sections	5.1	5.1	5.1	5.1	5.0	
	Pir1	Pir2	Pir3	Amy	Thal	Pt
Mean HSPA1 cells	1655.8	29835.1	9952.2	12622.4	61999.3	24200.2
SD	2195.0	53478.9	17138.3	25594.0	119297.1	45894.0
Mean CE (m=0)	0.544	0.482	0.414	0.582	0.433	0.509
Mean CV	1.326	1.792	1.722	2.028	1.924	1.896
CE²/CV²	0.169	0.072	0.058	0.082	0.051	0.072
Frame size (μm²)	4900	625	4225	3600	3600	1607
Grid size (μm²)	40000	25600	40000	78400	202500	77297
Average Sections	6.5	6.5	6.3	3.1	5.0	4.1

Table 2. Estimates of HSPA1 sampling parameters. Precision parameters for HSPA1 cell count for each region of interest: HSPA1 cells estimated count (mean value), standard deviation (SD), Gundersen coefficient of error second derivative (CE), mean inter-animal coefficient of variation (CV = SD/mean), CE²/CV² ratio, optical fractionator frame and grid size, average number of sections analysed.

	Hil	CA3	CA1	Ent
Mean HSPA5 cells	27832.2	95283.4	114747.5	185469.5
SD	16649.2	61177.5	76727.0	183515.4
Mean CE (m=0)	0.158	0.125	0.110	0.131
Mean CV	0.455	0.591	0.617	0.908
CE²/CV²	0.120	0.045	0.032	0.021
Frame size (μm²)	2500	2500	2500	3600
Grid size (μm²)	29929	58564	65025	116480
Average Sections	11.8	11.3	11.5	11.6
	PRh	Pir1	Pir2	Pir3
Mean HSPA5 cells	83558.9	9985.5	66784.2	67119.3
SD	56794.9	7820.5	31398.2	41184.9
Mean CE (m=0)	0.112	0.255	0.115	0.134
Mean CV	0.635	0.711	0.444	0.565
CE²/CV²	0.031	0.129	0.067	0.056
Frame size (μm²)	3600	1600	1600	3600
Grid size (μm²)	80080	22500	31684	81796
Average Sections	11.9	12.2	12.2	12.2

Table 3. Estimates of HSPA5 sampling parameters. Precision parameters for HSPA5 cell count for each region of interest: HSPA5 cells estimated count (mean value), standard deviation (SD), Gundersen coefficient of error second derivative (CE), mean inter-animal coefficient of variation (CV = SD/mean), CE²/CV² ratio, optical fractionator frame and grid size, average number of sections analysed.

	Hil	CA3	CA1	Ent
Mean HSPH4 cells	29441.9	78226.0	41995.9	154500.2
SD	15321.5	54355.3	29222.2	95614.2
Mean CE (m=0)	0.146	0.120	0.149	0.136
Mean CV	0.854	0.984	0.923	0.949
CE²/CV²	0.029	0.015	0.026	0.020
Frame size (µm²)	2500	2500	2500	3600
Grid size (µm²)	29929	58564	65025	173056
Average Sections	10.9	11.1	11.6	11.1
	PRh	Pir1	Pir2	Pir3
Mean HSPH4 cells	46780.4	4271.7	68101.2	73472.0
SD	35725.7	2306.1	33772.7	36953.8
Mean CE (m=0)	0.148	0.289	0.104	0.106
Mean CV	1.018	0.942	0.945	0.933
CE²/CV²	0.021	0.094	0.012	0.013
Frame size (µm²)	3600	1600	1600	3600
Grid size (µm²)	78400	22500	31684	81796
Average Sections	11.2	11.8	11.7	11.7

Table 4. Estimates of HSPH4 sampling parameters. Precision parameters for HSPH4 cell count for each region of interest: HSPH4 cells estimated count (mean value), standard deviation (SD), Gundersen coefficient of error second derivative (CE), mean inter-animal coefficient of variation (CV = SD/mean), CE²/CV² ratio, optical fractionator frame and grid size, average number of sections analysed.

4.2. Colocalisation analysis

4.2.1. HSPA1

Immunofluorescent micrographs were acquired by means of confocal laser scanning microscopy with a confocal laser scanning microscope equipped with argon (458, 488, 514 nm), DPSS 561-10 (405 nm) and a HeNe633 (633 nm) lasers. Some samples were scanned using Airyscan principle, a method combining 32 optical detectors (each representing 0.2 Airy unit) with a further deconvolution step to produce a superresolution image (KOROBCEVSKAYA et al., 2017). Images were captured at resolution of 1024 x 1024 pixels with pixel dwell 2.02 px/ μ s and double averaging of a single focal plane. The confocal images were obtained using a Plan-Apochromat 20x/0.8 NA and Plan-Apochromat 63x/1.4 NA objective. For image processing, Zeiss built-in software (ZEN software) was utilised. All samples have been inspected in all regions of hippocampus (CA1, CA3, Hil) as well as the parahippocampal cortices (PRh, Pir), both ipsilaterally and contralaterally (respectively to the electrode location), to evaluate colocalisation of heat shock proteins with labelling for cell markers. In all of above regions, at least one single-plane picture was acquired. In some regions z-stack imaging was performed.

Two quantitative approaches were used to evaluate signal colocalisation. In HSPA1/GFAP and HSPA1/NeuN staining the shape of colour intensity scatterplot was inspected. ZEN software returns such plots in its "Colocal" function, allowing to estimate the amount of colocalising pixels. In case of colocalisation, one can observe a more or less scattered cloud in the third quadrant of the plot (Fig. 6), while

lack of colocalisation leaves two clouds of points aligned along x- and y-axis (quadrant 1 and 2). This method is known and widely utilised in flow cytometry and has also its use in image analysis (DUNN et al., 2011). To exclude the background signal, three different regions visually assessed as background were used to estimate thresholds for both compared channels using ZEN software's hairline bisector method. Additionally to a scatterplot, the software also highlights colocalising pixels in the image. This can be exported as an 8-bit mask and merged with the original image to indicate the exact location of given pixels.

Analysis of HSPA1, TLR4 and Iba1 was performed at high magnification (63x) by means of a Coloc2 plugin for ImageJ. This software expansion, in addition to plots described above, returns several values describing colocalisation in wide extent. The ones used in this analysis were Pearson correlation coefficient (PCC), used broadly as a measure of a strength of association between two variables, and intensity correlation quotient, described for fluorescence colocalisation specifically (LI et al., 2004; DUNN et al., 2011). PCC values range between -1 and +1, where PCC = +1 means a perfect linear relation between fluorescence intensities, PCC = -1 – inverse relation and PCC = 0 – lack of correlation. ICQ derives from PCC and measures the extent in which intensities vary around their respective mean (LI et al., 2004). The value range varies between -0.5 and +0.5, where $-0.5 \geq ICQ > 0$ define a segregated staining, $ICQ \approx 0$ defines a random (or mixed) staining, and $0 < ICQ \leq +0.5$ defines a dependent staining. At least three regions of interest encompassing TLR4-positive cells were traced in each picture, returning values for

PCC and ICQ. The mean for each region in each animal was calculated. A cut off value of 0.5 for PCC and of 0.25 for ICQ for colocalisation purposes.

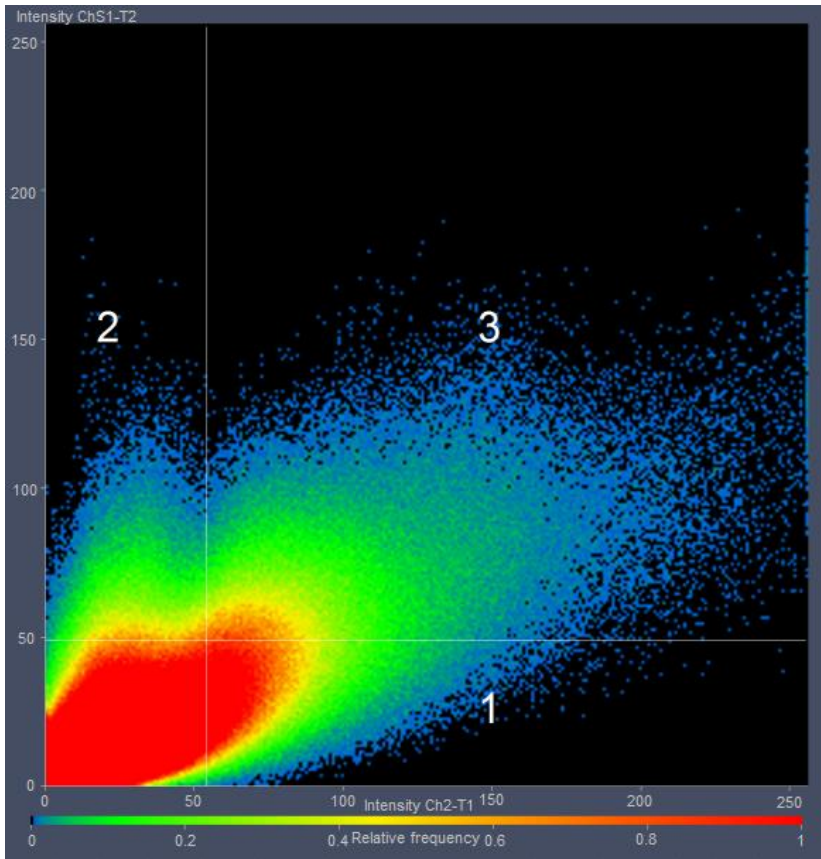


Figure 6. Colocalisation estimation, using the scatterplot method. In the diagram, each dot represents a value of red and green intensities for each pixel (X-axis: red signal, Y-axis: green signal). If a pixel demonstrates a colocalising signal of both colours, it is located in the quadrant 3 of the scatter plot. Continued on page 85.

Figure 6. Continued. Pixels showing purely red signal belong to the quadrant 1, while green ones – to the quadrant 2. Quadrant 4 gathers the information about the pixels from the background.

4.2.2. HSPA5 and HSPH4

Confocal laser scanning microscopy was performed, employing the same hardware as described above. Images were captured at resolution of 1024 X 1024 pixels with pixel dwell 2.02 px/ μ s and in order to improve the signal-to-noise ratio, two scans of one focal plane were averaged. Images were obtained using Plan-Apochromat 20x/0.8 NA and Plan-Apochromat 63x/1.4 NA objectives, then further processed with ZEN software.

All animals were visually inspected in hilus, CA1, CA3, perirhinal and piriform cortices to assess and locate the presence of HSPH4 and HSPA5 labelled cells. Where signal was located, 5 to 7 single confocal plane representative images were acquired at low magnification both in ipsilateral and contralateral hemispheres. In case the probes signal was not clearly identifiable, both higher magnification and z-stack micrographs were captured in order to increase image resolution.

To analyse colocalisation of HSPA5 and GFAP in detail, low magnification (20x) pictures were processed by ZEN software (Blue edition) and investigated by means of the abovementioned “Colocal” function of the program. Briefly, contours of two selected cells in the field of view were traced and later on, their PCC was estimated. To set a threshold to differentiate a signal from the background noise, a built-in “Costes” function. This allows the software to set a threshold according to a statistical significance test developed by Costes – it evaluates the probability that the calculated value of PCC between the

two channels of interest is significantly greater than values of PCC measured in randomly overlapping pixels (COSTES et al., 2004). This approach removes the bias of visual interpretation and allows automatization of the thresholding process.

PCC measured based on cells' signal was afterwards expressed as a mean value for each group of animals. A cut-off threshold of PCC = 0.5 was set to distinguish the colocalising signal from randomly overlapping pixels.

4.3. Optical density

Since canine tissue samples were taken from animals *post mortem*, a highly standardised tissue sampling procedure as the one carried out in rats was not possible. For this reason, a stereological cell count could not be performed and instead levels of HSPA5 and HSPH4 were quantified by means of optical density (OD) and area of the staining for these two proteins.

Images were captured at 20x magnification using a brightfield microscope equipped with a single chip charge-coupled device (CCD) colour and an AMD Athlon 64 processor based computer with image capturing software. Images were analysed by ImageJ software as described by SCHNEIDER et al. (2012).

Regions of interest included hippocampal dentate gyrus (DG), hilus, CA1, CA3 and parahippocampal cortex (PHC). Due to lack of standardised sources regarding detailed anatomy of canine brain, PHC has not been divided into subregions, unlike in rats. In each region, five representative pictures were acquired at 40x magnification, resulting in up to 25 visual fields (297.22 x 222.70 μm)

obtained from each animal.

For optical density analysis, at first we performed calibration in accordance with instructions on the software website (IMAGEJ). Images were then analysed as follows: initially pictures were cropped to contain only the region of interest and exclude artefacts. Afterwards, images were processed with the colour deconvolution plugin (vector Hematoxylin-DAB) described by RUIFROK and JOHNSTON (2001) that generates three 8-bit images (brown, blue and green), of which only the brown one, corresponding to DAB, was further processed. Histogram-based automatic triangle threshold (ZACK et al., 1977) was applied to images in order to select specific signal over the background. Thresholded area and mean OD values from all pictures analysed were averaged for each region and further used for statistical analysis.

5. Statistics

Statistical analysis was performed with GraphPad Prism 5.04. Estimated cell counts from each time point in all regions, as well as the volumes calculated by the Stereo Investigator software were compared between the ipsilateral and contralateral site using a one-way analysis of variance (ANOVA) followed by Bonferroni *post hoc* test. Cell density in HSPA1, HSPA5 and HSPH4 immunostaining was compared between SE and control animals in all regions within each time point by using the unpaired Student's t-test. Data are presented as a mean \pm SEM and a p value < 0.05 is considered statistically significant.

Optical density and positive area in HSPA5 and HSPH4 in dogs was conducted using a one-way ANOVA with a Bonferroni *post hoc* test to indicate differences between particular groups.

In the 2d post-SE time point, HSPA1-NeuN colocalisation area was analysed using a one-way ANOVA in order to compare the difference of colocalisation levels in relevant hippocampal (hilus, CA3, CA1) and parahippocampal (perirhinal cortex, piriform cortex) regions.

V. RESULTS

1. HSPA1 expression in the rat model of epileptogenesis

The analysis of immunohistochemically stained brain tissue provided comprehensive information about HSPA1 expression pattern in regions relevant for epileptogenesis. On a cellular level, HSPA1 signal was predominantly distributed in the soma, with some cells expressing the protein also in axons and dendrites. Control animals showed sparse HSPA1-positive cells in all investigated brain areas at every time point. Similar pattern has been observed in samples from status epilepticus animals in the latency phase and in the chronic phase with SRSs. In the early post-SE phase the staining was much more intense, with higher number of positive cells (assessed visually), but also with intensified specific diffuse signal in hilus and in CA3 as well as, to less extent, in CA1 subregions of the hippocampus (Fig. 7F). Stained cells were located mainly in the pyramidal layer of CA1 and CA3 and morphologically resembled neurons. Diffuse expression localised in regions neighbouring to the pyramidal layer, namely stratum lacunosum-moleculare, stratum radiatum, stratum lucidum and the stratum oriens.

1.1. HSPA1 expression levels in the course of epileptogenesis

Ipsilateral and contralateral cell counts revealed no difference between the both sides for all evaluated groups, therefore the total cell number from them was summed up, so for further analyses a single value represented each region in each animal. The electrical insult elicited the strongest effect on the expression of HSPA1 in the early post-SE phase, a milder and more localised effect in the latency phase and no significant effect in the chronic phase of the epileptogenesis. Older animals tended to exhibit a higher overall HSPA1 expression.

Figure 7. Quantification of HSPA1 cellular expression in hippocampus, thalamus and amygdala. Cell density of HSPA1 stereological cell count in (A) hilus, (B) CA3, (C) CA1, (D) thalamus and (E) amygdala. Each data point represents cell density of the counts from ipsilateral and contralateral sides summed together. Low magnification representative images of the hippocampus and the parahippocampal cortex from the early post-insult phase are presented in (F). HSPA1 signal in SE animals is intense compared to controls. Cell soma as well as processes are visible. A diffuse pattern is also present in the hilus and CA3 and to lesser extent in CA1. All data are presented as mean (dashed line) \pm SEM, * $p < 0.05$, paired Student's t-test for each time point. CTR: electrode implanted controls, SE: electrically stimulated animals, 2d: two days post-SE, 10d: 10 days post-SE, 8w: 8 weeks post-SE.

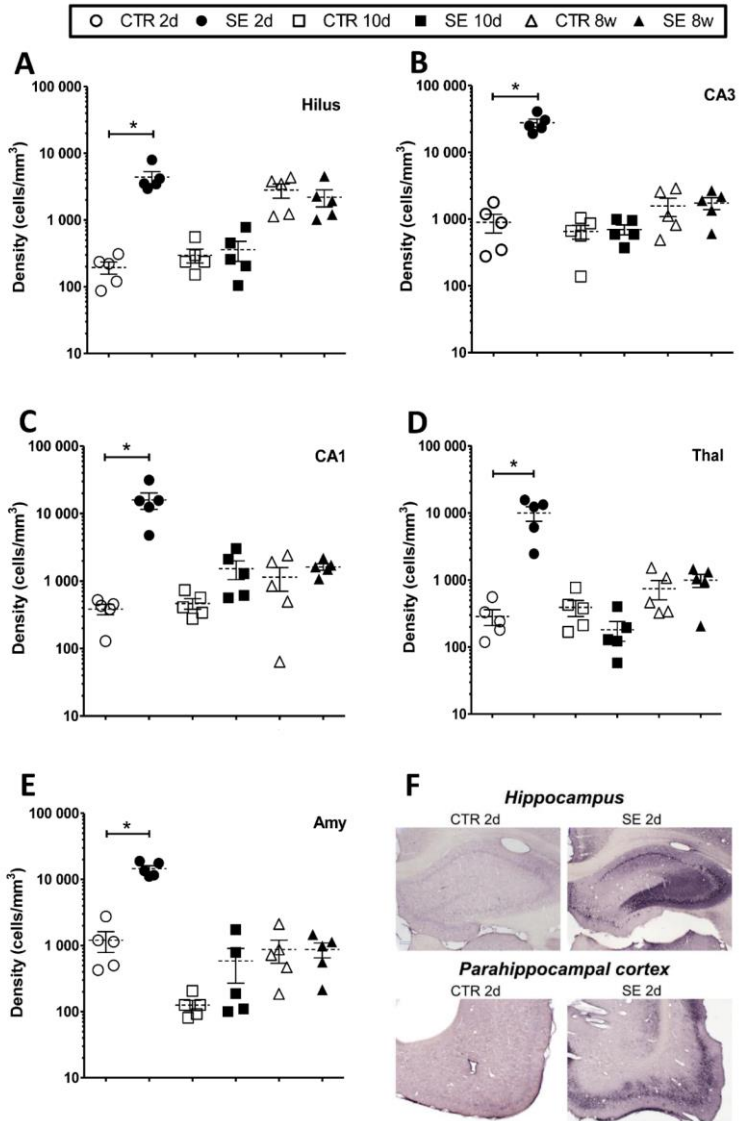


Figure 7. Description on page 90.

The most prominent effect was observed in the hippocampus, showing significant upregulation of HSPA1 expression in the acute phase in all regions. Stimulated animals showed a 23-fold increase ($p = 0.0017$; Fig. 7A) in HSPA1 positive cells in the hilus, a 30-fold increase ($p < 0.0001$; Fig. 7B) in CA3 and a 41-fold increase ($p = 0.0070$; Fig. 7C) in CA1. In the parahippocampal cortex, HSPA1 overexpression was evident two days following SE, but with a milder effect in comparison to the one observed in the hippocampus. The strongest effect has been observed in the perirhinal cortex and in the third layer of the piriform cortex, which lasted also in the latency phase. In PRh a 17-fold increase ($p < 0.0001$; Fig. 8A) in HSPA1 positive cells was found between animals in the early post-SE phase compared to respective controls. A 5-fold increase ($p = 0.0083$) in cell density was found ten days following SE. A similar pattern was also found in the Pir3, where HSPA1-positive cell density presented a 18-fold increase ($p < 0.0001$; Fig. 8D) 2 days after SE and a 4-fold increase ($p = 0.0270$) 10 days after SE. A moderate effect was visible in other layers of the piriform cortex with a 12-fold increase ($p < 0.0001$; Fig. 8C) in the second layer and a 3-fold increase ($p = 0.0037$; Fig. 8B) in the first layer in the early post-insult phase. At the same time point, the analysis revealed a 10-fold increase in the entorhinal cortex ($p < 0.0001$; Fig. 8D). In the parietal association cortex, a strong effect was visible only in the early post-insult phase with a 48-fold increase of the HSPA1 cell density ($p < 0.0001$; Fig. 8F). A distinctive effect was visible also in other associated brain areas: in the thalamus a 35-fold increase ($p = 0.0042$; Fig. 7D) was observed, while the effect was milder in the amygdala with a 12-fold increase ($p < 0.0001$; Fig. 7E) in

HSPA1 positive cells.

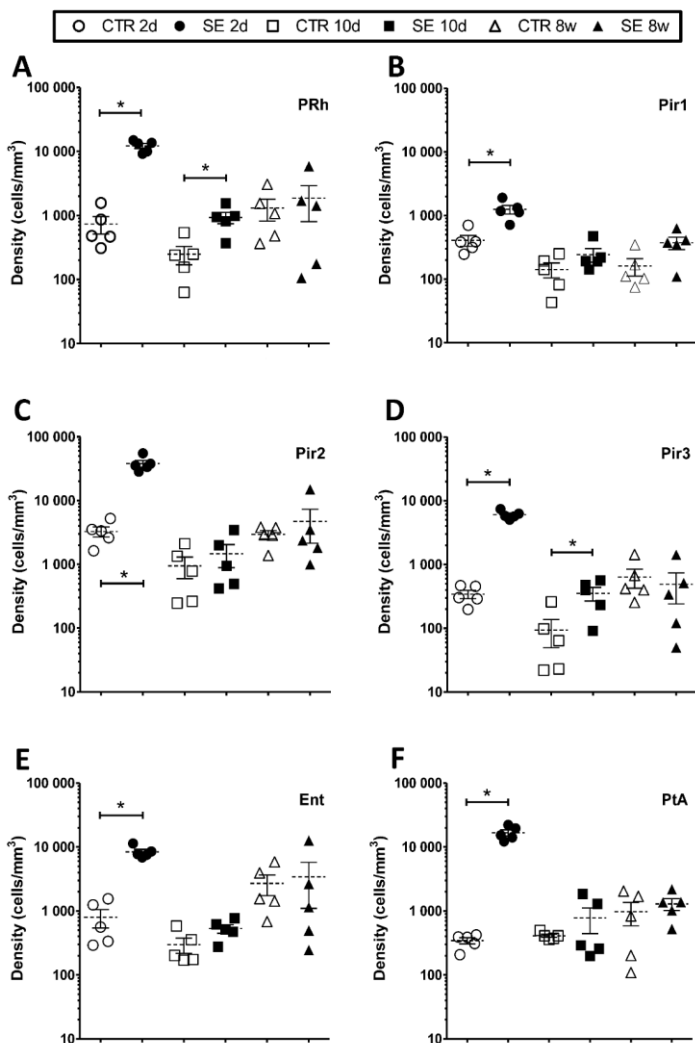


Figure 8. Description on page 94.

Figure 8. Quantification of HSPA1 cellular expression in the parahippocampal and parietal cortices. Cell density of HSPA1 stereological cell count in (A) perirhinal cortex, (B) piriform cortex layer 1, (C) piriform cortex layer 2, (D) piriform cortex layer 3, (E) entorhinal cortex and (F) parietal cortex. All data are presented as mean (dashed line) \pm SEM, * $p < 0.05$, paired Student's t-test for each time point. CTR: electrode implanted controls, SE: electrically stimulated animals, 2d: two days post-SE, 10d: 10 days post-SE, 8w: 8 weeks post-SE.

1.2. Profiling of HSPA1 expression in various cell types

Double and triple fluorescent immunolabelling provided a comprehensive overview of expression on a cellular level. Double staining of HSPA1 with the marker for neuronal nuclei (NeuN) revealed colocalisation of signal from both molecules in all considered regions (Fig. 9). Neuronal expression of HSPA1 was present in animals from both, SE and control groups. The area of colocalisation (Fig. 10) varied however among regions with higher levels in stimulated animals than in the controls. This however should be interpreted considering the overall lower number of HSPA1 immunopositive cells in the control animals.

Double immunofluorescent labelling for HSPA1 and astrocytic marker GFAP demonstrated no colocalisation in the pixel-by-pixel analysis of both signals (Fig. 11). This suggests no relevant expression of HSPA1 in astrocytes in relevant regions at given time points. Few colocalising dots present in cells are rather an indication of a local contact between astrocytes and HSPA1-positive cells (presumably neurons), which

suggests analysis of Z-stacked pictures acquired at high magnification (63X).

Triple immunofluorescent staining involving markers for HSPA1, TLR4 and microglia (Iba1) revealed a strong colocalisation of the first two (PCC = 0.74, ICQ = 0.31, n = 33; Figure 11). Interactions between Iba1 and HSPA1 were found to be much weaker (PCC = -0.16, ICQ = 0.06, n = 33), indicating no biologically relevant expression of HSPA1 in microglia. Similar correlation was observed also for the interaction between TLR4 and Iba1 (PCC = -0.21, ICQ = 0.05, n = 33). Microglial cells visualised by the staining were found in the near vicinity of HSPA1 expressing cells, and they morphologically appeared to be in an activated state (larger cell bodies, shorter processes as compared to control animals). Some of activated microglial cells engulfed HSPA1-positive cells, suggesting a direct contact between them.

Figure 9. Neuronal expression of HSPA1. Low magnification (20x) representative microphotographs of the subregions of the hippocampus and the parahippocampal cortex. For each region are presented: A - HSPA1 positive cells in red, B - NeuN positive cells in green, C - the merged image with Hoechst 33342 superimposed with the colocalisation white mask and D - colocalisation scatterplot computed by the software. The scatterplot is typical for two colocalising probes presenting a big cloud of colocalising pixels in the quadrant 3 (top right), which corresponds to the white area mask visible in the column C.

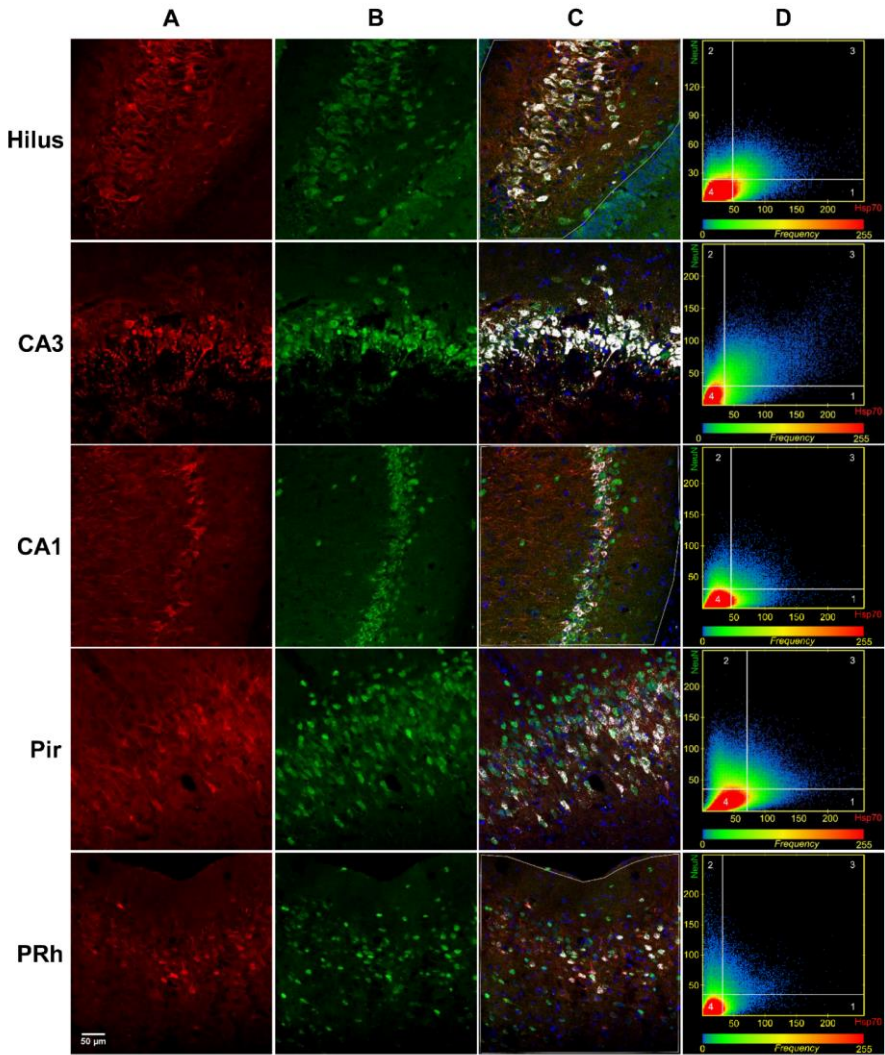


Figure 9. Description on page 95.

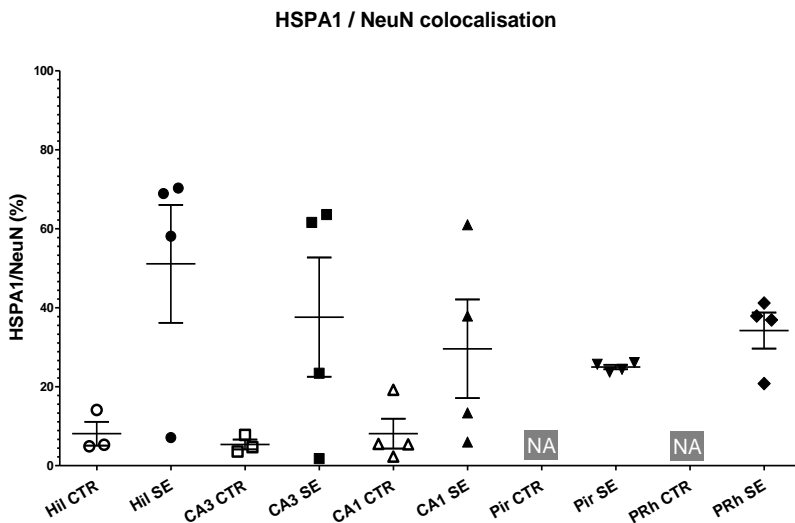
SE One-way ANOVA $P=0.5512$ (Bonferroni)

Figure 10. Comparison of area of colocalisation in the HSPA1/NeuN staining. Each dot represents a value for one animal from a given group. SE animals show higher area of colocalisation (following the overall trend of higher HSPA1-positive cell amount), but they also demonstrate a higher variance than controls. In some regions of interest (piriform and perirhinal cortex), no HSPA1-positive cells were observed.

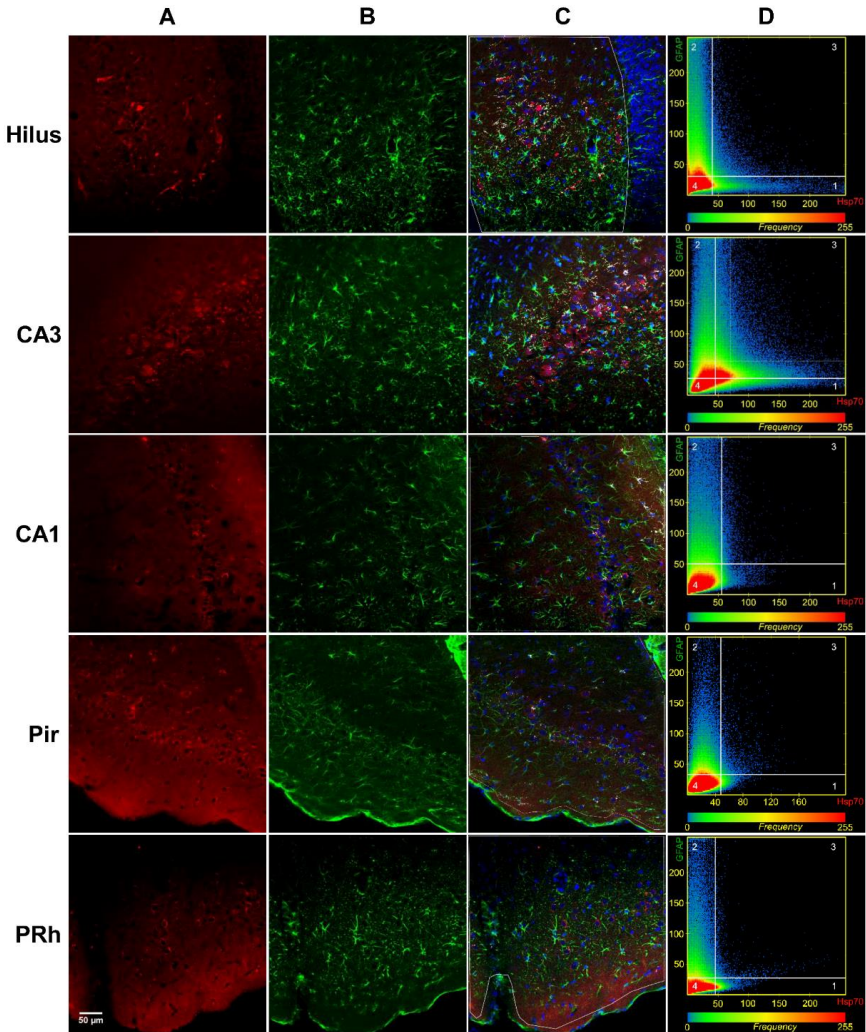


Figure 11. Lack of astroglial expression of HSPA1. Low magnification (20x) representative microphotographs of the hippocampus and the parahippocampal cortex. Continued on page 99.

Figure 11. Continued. For each region are presented in columns: A - HSPA1 positive cells in red, B - GFAP positive cells in green, C - the merged image with Hoechst 33342 superimposed with the colocalisation white mask and D - colocalisation scatterplot computed by the software. The scatterplot is typical for two independent, not colocalising probes presenting a scarce single colocalising pixels in the quadrant 3 (top right), which corresponds to the white area mask visible in the column C. Pixels located in the quadrant 1 represent an exclusive red signal of HSPA1 while the ones in the quadrant 2 – an exclusive green signal of GFAP.

Figure 12. Colocalisation of HSPA1 with its receptor (TLR4) and lack of HSPA1 expression in the microglia. High magnification representative microphotographs of triple immunolabelled cells in the perirhinal cortex. Merge image (A) of single channels for HSPA1 (B), TLR4 (C) and Iba1 (D) with a region of interest of three cells overlayed. An example of colocalisation analysis (E) where for each marker combination (first row: HSPA1/TLR4; second row: HSPA1/Iba1; third row: Iba1/TLR4) is presented a scatterplot relative to the region of interest (Cells #1-3).

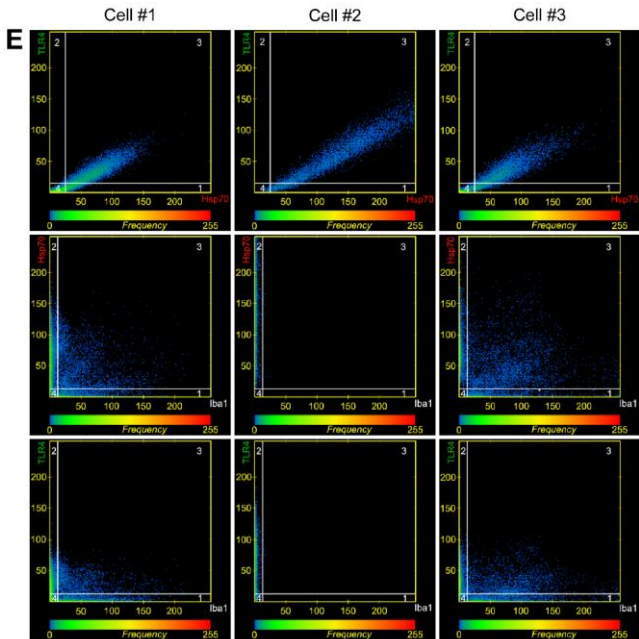
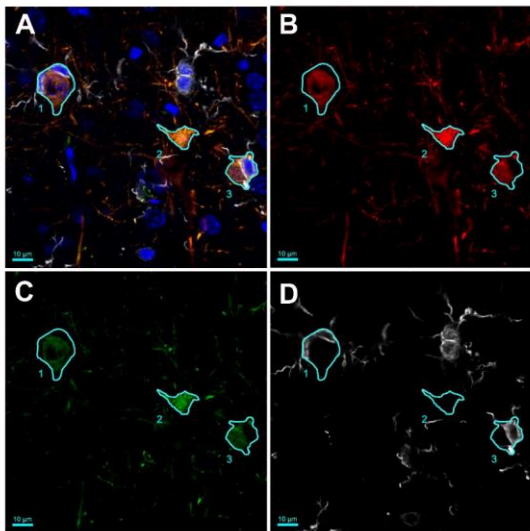


Figure 12. Description on page 99.

2. HSPA5 and HSPH4 expression in epilepsy

2.1. Rat model of epileptogenesis

This study aimed to describe the expression profile of the cognate of HSPA8 in the endoplasmic reticulum (HSPA5) and of its cochaperone (HSPH4) in the course of epileptogenesis in the rat electrical SE model. Immunohistochemical staining revealed information about their distribution in the investigated regions. The staining pattern was similar in both SE and control animals, with HSPA5 signal distributed predominantly in cell soma. The signal was present mostly in the close vicinity to the cell nucleus (as expected of the protein present in the ER), but also in cytosol, reaching in some cases into the processes (Fig. 13I-L). HSPH4 followed the somatic expression pattern (Fig.14I-P), but diffused also in the extracellular matrix in stratum lacunosum-moleculare, stratum radiatum, stratum lucidum and stratum oriens of the Cornu Ammonis.

No differences in the cell count nor in the volume analysis were observed between the hemispheres, so the numbers from the contralateral and ipsilateral sides were summed up and expressed as cell density (cell number over volume) in a single number representing a value for each region in each animal, analogically to the analysis of HSPA1. The effect of status epilepticus on the expression of both proteins was seen mostly in the latency phase. In the acute phase the effect of the stimulation was marginal and no difference was observed

in the chronic phase with spontaneous recurrent seizures.

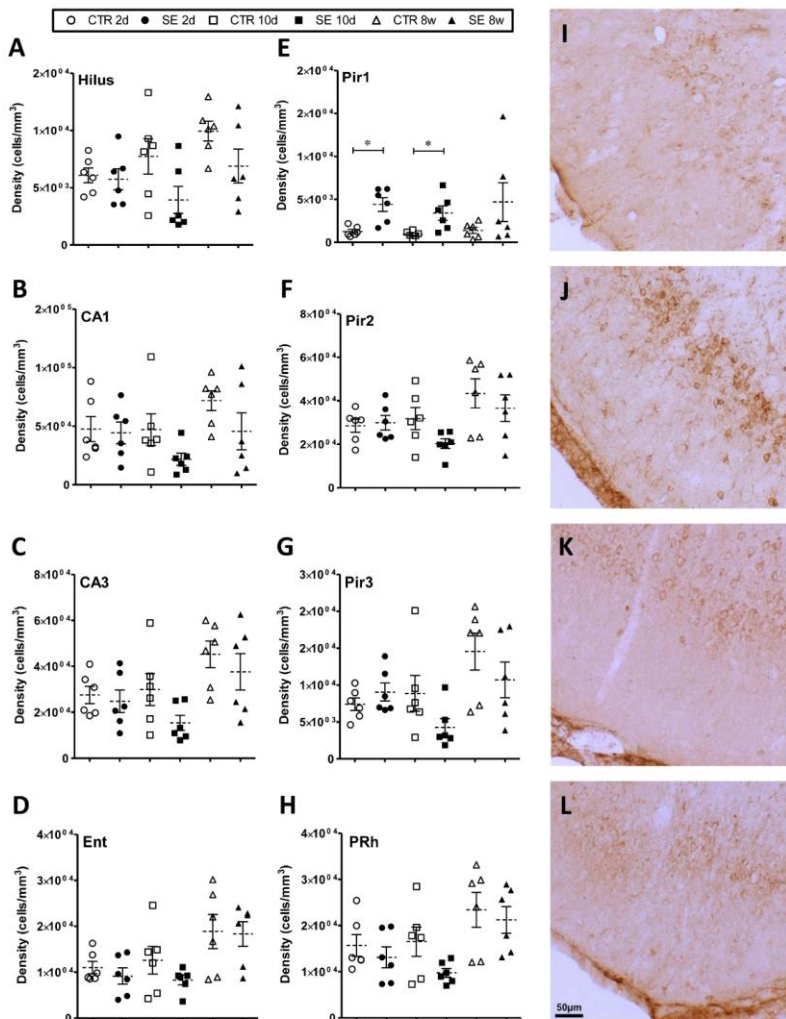


Figure 13. Description on page 103.

Figure 13. Quantification of the cellular expression of HSPA5 in rat. Cell density of HSPA5 stereological cell counting in the hippocampus (A: hilus, B: CA1, C: CA3) and parahippocampal cortices (D: entorhinal cortex, E: piriform cortex layer 1, F: piriform cortex layer 2, G: piriform cortex layer 3, H: perirhinal cortex). Each data point represents cell density of the counts from the ipsilateral and contralateral sides summed together. Representative images of piriform cortex illustrating the increase of HSPA5 positive cells in SE (J, L) compared to control animals (I, K). All data are presented as mean (dashed line) \pm SEM, * $p < 0.05$, paired Student's t-test for each time point. CTR: Electrode-implanted controls, SE: electrically stimulated animals, 2d: two days post-SE, 10d: 10 days post-SE, 8w: 8 weeks post-SE

HSPA5

The analysis of the density of HSPA5-positive cells revealed upregulation of protein expression in SE animals in the parahippocampal cortex, specifically in the piriform cortex layer 1, during the acute post-insult phase (3.5-fold increase; $t(5) = 3.773$, $p = 0.013$; Fig. 12E) and in the latency phase (3.6-fold increase; $t(5) = 2.903$, $p = 0.0337$; Fig.13E). Since anterior and posterior segments of the piriform cortex are known to exhibit differences in histology and in function (the ventrorostral part of Pir incorporates a distinct chemoconvulsant trigger zone, low in GABAergic inputs of inhibitory neurons, called area tempestas), cell counting results were analysed separately for both parts of the region. Lateral olfactory tract was employed as an anatomical indicator of the anterior Pir according to LOSCHER and EBERT (1996). In the acute phase, immunostained cell density was increased in SE animals in comparison to controls ($t(5) = 3.035$, $p = 0.0289$; data not shown) in the anterior piriform

cortex. In the latency phase (10 days after SE), the increase in positive cell number was significant in status epilepticus rats compared to control animals ($t(5) = 3.33$, $p = 0.0208$) in the posterior part of Pir, with a strong trend towards significance in the anterior moiety. The other layers of the piriform cortex, as well as other regions of interest in the rat brain, did not demonstrate any significant differences related to the status epilepticus (Figure 13A-D, F-H).

HSPH4

Quantification of HSPH4 revealed a more distinct influence of SE on protein expression, both in the hippocampus, and in the parahippocampal cortex. This effect was however present exclusively in the latency period. Among hippocampal regions, the upregulation was pronounced in the CA1 with a 1.7-fold increase in the SE animals as compared to controls ($t(8) = 2.381$; $p = 0.0445$; Fig.14B). In the parahippocampal cortex, HSPH4 expression was found to be upregulated in the entorhinal (1.9-fold; $t(9) = 3.511$; $p = 0.0066$; Fig. 14D), in the perirhinal (2.3-fold; $t(9) = 3.663$; $p = 0.0052$; Fig.14H) and in the piriform cortex layer 2 (1.6-fold; $t(9) = 3.456$; $p = 0.0072$; Fig.14F). No significant difference has been observed in the remaining regions of the temporal lobe (Fig.14A, C, E, G).

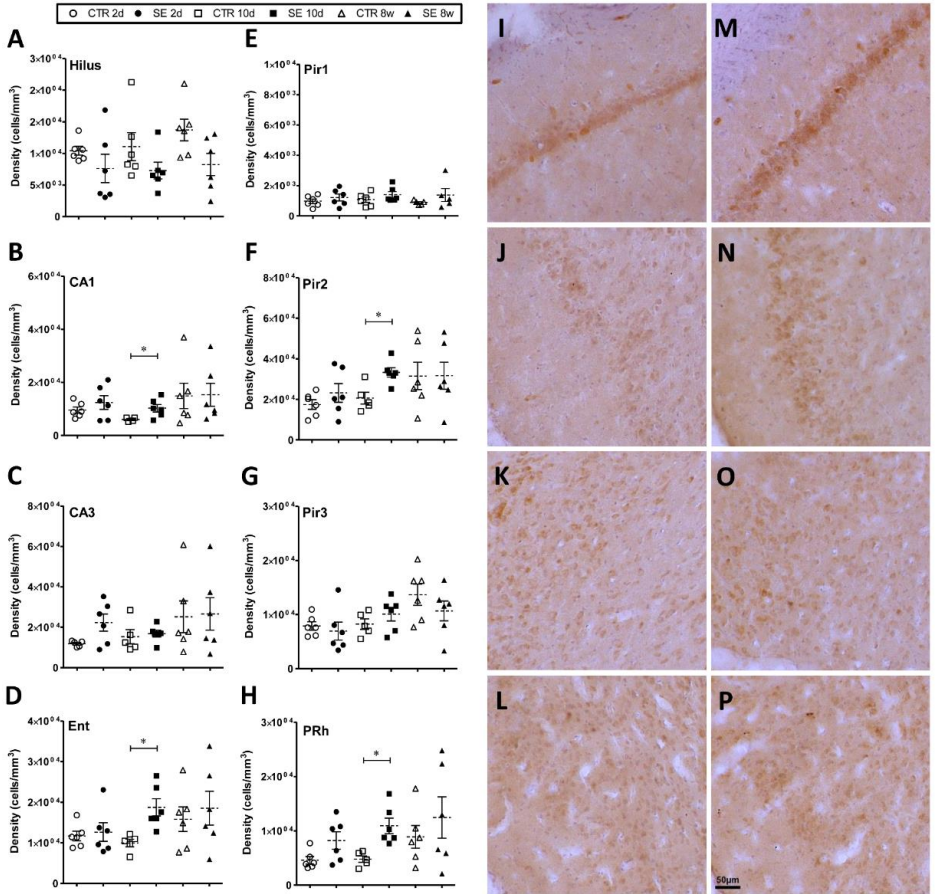


Figure 14. Quantification of the cellular expression of HSPH4 in rat. Cell density of HSPH4 stereological cell counting in the hippocampus (A: hilus, B: CA1, C: CA3) and parahippocampal cortices (D: entorhinal cortex, E: piriform cortex layer 1, F: piriform cortex layer 2, G: piriform cortex layer 3, H: perirhinal cortex). Each data point represents cell density of the counts from the ipsilateral and contralateral sides summed together. Continued on page 106.

Figure 14. Continued. All data are presented as mean (dashed line) \pm SEM, * $p < 0.05$, paired Student's t-test for each time point. CTR: Electrode-implanted controls, SE: electrically stimulated animals, 2d: two days post-SE, 10d: 10 days post-SE, 8w: 8 weeks post-SE.

2.2. HSPA5 and HSPH4 profiling in various cell populations

To characterise which types of brain cells express heat shock proteins of interest, we performed immunofluorescent double labelling of HSPA5 and HSPH4 with common neural and glial cell markers: NeuN, GFAP and Iba1 in the subregions of rat hippocampus and parahippocampal cortex.

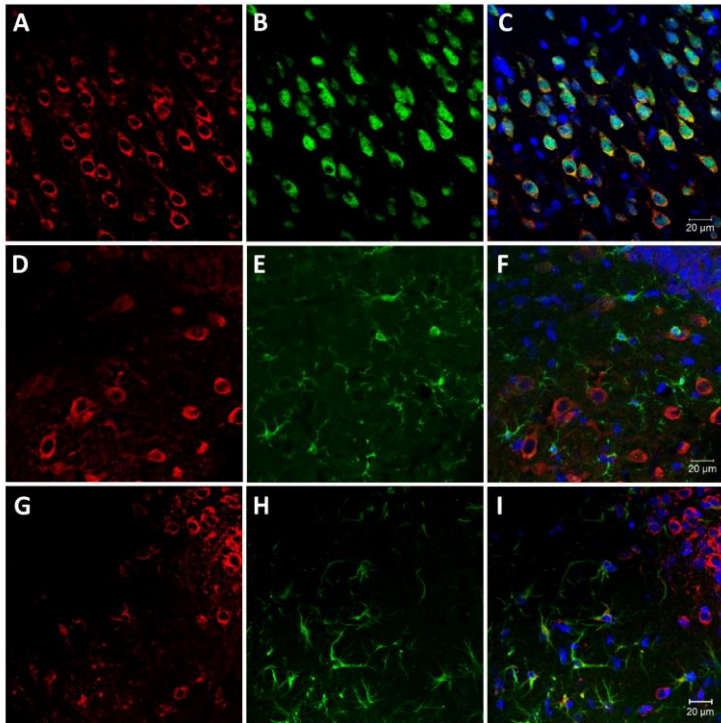


Figure 15. HSPA5 expression in various brain cell populations. Representative microphotographs (20x, digital zoom 2x) of double immunostaining of HSPA5 (A, D, G) with NeuN (B), Iba1 (E) and GFAP (H) respectively. In the merged images (C, F, I), with Hoechst 33342 counterstain visible in blue, it is possible to observe the protein's colocalisation with a neuronal marker (C) but not with a microglia marker (F). Colocalisation of HSPA5 with GFAP is restricted to several cells in the layer 1 of the piriform cortex (I).

The visual inspection of the immunostaining revealed colocalisation of HSPA5 with a neuronal marker (NeuN; Fig.15A-C) in all groups of

animals with the distribution of the heat shock protein in the close vicinity to the cell nucleus counterstained with Hoechst 33342. On the other hand, signal from a microglial marker (Iba1; Fig.15D-F) did not colocalise with the one of HSPA5 neither in SE nor in control animals. Double immunolabelling of HSPA5 with an astrocytic marker (GFAP; Fig.15G-I) demonstrated single scarce cells present in layer 1 of the piriform cortex (1-4 in the field of view) exhibiting colocalisation of the two proteins (Fig.16). The colocalisation could be detected predominantly in SE animals in the acute post-insult phase. Interestingly, in other regions this trend could not be confirmed and only neuronal expression of HSPA5 was observed.

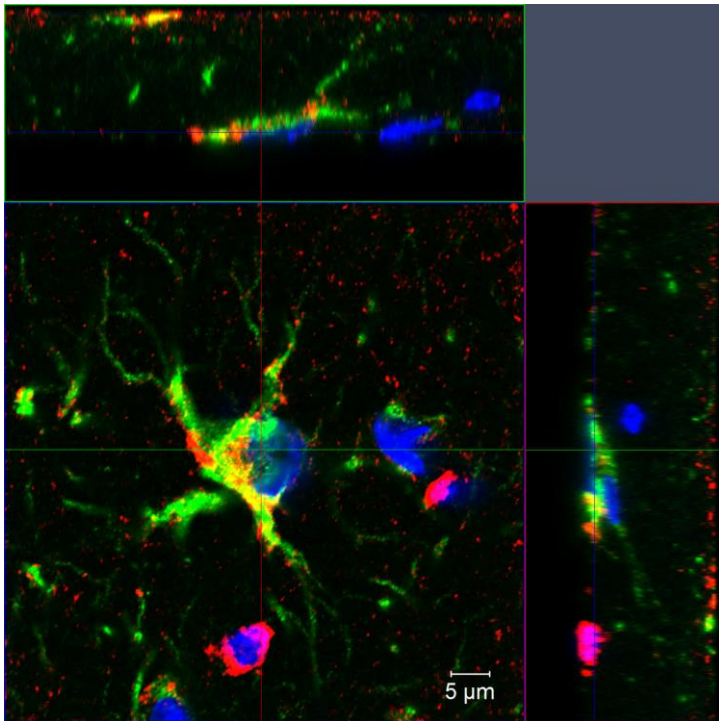


Figure 16. HSPA5 expression in cortical astrocytes. A representative high magnification Z-stack image demonstrating colocalisation of HSPA5 and astroglial marker GFAP within a cell in the piriform cortex layer 1 in a SE animal in the early post-insult phase. Several cells in the same region in the same group of animals presented a similar expression pattern.

These findings were confirmed by quantification of PCC of both signals in HSPA5/GFAP double staining (Table 5). The cut-off value of $PCC = 0.5$ was exceeded only in the piriform cortex in SE animals during the early post-insult phase. Results of other groups oscillated around $PCC = 0$, indicating no correlation between the signals of HSPA5 and GFAP, and thus – no colocalisation.

		Hilus	CA3	CA1	PRh	Pir
2d	CTR	0.10	0.04	-0.01	0.19	0.51
	SE	0.00	0.00	-0.05	0.01	0.05
10d	CTR	-0.14	0.00	-0.04	-0.07	0.23
	SE	0.00	0.00	0.14	0.09	0.04
12w	CTR	0.23	-0.15	-0.01	-0.06	0.05
	SE	0.05	0.03	0.08	0.00	-0.17

Table 5. Results of colocalisation analysis in HSPA5/GFAP staining. Reported are values for Pearson's correlation coefficient in different groups in all the time points in five investigated regions. Only SE animals showed temporally and regionally restricted expression of HSPA5 in astroglia. Threshold value for PCC indicating colocalisation was set for PCC = 0.5.

Double immunofluorescent staining of HSPH4 with NeuN (Fig.17A-C) also revealed colocalisation between the two markers in all investigated regions. HSPH4 signal presented more cytoplasmic localisation as compared to the HSPA5 signal. No colocalisation between HSPH4 and Iba1 was observed (Fig.17D-F) and in contrast to HSPA5, the labelling of HSPH4 with GFAP did not demonstrate colocalisation of these two proteins (Fig.17G-I). The abovementioned trends were present in experimental as well as in control animals.

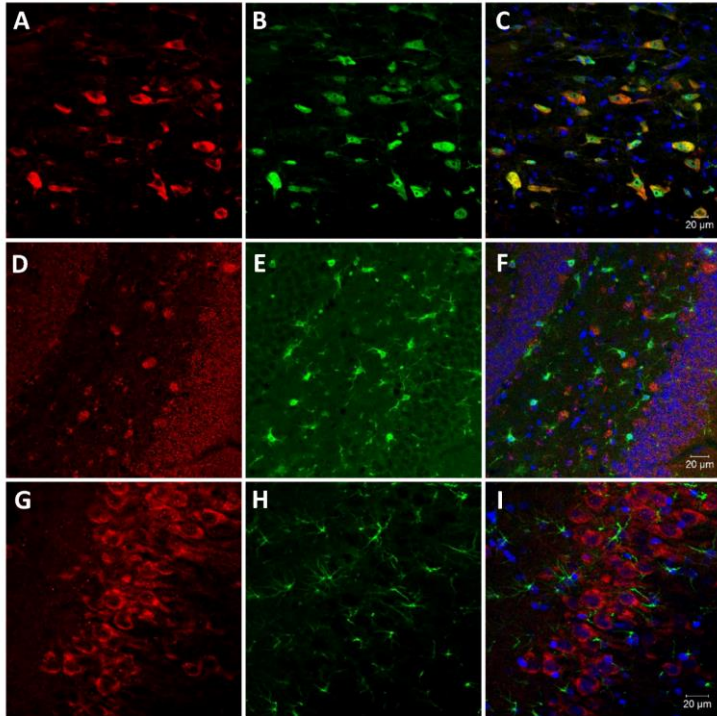


Figure 17. HSPH4 expression in various brain cell populations. Representative microphotographs of double immunostaining of HSPH4 (A, D, G) with NeuN (B), Iba1 (E) and GFAP (H) respectively. In the merged images (C, F, I), with Hoechst 33342 counterstain visible in blue, it is possible to observe the protein's colocalisation with a neuronal marker (C), but neither with a microglia (F), nor with an astrocyte marker (I).

2.3. HSPA5 and HSPH4 expression profiles in dogs

The analysis of immunohistochemically stained canine brain tissue revealed a similar location of the HSPA5 signal as in rats: in the cell

soma, in close vicinity of the nucleus, suggesting an expression inside the ER (Fig.18E). The majority of positive cells was present in stratum pyramidale of CA1 and CA3 regions of hippocampus as well as in the hilus of the dentate gyrus. In the parahippocampal cortex, the most cell dense region was layer 2 of piriform cortex. The morphology of the majority of the stained cells showed similarity to pyramidal neurons and, sparsely, to astroglia. Nevertheless, no significant differences in optical density (data not shown) nor in stained area (Fig.18A-D, F) were found between different groups (data not shown).

Immunohistochemical staining of HSPH4 also exposed a cytoplasmic signal, which however proved to be more diffuse than the one of HSPA5 (Fig.18H). The expression pattern was similar to the one of HSPA5, where the pyramidal layer of CA1 and CA3 as well as the hilus of dentate gyrus stood out as consisting the most positive cells. The cell morphology was in this case also reminiscent of pyramidal neurons, with the most signal gathered in the cell soma. The quantitative analysis considering the aetiology of the disease revealed a significant change in positively stained area in CA1 [$F(3,43) = 5,569$, $p = 0,0045$; Fig.17K]. *Post hoc* comparison between individual groups exposed area enlargement in animals with structural epilepsy as compared to the patient control group of 151%. A trend toward significant differences was observed in the molecular layer of dentate gyrus [$F(3,42) = 2,495$, $p = 0,0729$; Fig.18J].

The quantitative analysis of the positively stained area for cluster, status epilepticus and control groups revealed a significant difference in CA1 [$F(2,44) = 3,31$, $p = 0,0459$; data not shown]. Bonferroni's

Multiple Comparison Test showed no statistically significant differences between respective groups. In CA3 and hilus a trend towards significance was observed [CA3: $F(2,40) = 3,121$, $p = 0,055$; Hil: $F(2,43) = 2,75$; $p = 0,0752$; data not shown]. No statistically significant difference was spotted between these groups in the analysis of OD (data not shown).

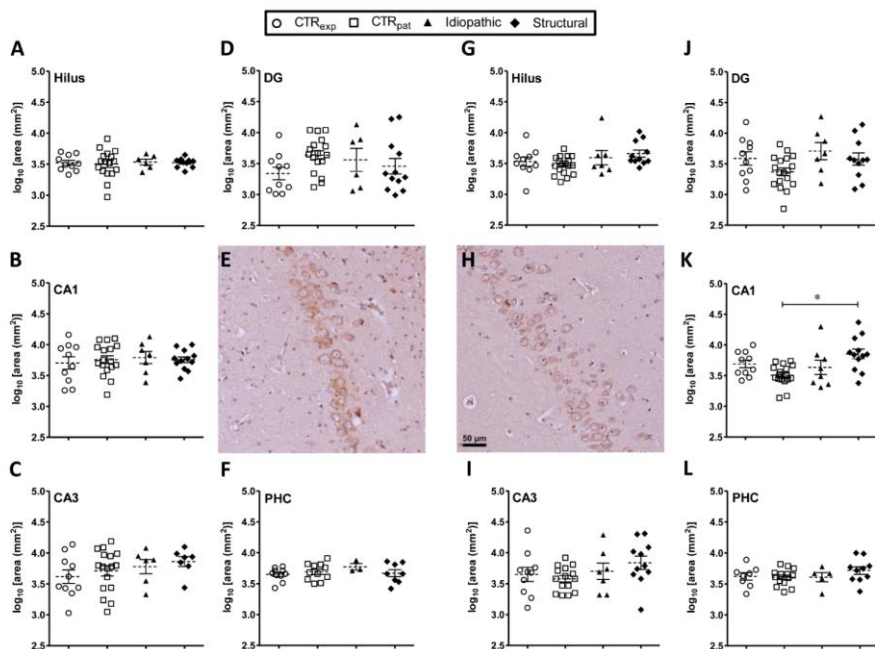


Figure 18. HSPA5 and HSPH4 quantification in canine tissue. Immunopositive area respectively for HSPA5 and HSPH4 in hilus (A, G), CA1 (B, K), CA3 (C, I), DG (D, J) and parahippocampal cortex (F, L). Data points correspond to averaged immunopositive area for HSPA5 and HSPH4 measured in each animal. Representative images of CA1 region staining for HSPA5 (E) and HSPH4 (H) in animals with structural epilepsy. All data are presented as mean (dashed line) \pm SEM, * $p < 0.05$, one-way ANOVA with Bonferroni *post hoc* test. CTR_{exp}: control dogs without neurological diseases used in parasitological studies. CTR_{pat}: control dogs without neurological diseases treated in the clinic. Idiopathic: patients with idiopathic epilepsy, subtype unknown cause and no identification of structural epilepsy. Structural: patients with epilepsy caused by identified cerebral pathology.

VI. DISCUSSION

The goal of this study was to describe the expression profiles of HSP family members during epileptogenesis, taking into consideration the development of the process and pathophysiological changes in its distinct phases. This description can be of use for further assessment of the proteins' suitability as targets for anti-epileptogenic treatment as well as for finding a suitable time window for therapeutical approaches. Targeting HSPA1-mediated inflammatory signalling has already been proposed for several diseases (SAMBORSKI & GRZYMISLAWSKI, 2015; BERNARDO et al., 2016; KIRKEGAARD et al., 2016; KUMAR et al., 2016; KIM et al., 2018), also for epilepsy (YENARI et al., 1998; YANG et al., 2008; HU et al., 2019). The characterisation of the expression pattern of two other heat shock proteins, HSPA5 and HSPH4, is relevant for better understanding of processes occurring in a specific cell compartment, namely in the endoplasmic reticulum, following status epilepticus. It also provides a bigger picture in terms of heat shock reaction and its possible consequences in the course of epileptogenesis.

1. HSPA1

Preliminary immunohistochemical staining performed in the large-scale proteomics study in the electrical post-SE rat model in our lab provided evidence for an early induction of HSPA1 in the hippocampus and in the parahippocampal cortex following the insult (WALKER et

al., 2016). Detailed quantitative analysis of the regions relevant for the development of temporal lobe epilepsy confirmed these findings, and added specific information regarding changes in the expression following status epilepticus. All regions analysed showed a noticeable induction of HSPA1, with the effect especially pronounced in hippocampal subregions and in the piriform cortex, areas prone to neuronal cell damage as the consequence of SE. This regulation seems to be in accordance with the role of HSPA1 as an inhibitor of apoptosis (BENARROCH, 2011; KIM et al., 2018) and seems to act as a protective mechanism following the insult and the subsequent cell stress and damage. HSPA1 overexpression has already proven to exert neuroprotective effects and to increase neuronal survival in stroke and epilepsy models (YENARI et al., 1998). Chemical induction of SE triggers a rapid increase in HSPA1 expression rates in several studies (VASS et al., 1989; YANG et al., 2008; LIVELY & BROWN, 2011). Those previous studies were not however based on unbiased stereological cell quantification, which was utilised in our project. The electric SE model used for purposes of this study excludes also possible direct effects of chemoconvulsants, providing unambiguous confirmation of findings in abovementioned experiments.

The rapid induction of HSPA1 expression was observed in all regions of interest, the extended effect, lasting at least ten days, was however evident only in the layer 3 of the piriform cortex and in the perirhinal cortex. These findings suggest HSPA1-related signalling may play a role also in the latency phase of epileptogenesis, although its effect is limited anatomically. In general, HSPA1 expression seems to be declining with progression of the process of epileptogenesis, being

relevant only locally in some parahippocampal regions. This seems to be further confirmed by a lack of changes in expression rates during the chronic phase with spontaneous recurring seizures, when HSPA1 levels in animals surviving SE show no difference in comparison to controls. This stays in line with results of the large-scale proteomic analysis performed in the same model (WALKER et al., 2016).

In total, the findings argue against a prolonged relevant functional role of HSPA1 after single seizure event. Earlier analysis of human tissue from patients with temporal lobe epilepsy revealed only scarce HSPA1-positive cells (YANG et al., 2008; NAKAYAMA et al., 2017). Also in brain samples from canine epileptic patients, HSPA1 levels were changed to low extent solely in the piriform cortex, while hippocampus remained unaffected (VON RUDEN et al., 2020). Thus, both experimental and clinical data suggest that the cellular events associated with recurrent short single seizures present in the chronic phase seem to be insufficient to trigger HSPA1 upregulation. In general, the most suitable time point for targeting HSPA1-related processes seems to be the early phase following the insult. Nevertheless, further studies would be necessary to indicate a suitable time window within the post-insult phase, especially since HSPA1 upregulation has been already described to be significant in a period of 24 hours after SE in the kainate model (CHANG et al., 2014).

To better understand the role of HSPA1 in the epileptogenic process, it is crucial to describe pathology-associated regulation of its expression in various cell populations. We decided to analyse the overall neuronal population as well as glial cell types most relevant for

neuroinflammation, namely microglia and astrocytes. Immunohistochemical analysis of double and triple labelled cells revealed a predominant induction of HSPA1 expression in neurons. These results stay in line with findings from chemically induced post-SE rat models, which also described neuronal overexpression (VASS et al., 1989; YANG et al., 2008; LIVELY & BROWN, 2011). It has already been suggested for HMGB1 that neuronal cell stress might serve as the first trigger for enhanced DAMP signalling following an epileptogenic insult (PAUDEL et al., 2018). Release of danger signals from injured cells can afterwards signal via Toll-like receptors and mediate an excessive response of the innate immune system. The resulting pro-inflammatory signalling events seem to contribute to epileptogenesis. As HSPA1 is known to serve as a ligand of TLR4 receptors, it might modulate respective molecular responses occurring during the early phase following a brain insult.

In contrast to the pronounced induction in neurons, we did not obtain evidence for a relevant regulation in astrocytes and only observed a very weak expression in microglia. On the one hand, it might give an impression that activation of glia cells does not influence HSPA1 expression rates following SE. However, considering the half-life of the protein of approximately 18 hours (GERNER et al., 2002) and the promptitude of HSPA1 response (CLOUTIER & COULOMBE, 2013; CHANG et al., 2014), it is plausible that we analysed cells after the peak of their HSPA1 expression. Furthermore, different types of stressors seem to cause different patterns of cellular HSPA1 regulation. For instance, the analysis following hyperthermia induced in rats revealed a more intense upregulation of HSPA1 in microglia as

compared to neurons and astrocytes (PAVLIK & ANEJA, 2007). Inducible form of HSPA1 was also reported to be expressed mostly in neurons and not to be expressed in astrocytes in a rat stroke model (AGULLA et al., 2013). Henceforth, the cellular pattern of HSPA1 expression seems to depend on the type of insult and glial cells might be less responsive to the stress associated to status epilepticus than neurons.

To understand why HSPA1 expression is so significant in neurons, one has to consider pathophysiology of a seizure. Prolonged hyperactivity of excitatory neurons leads to prominent glutamate release. Following extended NMDA receptor signalling can result in a cell stress, which can serve as a trigger for the induction of HSPA1. The protein is known to protect hippocampal neurons from excessive extracellular glutamate with subsequent excessive activation of NMDA receptors (AYALA & TAPIA, 2008). However, there seems to be a link between HSPA1 expressing neurons and microglial cells, which is indirectly supported by the presence of microglia in close proximity of HSPA1/TLR4 immunopositive cells. Furthermore, these microglial cells exhibit a morphology reflecting an activated state and in several cases they seem to engulf HSPA1-expressing neurons, advocating for a putative influence of neuronal HSPA1 expression on glial cells in their vicinity.

Whether HSPA1 overexpression leads to any functional consequences, remains an open question. Intracellular HSPA1 is believed to have an important role in neuroprotection, since its expression can limit generation of pro-inflammatory mediators and

reactive oxygen species (KIM & YENARI, 2013). At the same time, extracellular HSPA1 is a well-known ligand of Toll-like receptors 2 and 4, of which TLR4 cascade is a relevant contributor to seizure generation. It still remains unknown, whether HSPA1 serves as an agonist, an antagonist, or partial agonist/antagonist of TLR4, and results regarding this matter so far are contradictory (ASEA et al., 2000; ASEA et al., 2002; SINGLETON & WISCHMEYER, 2006; FERAT-OSORIO et al., 2014). Recent studies reported that HSPA1 induction during seizures leads to proteasomal degradation of Kv4-KChIP4a channel complexes responsible for generating a neuronal A-type current (HU et al., 2019). A-type channels are activated in response to hyperpolarisation and their activity tends to delay the following depolarisation. Their degradation can therefore lead to shortening of the period between the action potentials. This may serve as a link between overexpression of HSPA1 and pathophysiology of epileptogenesis. The HSPA1-mediated proteasomal degradation of potassium channel complex might also occur during early phases of epileptogenesis thereby contributing to network reorganisation and changes leading to hyperexcitability.

The functional impact of HSPA1 in the generation of a hyperexcitable network was studied extensively in our working group. Two experiments were performed, encompassing genetic and pharmacological regulation of HSPA1 expression. Findings from knockout mice lacking inducible HSPA1 showed increased seizure thresholds, more severe seizures, and enhanced microglia activation, which supports a protective role of the protein. However, treatment with the HSPA1 inducing compound celastrol as well as HSPA1

overexpression in mice lines also increased seizure severity (VON RUDEN et al., 2018; VON RUDEN et al., 2019).

In summary, as mentioned above, the putative final functional role of HSPA1 in epileptogenesis remains unclear, with studies indicating its neuroprotective role as well as detrimental effects following HSPA1 administration or internal overexpression present. The ambiguous findings might also mirror the fact that activation of glia can serve both a protective function and, on the other hand, if the activation becomes excessive and persistent, it can also contribute to the pathophysiology and disease progression (RAVIZZA et al., 2011; PITKANEN et al., 2015). The pronounced upregulation of HSPA1 expression in epileptogenesis described in this study reflects an endogenous mechanism modulating the induction of inflammatory signalling and the onset of molecular, cellular, and network reorganisation resulting in the generation of a hyperexcitable epileptic network. Nevertheless, further research is indispensable to decisively determine the role of HSPA1 in the epileptogenic process and develop treatment approaches, based either on inhibition or on enhancement of HSPA1 function.

2. HSPA5 and HSPH4

The present study focused also on the analysis of the expression patterns of two endoplasmic chaperones, HSPA5 and HSPH4, in the course of epileptogenesis modelled in the adult rat brain. Comprehensive information related to epileptogenesis-associated alterations in the levels of the abovementioned proteins is necessary to better understand the role of ER-stress and the related processes in the development of temporal lobe epilepsy. It might be also of use while assessing putative therapeutic approaches targeting the unfolded protein response. Additionally, information about time-windows when the alterations are the most pronounced is of high relevance to the temporal placement of eventual anti-epileptogenic intervention. Quantitative analysis of immunohistochemical stainings in rats confirmed the findings from a previous proteomics study in the electrical post-SE model, where an early induction of HSPA5 and late upregulation of HSPH4 was indicated (WALKER et al., 2016). In addition, analogically to the HSPA1 examination, it provided a detailed information about the expression patterns in different subregions of the hippocampus and the parahippocampal cortex.

Both proteins of interest underwent changes in expression patterns during the latency phase following SE, showing a significant upregulation in subregions of the temporal lobe crucial for the development of TLE. By definition, the latent period is described as the timespan following the brain insult when molecular and cellular mechanisms leading to the onset of clinical seizures are progressing. Analysis of immunohistochemically stained brain rat tissue revealed

the most pronounced alterations of HSPA5 and HSPH4 during this phase. This suggests that pathophysiological events linked to the commencing epileptogenic process modify the expression of the two ER chaperones, and that status epilepticus, as well as following early post-insult recovery phase, influence their levels to a lesser extent, having an impact only on HSPA5. Epileptogenesis has already been demonstrated to trigger upregulation of various markers of ER stress, including HSPA5, in the kindling models in rats (CHIHARA et al., 2011) and mice (ZHU et al., 2017). It is therefore plausible that cytomolecular changes in the neuronal circuitry in the course of epileptogenesis lead to increased endoplasmic reticulum stress with following upregulated expression of HSPA5 and HSPH4.

The expression pattern of both proteins varied in response to the epileptogenic insult, but this variation was restricted regionally. The piriform, the perirhinal and the entorhinal cortex as well as CA1 region of the hippocampus were the areas affected the most. The piriform cortex demonstrated changes in expression levels of both proteins of interest. However, HSPA5 showed alterations as the consequence of status epilepticus restricted only to layer 1, the most superficial part of the region consisting mostly of axons and glial cells, while HSPH4 exhibited changes in the layer 2, the portion of the piriform cortex containing the most of the neuronal cell bodies. The piriform cortex, due to its interconnectivity to other hyperexcitability-prone areas as well as to its low inhibitory GABAergic connectivity, especially in area *tempesta*, is a region particularly susceptible to pro-convulsive stimulation and capable of generating seizures (PIREDDA & GALE, 1985). It is plausible that strong hyperexcitatory activity of neurons of

the piriform cortex causes the most pronounced effect on HSPA5 and HSPH4 expression among all the investigated regions.

HSPH4 levels were found to be upregulated in SE animals also in the perirhinal and the entorhinal cortices. These two temporal lobe subregions play an important role in the brain connectivity serving as an interface of sensory inputs between the hippocampal formation and other limbic as well as cortical areas, relaying the signal in both directions (WITTER & GROENEWEGEN, 1986). As a result of their strategic location and high interconnectivity, the abovementioned regions serve as crucial elements for the progression of epileptogenic alterations (VISMER et al., 2015). In the hippocampus, HSPH4 was upregulated in CA1 region in SE rats and in dogs with structural epilepsy. This Cornu Ammonis subregion is involved in a complex circuitry, particularly vulnerable to abnormal neuronal activity and susceptible to long-term potentiation of their principal neurons, leading in the end to construction of a primary focus able to exhibit spontaneous epileptiform discharges (DESHMUKH & KNIERIM, 2012). The upregulation of HSPH4 on the spot of development of a putative epileptic focus as well as in the regions highly connected to it further supports a conclusion that ER stress might be related to the process of epileptogenesis.

Qualitative analysis of HSPA5 and HSPH4 expression in different brain cell populations revealed a predominant colocalisation of both proteins with a neuronal marker (NeuN) and no colocalisation with a microglial marker (Iba1). Restricted colocalisation has been observed between an astrocytic marker (GFAP) and HSPA5, but not HSPH4.

These findings suggest that high ER stress is exerted on neurons, which are the main cells involved in the development of dysfunctional circuitry in the course of epileptogenesis. The glial response to the conditions following status epilepticus was in this case either too weak, or the selected time points of two days, ten days and eight weeks after the initial insult did not allow us to grasp any relevant changes in these cell populations. For instance, in case of rapid glial response it might have been too late to notice HSPH4 alterations in glia, due to the short half-life of the protein, estimated for around 10.77 hours (XIAO & WU, 2017). Admittedly, the half-life of HSPA5 is relatively long, it is however present in high basal concentrations in the cells (PREISSLER & RON, 2019), therefore its alterations could have been imperceptible. Additionally, high variance of these basal values in the control groups can further clarify relatively low and limited HSPA5 upregulation in the investigated areas.

Neuronal HSPA5 and HSPH4 proved to exert protective effects as a response to stress factors. HSPA5 acted neuroprotectively in a stroke mouse model by binding to and decreasing an overactivation of the protein kinase RNA-like endoplasmic reticulum kinase (PERK) arm of the UPR, which leads to deleterious consequences for cellular homeostasis (LOUESSARD et al., 2017). The protein plays also a relevant role in neuroprotection in many common neurodegenerative diseases, like Alzheimer's disease, Parkinson's disease and amyotrophic lateral sclerosis (CASAS, 2017), promoting cell survival and decreasing degeneration. HSPH4 has been demonstrated to be expressed by neurons in response to glutamate. The cells showed higher viability following kainate administration in transgenic mice

overexpressing the protein (KITAO et al., 2001). HSPH4 overexpression was also confirmed following hypoxic stress in neuronal culture (TAMATANI et al., 2001). A crucial role in cell survival is also displayed in physiological conditions such as brain development. HSPH4 is induced in cerebellar Purkinje cells in mice during a period of their highest vulnerability to cell death and targeted neuronal HSPH4 overexpression improved neuronal viability in Purkinje cell layer over the critical period (KITAO et al., 2004). Since HSPA5 and HSPH4 seem to be of high importance for promotion of neuronal survival and decrease of neurodegeneration, both in physiological and pathological conditions, it is plausible that similar neuroprotective mechanisms might apply in case of status epilepticus and its early results as well as subsequent epileptogenic processes.

Since the rat model of electrical SE takes into consideration highly standardized, laboratory conditions, a glimpse into more unpredictable clinical environment can add more relevant information to the picture of HSPA5 and HSPH4 expression in epileptic brain. For that purpose, analysis on the canine brain tissue was performed. Data from patients handled in the clinics can be directly compared to the results obtained from the chronic phase with spontaneous recurrent seizures in the rat model, since this phase mirrors the actual presentation of TLE. Rats used in this study presented no significant differences in levels of HSPA5 and HSPH4 between experimental and control group during this phase. On the other hand, analysis performed in the immunohistochemically stained brain samples collected from dogs, indicated an increase of area of the HSPH4 staining in patients with structural type of epilepsy. No differences were however observed in

case of HSPA5.

There is discrepancy in the data between the rat and the dog models and its nature is not completely clear. It might be related to differences between the two species and could be influenced by drug treatment, duration of the disease, age, breed, co-morbidities etc. However, this finding might to some extent suggest that ER stress-related response might be involved also when symptoms are fully developed, so therapeutic targeting of the respective heat shock protein could be advantageous also in the chronic phase of the disease. Additional research involving more clinical cases is nevertheless necessary to elucidate the relevance of HSPA5 and HSPH4 to TLE manifestation.

In addition to regulation of protein expression itself, one has to address posttranslational regulation of function as well. In the ER, HSPA5 is present in two distinct states, active or inactive, which depends on AMPylation, locking the protein in low-affinity state for its substrates (PREISSLER & RON, 2019). HSPA5 may also be deposited into a pool of temporarily inactive proteins in a process of oligomerisation (PREISSLER & RON, 2019). Therefore, in an environment where substrates of the chaperone are lacking, HSPA5 can still be abundant in cells, but either in its inactive AMP-bound form, or accumulated in form of oligomers. All of these posttranslational alterations of HSPA5 were not in the scope of this study, therefore it might be of future interest to investigate a presumptive impact of epileptogenic insult on HSPA5 cellular fractions.

The unfolded protein response has been already proposed as a possible target of novel therapeutic strategies. The process has been

discussed in terms of anti-cancer therapy (WANG et al., 2018b), in cardiovascular disease (ZHANG et al., 2019) as well as in neurodegenerative diseases (HUGHES & MALLUCCI, 2019; MARTINEZ et al., 2019). Modulation of HSPA5 levels has been suggested in oncology. Cleavage of HSPA5 polypeptides was demonstrated to result in lower cancer cell survival (BACKER et al., 2011). Several therapeutic agents regulating HSPA5 expression have been described in models of Parkinson's disease, where they exerted a neuroprotective effects (ENOGIERU et al., 2019).

Possible therapy strategies could be also developed, considering the physical and functional link between endoplasmic reticulum and mitochondria. Both organelles are in close contact by their membranes, where 20% of the mitochondrial surface is linked directly to the ER (KORNMANN et al., 2009). These linking sites through which ER communicates with mitochondria are referred to as mitochondrial-associated membranes (MAMs) and their interaction is critical for calcium signaling flowing from the ER into the mitochondria (MALHOTRA & KAUFMAN, 2011). The machinery of the MAMs involved in calcium efflux consists of inositol triphosphate receptor (IP3R), an important Ca^{2+} channel, as well as sigma-1R receptor, which along with HSPA5 forms a complex bound to IP3R (MALHOTRA & KAUFMAN, 2011). Under conditions of ER stress, sigma-1 receptors have been demonstrated to dissociate from HSPA5 and interact directly with IP3R, subsequently prolonging calcium signaling from the ER to mitochondria and ultimately promoting cell survival (NGUYEN et al., 2015). Targeting sigma-1R is a concept already being discussed in epileptology, since allosteric modulations

of the receptor provided anti-seizure effects in pentylenetetrazole and kainic acid-induced status epilepticus rat models (GUO et al., 2015; VAVERS et al., 2017). Additional modulation of HSPA5, which plays a key role in sigma-1R functionality, might be of further advantage in developing therapy approaches targeted towards this complex.

Interestingly, the unfolded protein response seems to be connected to inflammation and subsequent production of cytokines (SMITH, 2018). In a study performed on cultured macrophages, production of anti-inflammatory interleukin 10 was greatly reduced by ER stress, while the levels of pro-inflammatory interleukin 12 messenger RNA were elevated (ZHANG et al., 2019). In the course of the UPR, a chaperone protein known as heat shock protein C4 (HSPC4, also known as 94 kDa glucose-regulated protein, GRP94, and HSP90B1) is upregulated in response to misfolded proteins. HSPC4 is recognised to regulate levels of TLRs by folding TLR1, 2, 4, 7 and 9 specifically (TIMBERLAKE et al., 2018), influencing directly their expression in cell membranes and, subsequently, the intensity of the inflammatory response in the cell. It is therefore plausible that cellular stress associated with excessive excitatory signaling during status epilepticus triggers upregulation of HSPC4 throughout the unfolded protein response. Consequently, TLRs expression gets upregulated, facilitating initiation of production of pro-inflammatory cytokines in the cell as well as their release into the extracellular matrix, which establishes an environment promoting seizure generation, but also further exacerbating the UPR, creating a positive feedback loop (SMITH, 2018).

This further connects heat shock proteins and processes involving HSPs to epileptogenesis, which makes them promising candidates for future therapeutic targets. In the case of HSPA5 and HSPH4 however, additional studies with genetic and pharmacological modulation of both proteins with subsequent analysis of the consequences in animal models of temporal lobe epilepsy are necessary to elucidate their impact on the process of the development of the disease.

VII. CONCLUSIONS

All heat shock proteins of interest analysed in this study exhibited altered expression patterns in the course of epileptogenesis. Moreover, HSPH4 underwent changes also in case of canine patients diagnosed with structural epilepsy. Those findings prove that epileptic events influence the expression rates of proteins involved in response to stress and are involved in inflammatory reactions (HSPA1) and in unfolded protein response (HSPA5, HSPH4).

HSPA1 was intensely upregulated in the early phase following status epilepticus, therefore it is plausible that the protein might contribute to excessive inflammation which later on contributes to cellular and molecular changes leading to formation of hyperexcitable networks and generation of epileptic focus. Therefore, targeting HSPA1 in the early post-insult phase could be worth of consideration in development of novel therapeutic approaches.

HSPA5 and HSPH4 exhibited the most pronounced upregulation mainly in the latency phase of the epileptogenesis. This finding suggests that endoplasmic stress is exerted on cells when the cytomolecular epileptogenic changes progress in the brain tissue. Furthermore, this result indicates that therapy strategies targeting these proteins should be aimed on this time point of the process.

VIII. SUMMARY

Epilepsies are common chronic diseases with high burden both in veterinary practice and in human medicine. Due to many obstacles in standard therapeutic procedures leading to ineffective treatment, development of new targeting strategies is necessary. A good starting point is preventing or hindering the process of epileptogenesis, when all the mechanisms driving the pathologic alterations in the brain commence and proceed.

The link between epileptogenesis and inflammation has been already established. It is known that epileptogenic insults can start inflammatory processes as well as that inflammation can sustain and progress epileptogenesis. Therefore, modification of pro-inflammatory signalling within a cell would make a possibly efficient therapy strategy. Among cascades leading to inflammation, the one of Toll-like receptor 4 (TLR4) is of particular interest, due to its known contribution to generation of seizures. Ligands of TLR4 include pathogen-derived as well as endogenous molecules, among them heat shock protein A1 (HSPA1).

The unfolded protein response is a set of processes started by stress exerted on endoplasmic reticulum. Gathering of misfolded peptides is a factor precipitating the response, which in the end leads to upregulation of chaperones. Among them, heat shock protein A5 (HSPA5) and heat shock protein H4 (HSPH4) play important roles in bringing back the homeostasis inside the organelle. The unfolded protein response is known to contribute to many neurological

disorders.

To investigate alterations that the three heat shock proteins undergo following an epileptogenic insult, single and multiple immunohistochemistry was performed in brains collected from rats of temporal epilepsy model as well as in canine tissue from clinical cases. In the rat temporal lobe epilepsy model, stereological cell counting revealed a clear upregulation of HSPA1 expression in all investigated regions of the hippocampus and the parahippocampal cortex in the early post-insult phase. Upregulation of HSPA5 and HSPH4 expression was spatially restricted, present predominantly in the parahippocampal cortex, mostly in the latency phase. All of the heat shock proteins were expressed by neurons, and restricted expression was observed in microglia (HSPA1) and in astroglia (HSPA5). In canine tissue, quantitative analysis revealed an increase of HSPH4 expression in brains collected from patients diagnosed with structural epilepsy in Cornu Ammonis 3 region of the hippocampus.

These findings advocate an influence of status epilepticus and of the subsequent epileptogenic process on regulation of heat shock proteins expression. Considering involvement of HSPA1 in inflammatory cascade, possible modifications of expression of this protein could be a suitable therapeutic strategy. However, it has to be firstly elucidated, whether HSPA1 acts protectively or deleteriously as an element of the Toll-like receptor 4 inflammatory cascade.

At the same time, hampering the progression of the process may be achieved by modifications of endoplasmic heat shock proteins, HSPA5 and HSPH4, involved in local stress response and expressed

predominantly during the latency phase. More research however is necessary, involving genetic and pharmacological modulation of both proteins *in vivo*.

IX. ZUSAMMENFASSUNG

Epilepsien sind chronische, höchstbelastende Erkrankungen, die sowohl in der Veterinär- als auch in der Humanmedizin weit verbreitet sind. Viele Patienten sprechen nicht auf eine pharmakologische Therapie an und können daher nicht effektiv behandelt werden. Aus diesem Grund ist die Entwicklung neuer therapeutischer Strategien und das Finden neuer therapeutisch nutzbarer Zielstrukturen notwendig. Dabei ist es ein Hauptziel der epileptologischen Forschung Strategien zu entwickeln, die den Prozess der Epilepsieentstehung unterbrechen. Aus der Literatur ist bekannt, dass epileptische Anfälle inflammatorische Prozesse induzieren und dass inflammatorische Prozesse die Epileptogenese induzieren und forcieren können. Deswegen könnte eine Modifizierung von pro-inflammatorischen Signalkaskaden möglicherweise eine effiziente Präventionsstrategie darstellen. In diesem Zusammenhang ist die Toll-like-Rezeptor-4(TLR4)-Signalkaskade von besonderem Interesse. Die Liganden des TLR4 umfassen verschiedene endogene Moleküle, unter anderem auch das Hitze-Schock-Protein A1 (HSPA1).

Die zelluläre Antwort auf ungefaltete Proteine umfasst komplexe Reaktionen, die durch zelluläre Stressfaktoren ausgelöst werden, welche das endoplasmatische Retikulum beeinflussen. Die Kumulation von fehlerhaft gefalteten Peptiden ist ein Faktor, der die Antwort beschleunigt, was im Endeffekt zur Hochregulierung von Chaperon-Proteinen führt. Unter den Chaperon-Proteinen spielen Hitze-Schock-Protein A5 (HSPA5) und Hitze-Schock-Protein H4 (HSPH4) eine wichtige Rolle für die Wiederherstellung der

Homöostase. Die zelluläre Antwort auf ungefaltete Proteine scheint zur Pathophysiologie verschiedener neurologischer Erkrankungen beizutragen.

Um die Veränderungen der Expressionsraten der drei Hitze-Schock-Proteine in Folge von epileptischen Anfällen zu untersuchen, wurden qualitative und quantitative immunhistochemische Untersuchungen an Gehirnschnitten von Ratten während der Epileptogenese sowie an Gehirnen von Hundepatienten durchgeführt. In der frühen Post-Insult-Phase des Rattenmodells der Temporallappenepilepsie konnte durch stereologische Zellzählung eine erhöhte Zahl HSPA1-exprimierender Zellen in allen untersuchten Regionen des Hippocampus und des parahippocampalen Cortex in der frühen Post-Insult-Phase nachgewiesen werden. Eine Überexpression von HSPA5 und HSPH4 zeigte sich hingegen nur in einzelnen Hirnregionen, wie dem parahippocampalen Cortex. Alle im Rahmen dieses Forschungsprojektes analysierten Hitze-Schock-Proteine waren in Neuronen exprimiert und zusätzlich vereinzelt in Mikrogliazellen (HSPA1) und in Astrozyten (HSPA5). Die quantitative Analyse im Hundegewebe zeigt eine Erhöhung der HSPH4-Expression in der Cornu-Ammonis-3-Region des Hippocampus in Gehirnen von Patienten mit struktureller Epilepsie.

Die Ergebnisse zeigen, dass ein Status Epilepticus als epileptogener Insult und der Prozess der Epileptogenese einen Einfluss auf die Expression von Hitze-Schock-Proteinen ausübt. Angesichts der Beteiligung von HSPA1 in der Inflammationskaskade könnte möglicherweise eine gezielte Modulation der Expression dieses

Proteins eine geeignete neue Therapiestrategie darstellen. Allerdings muss zuerst abgeklärt werden, ob HSPA1 als ein Element der TLR4-Entzündungskaskade nach epileptogenen Insulten protektive oder schädliche Eigenschaften besitzt.

Möglicherweise könnte der Prozess der Epileptogenese außerdem durch eine Modulation der endoplasmatischen Hitze-Schock-Proteine, HSPA5 und HSPH4, beeinflusst werden. Diese beiden Proteine sind an der lokalen Stressantwort beteiligt und werden vorüberwiegend in der Latenzphase der Epileptogenese exprimiert. Weiterführende funktionelle Studien, insbesondere die genetische und pharmakologische Modulation dieser Proteine *in vivo*, sind jedoch eine Voraussetzung, um eine abschließende und umfassende Aussage treffen zu können.

X. LIST OF REFERENCES

Agulla J, Brea D, Campos F, Sobrino T, Argibay B, Al-Soufi W, Blanco M, Castillo J, Ramos-Cabrer P. In vivo theranostics at the peri-infarct region in cerebral ischemia. *Theranostics* 2013; 4: 90-105.

Aksoy MO, Kim V, Cornwell WD, Rogers TJ, Kosmider B, Bahmed K, Barrero C, Merali S, Shetty N, Kelsen SG. Secretion of the endoplasmic reticulum stress protein, GRP78, into the BALF is increased in cigarette smokers. *Respir Res* 2017; 18: 78.

Alexanian A, Sorokin A. Cyclooxygenase 2: protein-protein interactions and posttranslational modifications. *Physiol Genomics* 2017; 49: 667-81.

Asea A, Kraeft SK, Kurt-Jones EA, Stevenson MA, Chen LB, Finberg RW, Koo GC, Calderwood SK. HSP70 stimulates cytokine production through a CD14-dependant pathway, demonstrating its dual role as a chaperone and cytokine. *Nat Med* 2000; 6: 435-42.

Asea A, Rehli M, Kabingu E, Boch JA, Bare O, Auron PE, Stevenson MA, Calderwood SK. Novel signal transduction pathway utilized by extracellular HSP70: role of toll-like receptor (TLR) 2 and TLR4. *J Biol Chem* 2002; 277: 15028-34.

Asea AAA (2008) Heat shocks and the brain implications for neurodegenerative diseases and neuroprotection. Springer, [New York, NY

Asea AAA (2016) HEAT SHOCK PROTEIN-BASED THERAPIES. SPRINGER INTERNATIONAL PU, [Place of publication not identified]

Ayala GX, Tapia R. HSP70 expression protects against hippocampal neurodegeneration induced by endogenous glutamate in vivo. *Neuropharmacology* 2008; 55: 1383-90.

Backer MV, Backer JM, Chinnaiyan P. Targeting the unfolded protein response in cancer therapy. *Methods Enzymol* 2011; 491: 37-56.

Bankstahl M, Breuer H, Leiter I, Markel M, Bascunana P, Michalski D, Bengel FM, Loscher W, Meier M, Bankstahl JP, Hartig W. Blood-Brain Barrier Leakage during Early Epileptogenesis Is Associated with Rapid Remodeling of the Neurovascular Unit. *eNeuro* 2018; 5

Barnes Heller H. Feline Epilepsy. *Vet Clin North Am Small Anim Pract* 2018; 48: 31-43.

Beaucamp N, Harding TC, Geddes BJ, Williams J, Uney JB. Overexpression of hsp70i facilitates reactivation of intracellular proteins in neurones and protects them from denaturing stress. *FEBS Lett* 1998; 441: 215-9.

Bedner P, Dupper A, Huttmann K, Muller J, Herde MK, Dublin P, Deshpande T, Schramm J, Haussler U, Haas CA, Henneberger C, Theis M, Steinhauser C. Astrocyte uncoupling as a cause of human temporal lobe epilepsy. *Brain* 2015; 138: 1208-22.

Benarroch EE. Heat shock proteins: multiple neuroprotective functions and implications for neurologic disease. *Neurology* 2011; 76: 660-7.

Benson MJ, Manzanero S, Borges K. Complex alterations in microglial M1/M2 markers during the development of epilepsy in two mouse models. *Epilepsia* 2015; 56: 895-905.

Berendt M, Gredal H, Pedersen LG, Alban L, Alving J. A cross-sectional study of epilepsy in Danish Labrador Retrievers: prevalence and selected risk factors. *J Vet Intern Med* 2002; 16: 262-8.

Berendt M, Farquhar RG, Mandigers PJ, Pakozdy A, Bhatti SF, De Risio L, Fischer A, Long S, Matiasek K, Munana K, Patterson EE, Penderis J, Platt S, Podell M, Potschka H, Pumarola MB, Rusbridge C, Stein VM, Tipold A, Volk HA. International veterinary epilepsy task

force consensus report on epilepsy definition, classification and terminology in companion animals. BMC Vet Res 2015; 11: 182.

Bernardo BC, Weeks KL, Patterson NL, McMullen JR. HSP70: therapeutic potential in acute and chronic cardiac disease settings. Future Med Chem 2016; 8: 2177-83.

Bertram EH, Cornett J. The ontogeny of seizures in a rat model of limbic epilepsy: evidence for a kindling process in the development of chronic spontaneous seizures. Brain Res 1993; 625: 295-300.

Bioscience M. Counting Rules. 2019a:
<https://www.stereology.info/counting-rules/>. 27 Jul.

Bioscience M. Some CE Theory. 2019b:
<https://www.stereology.info/some-ce-theory/>. 27 Jul.

Braakman I, Bulleid NJ. Protein folding and modification in the mammalian endoplasmic reticulum. Annu Rev Biochem 2011; 80: 71-99.

Brandt C, Glien M, Potschka H, Volk H, Loscher W. Epileptogenesis and neuropathology after different types of status epilepticus induced by prolonged electrical stimulation of the basolateral amygdala in rats. Epilepsy Res 2003; 55: 83-103.

Brandt C, Volk HA, Loscher W. Striking differences in individual anticonvulsant response to phenobarbital in rats with spontaneous seizures after status epilepticus. Epilepsia 2004; 45: 1488-97.

Buckmaster PS, Lew FH. Rapamycin suppresses mossy fiber sprouting but not seizure frequency in a mouse model of temporal lobe epilepsy. J Neurosci 2011; 31: 2337-47.

Buckmaster PS. Does mossy fiber sprouting give rise to the epileptic state? Adv Exp Med Biol 2014; 813: 161-8.

Casas C. GRP78 at the Centre of the Stage in Cancer and Neuroprotection. *Front Neurosci* 2017; 11: 177.

Chang CC, Chen SD, Lin TK, Chang WN, Liou CW, Chang AY, Chan SH, Chuang YC. Heat shock protein 70 protects against seizure-induced neuronal cell death in the hippocampus following experimental status epilepticus via inhibition of nuclear factor-kappaB activation-induced nitric oxide synthase II expression. *Neurobiol Dis* 2014; 62: 241-9.

Charalambous M, Brodbelt D, Volk HA. Treatment in canine epilepsy-a systematic review. *BMC Vet Res* 2014; 10: 257.

Charalambous M, Pakozdy A, Bhatti SFM, Volk HA. Systematic review of antiepileptic drugs' safety and effectiveness in feline epilepsy. *BMC Vet Res* 2018; 14: 64.

Chen C, Bazan NG. Lipid signaling: sleep, synaptic plasticity, and neuroprotection. *Prostaglandins Other Lipid Mediat* 2005; 77: 65-76.

Chen J, Guo H, Zheng G, Shi ZN. Region-specific vulnerability to endoplasmic reticulum stress-induced neuronal death in rat brain after status epilepticus. *J Biosci* 2013; 38: 877-86.

Chihara Y, Ueda Y, Doi T, Willmore LJ. Role of endoplasmic reticulum stress in the amygdaloid kindling model of rats. *Neurochem Res* 2011; 36: 1834-9.

Clive R. Taylor LR (2006) *Education Guide: Immunohistochemical Staining Methods*, Fourth Edition. Dako Denmark A/S

Cloutier P, Coulombe B. Regulation of molecular chaperones through post-translational modifications: decrypting the chaperone code. *Biochim Biophys Acta* 2013; 1829: 443-54.

Collabolators GE. Global, regional, and national burden of epilepsy,

1990–2016: a systematic analysis for the Global Burden of Disease Study 2016. *The Lancet Neurology* 2019; 18: 357 - 75.

Costes SV, Daelemans D, Cho EH, Dobbin Z, Pavlakis G, Lockett S. Automatic and quantitative measurement of protein-protein colocalization in live cells. *Biophys J* 2004; 86: 3993-4003.

Danzer S. Mossy Fiber Sprouting in the Epileptic Brain: Taking on the Lernaean Hydra. *Epilepsy Curr* 2017; 17: 50-1.

De Maio A, Santoro MG, Tanguay RM, Hightower LE. Ferruccio Ritossa's scientific legacy 50 years after his discovery of the heat shock response: a new view of biology, a new society, and a new journal. *Cell Stress Chaperones* 2012; 17: 139-43.

Deshmukh SS, Knierim JJ. *Hippocampus*. *Wiley Interdiscip Rev Cogn Sci* 2012; 3: 231-51.

Devinsky O, Vezzani A, Najjar S, De Lanerolle NC, Rogawski MA. Glia and epilepsy: excitability and inflammation. *Trends Neurosci* 2013; 36: 174-84.

Devinsky O, Vezzani A, O'Brien TJ, Jette N, Scheffer IE, de Curtis M, Perucca P. *Epilepsy*. *Nat Rev Dis Primers* 2018; 4: 18024.

Dhanasekaran DN, Reddy EP. JNK signaling in apoptosis. *Oncogene* 2008; 27: 6245-51.

Dragovic Z, Broadley SA, Shomura Y, Bracher A, Hartl FU. Molecular chaperones of the Hsp110 family act as nucleotide exchange factors of Hsp70s. *EMBO J* 2006; 25: 2519-28.

Dube CM, Brewster AL, Richichi C, Zha Q, Baram TZ. Fever, febrile seizures and epilepsy. *Trends Neurosci* 2007; 30: 490-6.

Dunn KW, Kamocka MM, McDonald JH. A practical guide to evaluating colocalization in biological microscopy. *Am J Physiol Cell Physiol* 2011; 300: C723-42.

Ekimova IV, Nitsinskaya LE, Romanova IV, Pastukhov YF, Margulis BA, Guzhova IV. Exogenous protein Hsp70/Hsc70 can penetrate into brain structures and attenuate the severity of chemically-induced seizures. *J Neurochem* 2010; 115: 1035-44.

Engel J, Pedley TA. *Epilepsy : a comprehensive textbook*. 2008;

Enogieru AB, Omoruyi SI, Hiss DC, Ekpo OE. GRP78/BIP/HSPA5 as a Therapeutic Target in Models of Parkinson's Disease: A Mini Review. *Adv Pharmacol Sci* 2019; 2019: 2706783.

Erlen A, Potschka H, Volk HA, Sauter-Louis C, O'Neill DG. Seizure occurrence in dogs under primary veterinary care in the UK: prevalence and risk factors. *J Vet Intern Med* 2018; 32: 1665-76.

Eyo UB, Peng J, Swiatkowski P, Mukherjee A, Bispo A, Wu LJ. Neuronal hyperactivity recruits microglial processes via neuronal NMDA receptors and microglial P2Y12 receptors after status epilepticus. *J Neurosci* 2014; 34: 10528-40.

Eyo UB, Murugan M, Wu LJ. Microglia-Neuron Communication in Epilepsy. *Glia* 2017; 65: 5-18.

Ferat-Osorio E, Sanchez-Anaya A, Gutierrez-Mendoza M, Bosco-Garate I, Wong-Baeza I, Pastelin-Palacios R, Pedraza-Alva G, Bonifaz LC, Cortes-Reynosa P, Perez-Salazar E, Arriaga-Pizano L, Lopez-Macias C, Rosenstein Y, Isibasi A. Heat shock protein 70 down-regulates the production of toll-like receptor-induced pro-inflammatory cytokines by a heat shock factor-1/constitutive heat shock element-binding factor-dependent mechanism. *J Inflamm (Lond)* 2014; 11: 19.

Fernandez-Fernandez MR, Valpuesta JM. Hsp70 chaperone: a master player in protein homeostasis. *F1000Res* 2018; 7

Fisher RS, Acevedo C, Arzimanoglou A, Bogacz A, Cross JH, Elger CE, Engel J, Jr., Forsgren L, French JA, Glynn M, Hesdorffer DC, Lee BI, Mathern GW, Moshe SL, Perucca E, Scheffer IE, Tomson T, Watanabe M, Wiebe S. ILAE official report: a practical clinical definition of epilepsy. *Epilepsia* 2014; 55: 475-82.

Fisher RS, Cross JH, French JA, Higurashi N, Hirsch E, Jansen FE, Lagae L, Moshe SL, Peltola J, Roulet Perez E, Scheffer IE, Zuberi SM. Operational classification of seizure types by the International League Against Epilepsy: Position Paper of the ILAE Commission for Classification and Terminology. *Epilepsia* 2017; 58: 522-30.

Fong JJ, Sreedhara K, Deng L, Varki NM, Angata T, Liu Q, Nizet V, Varki A. Immunomodulatory activity of extracellular Hsp70 mediated via paired receptors Siglec-5 and Siglec-14. *EMBO J* 2015; 34: 2775-88.

Frey HH, Loscher W. Pharmacokinetics of anti-epileptic drugs in the dog: a review. *J Vet Pharmacol Ther* 1985; 8: 219-33.

Gao B, Tsan MF. Endotoxin contamination in recombinant human heat shock protein 70 (Hsp70) preparation is responsible for the induction of tumor necrosis factor alpha release by murine macrophages. *J Biol Chem* 2003; 278: 174-9.

Garcia-Finana M, Cruz-Orive LM, Mackay CE, Pakkenberg B, Roberts N. Comparison of MR imaging against physical sectioning to estimate the volume of human cerebral compartments. *Neuroimage* 2003; 18: 505-16.

Genest O, Wickner S, Doyle SM. Hsp90 and Hsp70 chaperones: Collaborators in protein remodeling. *J Biol Chem* 2019; 294: 2109-20.

Gerner C, Vejda S, Gelbmann D, Bayer E, Gotzmann J, Schulte-Hermann R, Mikulits W. Concomitant determination of absolute values of cellular protein amounts, synthesis rates, and turnover rates by quantitative proteome profiling. *Mol Cell Proteomics* 2002; 1: 528-37.

Gross RA. A brief history of epilepsy and its therapy in the Western Hemisphere. *Epilepsy Res* 1992; 12: 65-74.

Gundersen HJ. Stereology of arbitrary particles. A review of unbiased number and size estimators and the presentation of some new ones, in memory of William R. Thompson. *J Microsc* 1986; 143: 3-45.

Gundersen HJ, Jensen EB. The efficiency of systematic sampling in stereology and its prediction. *J Microsc* 1987; 147: 229-63.

Gundersen HJ, Jensen EB, Kieu K, Nielsen J. The efficiency of systematic sampling in stereology--reconsidered. *J Microsc* 1999; 193: 199-211.

Guo L, Chen Y, Zhao R, Wang G, Friedman E, Zhang A, Zhen X. Allosteric modulation of sigma-1 receptors elicits anti-seizure activities. *Br J Pharmacol* 2015; 172: 4052-65.

Hamamoto Y, Hasegawa D, Mizoguchi S, Yu Y, Wada M, Kuwabara T, Fujiwara-Igarashi A, Fujita M. Retrospective epidemiological study of canine epilepsy in Japan using the International Veterinary Epilepsy Task Force classification 2015 (2003-2013): etiological distribution, risk factors, survival time, and lifespan. *BMC Vet Res* 2016; 12: 248.

Henshall DC, Kobow K. Epigenetics and Epilepsy. *Cold Spring Harb Perspect Med* 2015; 5

Hong S, Van Kaer L. Immune privilege: keeping an eye on natural killer T cells. *J Exp Med* 1999; 190: 1197-200.

Hu F, Zhou J, Lu Y, Guan L, Wei NN, Tang YQ, Wang K. Inhibition of

Hsp70 Suppresses Neuronal Hyperexcitability and Attenuates Epilepsy by Enhancing A-Type Potassium Current. *Cell Rep* 2019; 26: 168-81 e4.

Hughes D, Mallucci GR. The unfolded protein response in neurodegenerative disorders - therapeutic modulation of the PERK pathway. *FEBS J* 2019; 286: 342-55.

ILAE. The 2014 Definition of Epilepsy: A perspective for patients and caregivers. 2014: <https://www.ilae.org/guidelines/definition-and-classification/the-2014-definition-of-epilepsy-a-perspective-for-patients-and-caregivers>. 29 Jul.

ImageJ NIOH, Bethesda,. Optical Density Calibration. <https://imagej.nih.gov/ij/docs/examples/calibration/>. 18 Mar.

Iori V, Iyer AM, Ravizza T, Beltrame L, Paracchini L, Marchini S, Cerovic M, Hill C, Ferrari M, Zucchetti M, Molteni M, Rossetti C, Brambilla R, Steve White H, D'Incalci M, Aronica E, Vezzani A. Blockade of the IL-1R1/TLR4 pathway mediates disease-modification therapeutic effects in a model of acquired epilepsy. *Neurobiol Dis* 2017; 99: 12-23.

Janssens S, Beyaert R. Role of Toll-like receptors in pathogen recognition. *Clin Microbiol Rev* 2003; 16: 637-46.

Jensen RL, Stone JL, Hayne RA. Introduction of the human Horsley-Clarke stereotactic frame. *Neurosurgery* 1996; 38: 563-7; discussion 7.

Kampinga HH, Hageman J, Vos MJ, Kubota H, Tanguay RM, Bruford EA, Cheetham ME, Chen B, Hightower LE. Guidelines for the nomenclature of the human heat shock proteins. *Cell Stress Chaperones* 2009; 14: 105-11.

Kandel EI. Soviet investigations in epilepsy. *Acta Neurochir Suppl*

(Wien) 1990; 50: 136-41.

Kandel ER, Schwartz JH, Jessell TM (2000) Principles of neural science, 4th edn. McGraw-Hill, Health Professions Division, New York. xli, 1414 p.

Kawai T, Akira S. The role of pattern-recognition receptors in innate immunity: update on Toll-like receptors. *Nat Immunol* 2010; 11: 373-84.

Kawasaki T, Kawai T. Toll-like receptor signaling pathways. *Front Immunol* 2014; 5: 461.

Kearsley-Fleet L, O'Neill DG, Volk HA, Church DB, Brodbelt DC. Prevalence and risk factors for canine epilepsy of unknown origin in the UK. *Vet Rec* 2013; 172: 338.

Keck M, van Dijk RM, Deeg CA, Kistler K, Walker A, von Ruden EL, Russmann V, Hauck SM, Potschka H. Proteomic profiling of epileptogenesis in a rat model: Focus on cell stress, extracellular matrix and angiogenesis. *Neurobiol Dis* 2018; 112: 119-35.

Kern J, Untergasser G, Zenzmaier C, Sarg B, Gastl G, Gunsilius E, Steurer M. GRP-78 secreted by tumor cells blocks the antiangiogenic activity of bortezomib. *Blood* 2009; 114: 3960-7.

Kim JY, Yenari MA. The immune modulating properties of the heat shock proteins after brain injury. *Anat Cell Biol* 2013; 46: 1-7.

Kim JY, Han Y, Lee JE, Yenari MA. The 70-kDa heat shock protein (Hsp70) as a therapeutic target for stroke. *Expert Opin Ther Targets* 2018; 22: 191-9.

Kirkegaard T, Gray J, Priestman DA, Wallom KL, Atkins J, Olsen OD, Klein A, Drndarski S, Petersen NH, Ingemann L, Smith DA, Morris L, Bornaes C, Jorgensen SH, Williams I, Hinsby A, Arenz C, Begley D,

Jaattela M, Platt FM. Heat shock protein-based therapy as a potential candidate for treating the sphingolipidoses. *Sci Transl Med* 2016; 8: 355ra118.

Kitao Y, Ozawa K, Miyazaki M, Tamatani M, Kobayashi T, Yanagi H, Okabe M, Ikawa M, Yamashima T, Stern DM, Hori O, Ogawa S. Expression of the endoplasmic reticulum molecular chaperone (ORP150) rescues hippocampal neurons from glutamate toxicity. *J Clin Invest* 2001; 108: 1439-50.

Kitao Y, Hashimoto K, Matsuyama T, Iso H, Tamatani T, Hori O, Stern DM, Kano M, Ozawa K, Ogawa S. ORP150/HSP12A regulates Purkinje cell survival: a role for endoplasmic reticulum stress in cerebellar development. *J Neurosci* 2004; 24: 1486-96.

Kornmann B, Currie E, Collins SR, Schuldiner M, Nunnari J, Weissman JS, Walter P. An ER-mitochondria tethering complex revealed by a synthetic biology screen. *Science* 2009; 325: 477-81.

Korobchevskaya K, Lagerholm BC, Colin-York H, Fritzsche M. Exploring the Potential of Airyscan Microscopy for Live Cell Imaging. *Photonics* 2017; 4: 41.

Kumar S, Stokes J, 3rd, Singh UP, Scissum Gunn K, Acharya A, Manne U, Mishra M. Targeting Hsp70: A possible therapy for cancer. *Cancer Lett* 2016; 374: 156-66.

Kwan P, Arzimanoglou A, Berg AT, Brodie MJ, Allen Hauser W, Mathern G, Moshe SL, Perucca E, Wiebe S, French J. Definition of drug resistant epilepsy: consensus proposal by the ad hoc Task Force of the ILAE Commission on Therapeutic Strategies. *Epilepsia* 2010; 51: 1069-77.

Li Q, Lau A, Morris TJ, Guo L, Fordyce CB, Stanley EF. A syntaxin 1, Galpha(o), and N-type calcium channel complex at a presynaptic nerve terminal: analysis by quantitative immunocolocalization. *J Neurosci* 2004; 24: 4070-81.

Lin BL, Wang JS, Liu HC, Chen RW, Meyer Y, Barakat A, Delseny M. Genomic analysis of the Hsp70 superfamily in *Arabidopsis thaliana*. *Cell Stress Chaperones* 2001; 6: 201-8.

Lively S, Brown IR. Induction of heat shock proteins in the adult rat cerebral cortex following pilocarpine-induced status epilepticus. *Brain Res* 2011; 1368: 271-80.

Loscher W, Schwartz-Porsche D, Frey HH, Schmidt D. Evaluation of epileptic dogs as an animal model of human epilepsy. *Arzneimittelforschung* 1985; 35: 82-7.

Loscher W, Ebert U. The role of the piriform cortex in kindling. *Prog Neurobiol* 1996; 50: 427-81.

Loscher W, Potschka H, Rieck S, Tipold A, Rundfeldt C. Anticonvulsant efficacy of the low-affinity partial benzodiazepine receptor agonist ELB 138 in a dog seizure model and in epileptic dogs with spontaneously recurrent seizures. *Epilepsia* 2004; 45: 1228-39.

Loscher W. Critical review of current animal models of seizures and epilepsy used in the discovery and development of new antiepileptic drugs. *Seizure* 2011; 20: 359-68.

Louessard M, Bardou I, Lemarchand E, Thiebaut AM, Parcq J, Leprince J, Terrisse A, Carraro V, Fafournoux P, Bruhat A, Orset C, Vivien D, Ali C, Roussel BD. Activation of cell surface GRP78 decreases endoplasmic reticulum stress and neuronal death. *Cell Death Differ* 2017; 24: 1518-29.

Magna M, Pisetsky DS. The role of HMGB1 in the pathogenesis of inflammatory and autoimmune diseases. *Mol Med* 2014; 20: 138-46.

Malhotra JD, Kaufman RJ. ER stress and its functional link to mitochondria: role in cell survival and death. *Cold Spring Harb Perspect Biol* 2011; 3: a004424.

Malyshev I (2013) Immunity, tumors and aging : the role of HSP70

Mambula SS, Calderwood SK. Heat shock protein 70 is secreted from tumor cells by a nonclassical pathway involving lysosomal endosomes. *J Immunol* 2006; 177: 7849-57.

Marin-Briggiler CI, Gonzalez-Echeverria MF, Munuce MJ, Ghersevich S, Caille AM, Hellman U, Corrigan VM, Vazquez-Levin MH. Glucose-regulated protein 78 (Grp78/BiP) is secreted by human oviduct epithelial cells and the recombinant protein modulates sperm-zona pellucida binding. *Fertil Steril* 2010; 93: 1574-84.

Maroso M, Balosso S, Ravizza T, Liu J, Aronica E, Iyer AM, Rossetti C, Molteni M, Casalgrandi M, Manfredi AA, Bianchi ME, Vezzani A. Toll-like receptor 4 and high-mobility group box-1 are involved in iktogenesis and can be targeted to reduce seizures. *Nat Med* 2010; 16: 413-9.

Maroso M, Balosso S, Ravizza T, Liu J, Bianchi ME, Vezzani A. Interleukin-1 type 1 receptor/Toll-like receptor signalling in epilepsy: the importance of IL-1beta and high-mobility group box 1. *J Intern Med* 2011; 270: 319-26.

Martin CB, Mirsattari SM, Pruessner JC, Pietrantonio S, Burneo JG, Hayman-Abello B, Kohler S. Deja vu in unilateral temporal-lobe epilepsy is associated with selective familiarity impairments on experimental tasks of recognition memory. *Neuropsychologia* 2012; 50: 2981-91.

Martinez A, Lopez N, Gonzalez C, Hetz C. Targeting of the unfolded protein response (UPR) as therapy for Parkinson's disease. *Biol Cell* 2019; 111: 161-8.

Mathieu P, Piantanida AP, Pitossi F. Chronic expression of transforming growth factor-beta enhances adult neurogenesis. *Neuroimmunomodulation* 2010; 17: 200-1.

McIntyre DC, Nathanson D, Edson N. A new model of partial status epilepticus based on kindling. *Brain Res* 1982; 250: 53-63.

Mody I. The GAD-given Right of Dentate Gyrus Granule Cells to Become GABAergic. *Epilepsy Curr* 2002; 2: 143-5.

Morales-Sosa M, Orozco-Suarez S, Vega-Garcia A, Caballero-Chacon S, Feria-Romero IA. Immunomodulatory effect of Celecoxib on HMGB1/TLR4 pathway in a recurrent seizures model in immature rats. *Pharmacol Biochem Behav* 2018; 170: 79-86.

Morgner N, Schmidt C, Beilsten-Edmands V, Ebong IO, Patel NA, Clerico EM, Kirschke E, Daturpalli S, Jackson SE, Agard D, Robinson CV. Hsp70 forms antiparallel dimers stabilized by post-translational modifications to position clients for transfer to Hsp90. *Cell Rep* 2015; 11: 759-69.

Nain M, Mukherjee S, Karmakar SP, Paton AW, Paton JC, Abdin MZ, Basu A, Kalia M, Vрати S. GRP78 Is an Important Host Factor for Japanese Encephalitis Virus Entry and Replication in Mammalian Cells. *J Virol* 2017; 91

Nakayama Y, Masuda H, Shirozu H, Ito Y, Higashijima T, Kitaura H, Fujii Y, Kakita A, Fukuda M. Features of amygdala in patients with mesial temporal lobe epilepsy and hippocampal sclerosis: An MRI volumetric and histopathological study. *Epilepsy Res* 2017; 135: 50-5.

Nguyen L, Lucke-Wold BP, Mookerjee SA, Cavendish JZ, Robson MJ, Scandinaro AL, Matsumoto RR. Role of sigma-1 receptors in neurodegenerative diseases. *J Pharmacol Sci* 2015; 127: 17-29.

Ni M, Zhang Y, Lee AS. Beyond the endoplasmic reticulum: atypical GRP78 in cell viability, signalling and therapeutic targeting. *Biochem J* 2011; 434: 181-8.

Ongerth T, Russmann V, Fischborn S, Boes K, Siegl C, Potschka H.

Targeting of microglial KCa3.1 channels by TRAM-34 exacerbates hippocampal neurodegeneration and does not affect ictogenesis and epileptogenesis in chronic temporal lobe epilepsy models. *Eur J Pharmacol* 2014; 740: 72-80.

Organisation WH. Epilepsy. 2019: <https://www.who.int/news-room/fact-sheets/detail/epilepsy>. 27 Jul.

Oswald Steward CSW, Paul F. Worley. Synaptic plasticity in epileptogenesis: Cellular mechanisms underlying long-lasting synaptic modifications that require new gene expression. *International Review of Neurobiology* 2001; 45: 269 - 92.

Packer RM, Shihab NK, Torres BB, Volk HA. Clinical risk factors associated with anti-epileptic drug responsiveness in canine epilepsy. *PLoS One* 2014; 9: e106026.

Pakozdy A, Halasz P, Klang A. Epilepsy in cats: theory and practice. *J Vet Intern Med* 2014; 28: 255-63.

Pandolfi F, Altamura S, Frosali S, Conti P. Key Role of DAMP in Inflammation, Cancer, and Tissue Repair. *Clin Ther* 2016; 38: 1017-28.

Panteliadis CP, Vassilyadi P, Fehlert J, Hagel C. Historical documents on epilepsy: From antiquity through the 20th century. *Brain Dev* 2017; 39: 457-63.

Parent JM, Kron MM. Neurogenesis and Epilepsy. In: Jasper's Basic Mechanisms of the Epilepsies. th, Noebels JL, Avoli M, Rogawski MA, Olsen RW, Delgado-Escueta AV, eds. Bethesda (MD): 2012:

Park JS, Gamboni-Robertson F, He Q, Svetkauskaite D, Kim JY, Strassheim D, Sohn JW, Yamada S, Maruyama I, Banerjee A, Ishizaka A, Abraham E. High mobility group box 1 protein interacts with multiple Toll-like receptors. *Am J Physiol Cell Physiol* 2006; 290:

C917-24.

Paudel YN, Shaikh MF, Chakraborti A, Kumari Y, Aledo-Serrano A, Aleksovska K, Alvim MKM, Othman I. HMGB1: A Common Biomarker and Potential Target for TBI, Neuroinflammation, Epilepsy, and Cognitive Dysfunction. *Front Neurosci* 2018; 12: 628.

Pavlik A, Aneja IS. Cerebral neurons and glial cell types inducing heat shock protein Hsp70 following heat stress in the rat. *Prog Brain Res* 2007; 162: 417-31.

Paxinos G, Watson C (2005) *The rat brain in stereotaxic coordinates*. Elsevier Academic Press, Amsterdam; Boston

Piredda S, Gale K. A crucial epileptogenic site in the deep prepiriform cortex. *Nature* 1985; 317: 623-5.

Pitkanen A. Therapeutic approaches to epileptogenesis--hope on the horizon. *Epilepsia* 2010; 51 Suppl 3: 2-17.

Pitkanen A, Lukasiuk K, Dudek FE, Staley KJ. *Epileptogenesis*. Cold Spring Harb Perspect Med 2015; 5

Pockley AG, Shepherd J, Corton JM. Detection of heat shock protein 70 (Hsp70) and anti-Hsp70 antibodies in the serum of normal individuals. *Immunol Invest* 1998; 27: 367-77.

Potschka H, Fischer A, von Ruden EL, Hulsmeier V, Baumgartner W. Canine epilepsy as a translational model? *Epilepsia* 2013; 54: 571-9.

Potschka H. Animal and human data: where are our concepts for drug-resistant epilepsy going? *Epilepsia* 2013; 54 Suppl 2: 29-32.

Preissler S, Ron D. Early Events in the Endoplasmic Reticulum Unfolded Protein Response. *Cold Spring Harb Perspect Biol* 2018;

Preissler S, Ron D. Early Events in the Endoplasmic Reticulum Unfolded Protein Response. *Cold Spring Harb Perspect Biol* 2019; 11

Racine R, Okujava V, Chipashvili S. Modification of seizure activity by electrical stimulation. 3. Mechanisms. *Electroencephalogr Clin Neurophysiol* 1972; 32: 295-9.

Rajkowska G, Clarke G, Mahajan G, Licht CM, van de Werd HJ, Yuan P, Stockmeier CA, Manji HK, Uylings HB. Differential effect of lithium on cell number in the hippocampus and prefrontal cortex in adult mice: a stereological study. *Bipolar Disord* 2016; 18: 41-51.

Ramón y Cajal S (1995) *Histology of the nervous system of man and vertebrates*. Oxford University Press, New York

Ravizza T, Balosso S, Vezzani A. Inflammation and prevention of epileptogenesis. *Neurosci Lett* 2011; 497: 223-30.

Ravizza T, Terrone G, Salamone A, Frigerio F, Balosso S, Antoine DJ, Vezzani A. High Mobility Group Box 1 is a novel pathogenic factor and a mechanistic biomarker for epilepsy. *Brain Behav Immun* 2018; 72: 14-21.

Remy S, Beck H. Molecular and cellular mechanisms of pharmacoresistance in epilepsy. *Brain* 2006; 129: 18-35.

Riazi K, Galic MA, Pittman QJ. Contributions of peripheral inflammation to seizure susceptibility: cytokines and brain excitability. *Epilepsy Res* 2010; 89: 34-42.

Richter-Landsberg C (2011) *Heat shock proteins in neural cells*. Springer, New York; London

Rodgers KM, Hutchinson MR, Northcutt A, Maier SF, Watkins LR, Barth DS. The cortical innate immune response increases local neuronal excitability leading to seizures. *Brain* 2009; 132: 2478-86.

Ruifrok AC, Johnston DA. Quantification of histochemical staining by color deconvolution. *Anal Quant Cytol Histol* 2001; 23: 291-9.

Samborski P, Grzymislowski M. The Role of HSP70 Heat Shock Proteins in the Pathogenesis and Treatment of Inflammatory Bowel Diseases. *Adv Clin Exp Med* 2015; 24: 525-30.

Santhakumar V, Aradi I, Soltesz I. Role of mossy fiber sprouting and mossy cell loss in hyperexcitability: a network model of the dentate gyrus incorporating cell types and axonal topography. *J Neurophysiol* 2005; 93: 437-53.

Sanz O, Estrada A, Ferrer I, Planas AM. Differential cellular distribution and dynamics of HSP70, cyclooxygenase-2, and c-Fos in the rat brain after transient focal ischemia or kainic acid. *Neuroscience* 1997; 80: 221-32.

Sarac S, Afzal S, Broholm H, Madsen FF, Ploug T, Laursen H. Excitatory amino acid transporters EAAT-1 and EAAT-2 in temporal lobe and hippocampus in intractable temporal lobe epilepsy. *APMIS* 2009; 117: 291-301.

Scaffidi P, Misteli T, Bianchi ME. Release of chromatin protein HMGB1 by necrotic cells triggers inflammation. *Nature* 2002; 418: 191-5.

Schneider CA, Rasband WS, Eliceiri KW. NIH Image to ImageJ: 25 years of image analysis. *Nat Methods* 2012; 9: 671-5.

Schwartz-Porsche D, Loscher W, Frey HH. Therapeutic efficacy of phenobarbital and primidone in canine epilepsy: a comparison. *J Vet Pharmacol Ther* 1985; 8: 113-9.

Sharma AK, Rani E, Waheed A, Rajput SK. Pharmacoresistant Epilepsy: A Current Update on Non-Conventional Pharmacological and Non-Pharmacological Interventions. *J Epilepsy Res* 2015; 5: 1-8.

Shen Y, Qin H, Chen J, Mou L, He Y, Yan Y, Zhou H, Lv Y, Chen Z, Wang J, Zhou YD. Postnatal activation of TLR4 in astrocytes promotes excitatory synaptogenesis in hippocampal neurons. *J Cell Biol* 2016; 215: 719-34.

Singleton KD, Wischmeyer PE. Effects of HSP70.1/3 gene knockout on acute respiratory distress syndrome and the inflammatory response following sepsis. *Am J Physiol Lung Cell Mol Physiol* 2006; 290: L956-61.

Sloviter RS, Zappone CA, Harvey BD, Frotscher M. Kainic acid-induced recurrent mossy fiber innervation of dentate gyrus inhibitory interneurons: possible anatomical substrate of granule cell hyperinhibition in chronically epileptic rats. *J Comp Neurol* 2006; 494: 944-60.

Smith JA. Regulation of Cytokine Production by the Unfolded Protein Response; Implications for Infection and Autoimmunity. *Front Immunol* 2018; 9: 422.

Sobieski C, Christian CA. Developmental Inflammation Takes a Toll: Early Immune Responses Increase Seizure Susceptibility via Astrocytic TLR4 Signaling. *Epilepsy Curr* 2017; 17: 370-1.

Sokka AL, Putkonen N, Mudo G, Pryazhnikov E, Reijonen S, Khiroug L, Belluardo N, Lindholm D, Korhonen L. Endoplasmic reticulum stress inhibition protects against excitotoxic neuronal injury in the rat brain. *J Neurosci* 2007; 27: 901-8.

Squire LR. *Encyclopedia of neuroscience*. 2009;

Tamatani M, Matsuyama T, Yamaguchi A, Mitsuda N, Tsukamoto Y, Taniguchi M, Che YH, Ozawa K, Hori O, Nishimura H, Yamashita A, Okabe M, Yanagi H, Stern DM, Ogawa S, Tohyama M. ORP150 protects against hypoxia/ischemia-induced neuronal death. *Nat Med* 2001; 7: 317-23.

Thom M. Review: Hippocampal sclerosis in epilepsy: a neuropathology review. *Neuropathol Appl Neurobiol* 2014; 40: 520-43.

Timberlake M, 2nd, Prall K, Roy B, Dwivedi Y. Unfolded protein response and associated alterations in toll-like receptor expression and interaction in the hippocampus of restraint rats. *Psychoneuroendocrinology* 2018; 89: 185-93.

Tsan MF, Gao B. Endogenous ligands of Toll-like receptors. *J Leukoc Biol* 2004; 76: 514-9.

Tsuchida S, Arai Y, Takahashi KA, Kishida T, Terauchi R, Honjo K, Nakagawa S, Inoue H, Ikoma K, Ueshima K, Matsuki T, Mazda O, Kubo T. HIF-1alpha-induced HSP70 regulates anabolic responses in articular chondrocytes under hypoxic conditions. *J Orthop Res* 2014; 32: 975-80.

Tsunemi S, Nakanishi T, Fujita Y, Bouras G, Miyamoto Y, Miyamoto A, Nomura E, Takubo T, Tanigawa N. Proteomics-based identification of a tumor-associated antigen and its corresponding autoantibody in gastric cancer. *Oncol Rep* 2010; 23: 949-56.

Turturici G, Sconzo G, Geraci F. Hsp70 and its molecular role in nervous system diseases. *Biochem Res Int* 2011; 2011: 618127.

UniProt. UniProtKB - P0DMV8 (HS71A_HUMAN). 2019a:
<https://www.uniprot.org/uniprot/P0DMV8>. 27 Jul.

UniProt. UniProtKB - Q9Y4L1 (HYOU1_HUMAN). 2019b:
<https://www.uniprot.org/uniprot/Q9Y4L1>. 27 Jul.

UniProt. UniProtKB - G1MDU7 (G1MDU7_AILME). 2019c:
<https://www.uniprot.org/uniprot/G1MDU7>. 27 Jul.

Uriarte A, Maestro Saiz I. Canine versus human epilepsy: are we up to date? *J Small Anim Pract* 2016; 57: 115-21.

Vabulas RM, Ahmad-Nejad P, Ghose S, Kirschning CJ, Issels RD, Wagner H. HSP70 as endogenous stimulus of the Toll/interleukin-1 receptor signal pathway. *J Biol Chem* 2002a; 277: 15107-12.

Vabulas RM, Wagner H, Schild H. Heat shock proteins as ligands of toll-like receptors. *Curr Top Microbiol Immunol* 2002b; 270: 169-84.

van Vliet EA, Otte WM, Wadman WJ, Aronica E, Kooij G, de Vries HE, Dijkhuizen RM, Gorter JA. Blood-brain barrier leakage after status epilepticus in rapamycin-treated rats I: Magnetic resonance imaging. *Epilepsia* 2016; 57: 59-69.

Vass K, Berger ML, Nowak TS, Jr., Welch WJ, Lassmann H. Induction of stress protein HSP70 in nerve cells after status epilepticus in the rat. *Neurosci Lett* 1989; 100: 259-64.

Vaughan DN, Jackson GD. The piriform cortex and human focal epilepsy. *Front Neurol* 2014; 5: 259.

Vaure C, Liu Y. A comparative review of toll-like receptor 4 expression and functionality in different animal species. *Front Immunol* 2014; 5: 316.

Vavers E, Svalbe B, Lauberte L, Stonans I, Misane I, Dambrova M, Zvejniece L. The activity of selective sigma-1 receptor ligands in seizure models in vivo. *Behav Brain Res* 2017; 328: 13-8.

Vega VL, Rodriguez-Silva M, Frey T, Gehrman M, Diaz JC, Steinem C, Multhoff G, Arispe N, De Maio A. Hsp70 translocates into the plasma membrane after stress and is released into the extracellular environment in a membrane-associated form that activates macrophages. *J Immunol* 2008; 180: 4299-307.

Venereau E, Ceriotti C, Bianchi ME. DAMPs from Cell Death to New Life. *Front Immunol* 2015; 6: 422.

Vezzani A, Moneta D, Richichi C, Aliprandi M, Burrows SJ, Ravizza T, Perego C, De Simoni MG. Functional role of inflammatory cytokines and antiinflammatory molecules in seizures and epileptogenesis. *Epilepsia* 2002; 43 Suppl 5: 30-5.

Vezzani A, Maroso M, Balosso S, Sanchez MA, Bartfai T. IL-1 receptor/Toll-like receptor signaling in infection, inflammation, stress and neurodegeneration couples hyperexcitability and seizures. *Brain Behav Immun* 2011a; 25: 1281-9.

Vezzani A, French J, Bartfai T, Baram TZ. The role of inflammation in epilepsy. *Nat Rev Neurol* 2011b; 7: 31-40.

Vezzani A, Aronica E, Mazarati A, Pittman QJ. Epilepsy and brain inflammation. *Exp Neurol* 2013a; 244: 11-21.

Vezzani A, Friedman A, Dingledine RJ. The role of inflammation in epileptogenesis. *Neuropharmacology* 2013b; 69: 16-24.

Vezzani A, Lang B, Aronica E. Immunity and Inflammation in Epilepsy. *Cold Spring Harb Perspect Med* 2015; 6: a022699.

Vezzani A, Fujinami RS, White HS, Preux PM, Blumcke I, Sander JW, Loscher W. Infections, inflammation and epilepsy. *Acta Neuropathol* 2016; 131: 211-34.

Vezzani A, Balosso S, Ravizza T. Neuroinflammatory pathways as treatment targets and biomarkers in epilepsy. *Nat Rev Neurol* 2019;

Vismer MS, Forcelli PA, Skopin MD, Gale K, Koubeissi MZ. The piriform, perirhinal, and entorhinal cortex in seizure generation. *Front Neural Circuits* 2015; 9: 27.

von Ruden EL, Wolf F, Keck M, Gualtieri F, Nowakowska M, Oglesbee M, Potschka H. Genetic Modulation of HSPA1A Accelerates Kindling Progression and Exerts Pro-convulsant Effects. *Neuroscience* 2018;

386: 108-20.

von Ruden EL, Wolf F, Gualtieri F, Keck M, Hunt CR, Pandita TK, Potschka H. Genetic and Pharmacological Targeting of Heat Shock Protein 70 in the Mouse Amygdala-Kindling Model. *ACS Chem Neurosci* 2019; 10: 1434-44.

von Ruden EL, Gualtieri F, Schonhoff K, Reiber M, Wolf F, Baumgartner W, Hansmann F, Tipold A, Potschka H. Molecular alterations of the TLR4-signaling cascade in canine epilepsy. *BMC Vet Res* 2020; 16: 18.

Vos MJ, Hageman J, Carra S, Kampinga HH. Structural and functional diversities between members of the human HSPB, HSPH, HSPA, and DNAJ chaperone families. *Biochemistry* 2008; 47: 7001-11.

Walker A, Russmann V, Deeg CA, von Toerne C, Kleinwort KJH, Szober C, Rettenbeck ML, von Ruden EL, Goc J, Ongerth T, Boes K, Salvamoser JD, Vezzani A, Hauck SM, Potschka H. Proteomic profiling of epileptogenesis in a rat model: Focus on inflammation. *Brain Behav Immun* 2016; 53: 138-58.

Wally Welker JIJ, Adrienne Noe. *Cell Stain Brain Atlas of the Domestic Dog (Basenji)*. 2015: 30 Jul.

Wang FX, Yang XL, Ma YS, Wei YJ, Yang MH, Chen X, Chen B, He Q, Yang QW, Yang H, Liu SY. TRIF contributes to epileptogenesis in temporal lobe epilepsy during TLR4 activation. *Brain Behav Immun* 2018a; 67: 65-76.

Wang H, Pezeshki AM, Yu X, Guo C, Subjectk JR, Wang XY. The Endoplasmic Reticulum Chaperone GRP170: From Immunobiology to Cancer Therapeutics. *Front Oncol* 2014; 4: 377.

Wang M, Wey S, Zhang Y, Ye R, Lee AS. Role of the unfolded protein response regulator GRP78/BiP in development, cancer, and

neurological disorders. *Antioxid Redox Signal* 2009; 11: 2307-16.

Wang M, Law ME, Castellano RK, Law BK. The unfolded protein response as a target for anticancer therapeutics. *Crit Rev Oncol Hematol* 2018b; 127: 66-79.

West MJ, Slomianka L, Gundersen HJ. Unbiased stereological estimation of the total number of neurons in the subdivisions of the rat hippocampus using the optical fractionator. *Anat Rec* 1991; 231: 482-97.

Williams PA, White AM, Clark S, Ferraro DJ, Swiercz W, Staley KJ, Dudek FE. Development of spontaneous recurrent seizures after kainate-induced status epilepticus. *J Neurosci* 2009; 29: 2103-12.

Witter MP, Groenewegen HJ. Connections of the parahippocampal cortex in the cat. III. Cortical and thalamic efferents. *J Comp Neurol* 1986; 252: 1-31.

Xiao H, Wu R. Quantitative investigation of human cell surface N-glycoprotein dynamics. *Chem Sci* 2017; 8: 268-77.

Yang T, Hsu C, Liao W, Chuang JS. Heat shock protein 70 expression in epilepsy suggests stress rather than protection. *Acta Neuropathol* 2008; 115: 219-30.

Yenari MA, Fink SL, Sun GH, Chang LK, Patel MK, Kunis DM, Onley D, Ho DY, Sapolsky RM, Steinberg GK. Gene therapy with HSP72 is neuroprotective in rat models of stroke and epilepsy. *Ann Neurol* 1998; 44: 584-91.

Yu L, Wang L, Chen S. Endogenous toll-like receptor ligands and their biological significance. *J Cell Mol Med* 2010; 14: 2592-603.

Zack GW, Rogers WE, Latt SA. Automatic measurement of sister chromatid exchange frequency. *J Histochem Cytochem* 1977; 25:

741-53.

Zhang G, Wang X, Gillette TG, Deng Y, Wang ZV. Unfolded Protein Response as a Therapeutic Target in Cardiovascular Disease. *Curr Top Med Chem* 2019; 19: 1902-17.

Zhang Y, Zhang X, Shan P, Hunt CR, Pandita TK, Lee PJ. A protective Hsp70-TLR4 pathway in lethal oxidant lung injury. *J Immunol* 2013a; 191: 1393-403.

Zhang YK, Liu JT, Peng ZW, Fan H, Yao AH, Cheng P, Liu L, Ju G, Kuang F. Different TLR4 expression and microglia/macrophage activation induced by hemorrhage in the rat spinal cord after compressive injury. *J Neuroinflammation* 2013b; 10: 112.

Zhao J, Wang Y, Xu C, Liu K, Wang Y, Chen L, Wu X, Gao F, Guo Y, Zhu J, Wang S, Nishibori M, Chen Z. Therapeutic potential of an anti-high mobility group box-1 monoclonal antibody in epilepsy. *Brain Behav Immun* 2017; 64: 308-19.

Zhu X, Dong J, Han B, Huang R, Zhang A, Xia Z, Chang H, Chao J, Yao H. Neuronal Nitric Oxide Synthase Contributes to PTZ Kindling Epilepsy-Induced Hippocampal Endoplasmic Reticulum Stress and Oxidative Damage. *Front Cell Neurosci* 2017; 11: 377.

Zuiderweg ER, Bertelsen EB, Rousaki A, Mayer MP, Gestwicki JE, Ahmad A. Allosteric in the Hsp70 chaperone proteins. *Top Curr Chem* 2013; 328: 99-153.

Zukor KA, Kent DT, Odelberg SJ. Fluorescent whole-mount method for visualizing three-dimensional relationships in intact and regenerating adult newt spinal cords. *Dev Dyn* 2010; 239: 3048-57.

XI. ADDENDUM

1. Software and devices

<i>Instrument</i>	<i>Producent</i>
Affinity Photo	Serif (Europe) Ltd, United Kingdom
Axiocam	Carl Zeiss Microscopy GmbH, Germany
Axiovision	AxioVision, RRID:SCR_002677, Carl Zeiss Microscopy GmbH, Germany
BH2 bright field microscope	Olympus, Japan
Centrifuge 5418	Eppendorf, Wesseling-Berzdorf, Germany
Confocal laser scanning microscope Zeiss LSM880	Zeiss LSM 880 with Airyscan, RRID:SCR_015963, Carl Zeiss Microscopy GmbH, Germany
Cover slips	H878.2, Carl Roth, Germany
Cryostat Microm HM560	Thermo Fisher Scientific, USA

EndNote X8	EndNote, RRID:SCR_014001, Clarivate Analytics, USA
Fiji	Fiji, RRID:SCR_002285, National Institutes of health, USA
GraphPad Prism 5	GraphPad Prism, RRID:SCR_002798, GraphPad Software Inc., USA
ImageJ	ImageJ, RRID:SCR_003070, National Institutes of health, USA
Keyence BZ X-710 fluorescent microscope	BZ X-710 fluorescent microscope, RRID:SCR_017202, Keyence, Japan
BZ Analyzer	BZ Analyzer software, RRID:SCR_017205, Keyence, Japan
Leica DMLB bright field microscope	Leica Microsystems GmbH, Germany
Magnetic stirrer with heating plate	VWR International GmbH, Germany
Magnetic stirring bars	VWR International GmbH, Germany
Microsoft Office	Microsoft Corporation, USA
Motorised stage	MBF Bioscience, USA
OCT Compound	Electron Microscopy Sciences – USA

Personal computer	Diverse
pH-meter	Hanna instruments, Croatia
Precision cover glasses thickness No. 1.5H	Paul Marienfeld GmbH & Co. KG, Germany
Shaker Unimax 1010	Heidolph Instruments GmbH & Co. KG, Germany
Stereo Investigator 11.0	Stereo Investigator, RRID:SCR_002526, MBF Bioscience, USA
SuperFrost Plus microscope slides	Thermo Fisher Scientific, USA
Vortexer LMS® VTX- 300OL Mixer UZUSIO	Hartenstein, Germany
Water bath Typ 24900	Medax Nagel GmbH & Co KG, Germany
Zen software: Black edition	ZEN Digital Imaging for Light Microscopy, RRID:SCR_013672, Carl Zeiss Microscopy GmbH, Germany
Zen software: Blue edition	ZEN Digital Imaging for Light Microscopy, RRID:SCR_013672, Carl Zeiss Microscopy GmbH, Germany

2. Solutions and substances

Solutions

3,3'-diaminobenzidine reaction solution

Antibody carriers (depending on the staining)

Block (depending on the staining)

Hoechst 33342 working solution

Hydrogen peroxide working solution

PBS

PBS-T

Sodium citrate buffer

TBS

TBS-T

Tris-Nickel solution

Substances

Substance	Producer
<i>Primary antibodies:</i>	
Anti-GFAP antibody (mouse, monoclonal, clone 2A5)	Abcam Cat# ab4648, RRID:AB_449329, Lot# GR309691-7
Anti-GFAP antibody (rabbit, polyclonal)	Abcam Cat# ab7260, RRID: AB_305808, Lot# 2549361
Anti-GRP78 BiP antibody (rabbit, polyclonal)	Abcam Cat# ab21685, RRID:AB_2119834, Lot# GR3192839-1
Anti-Hsp70/Hsp72 antibody (mouse, monoclonal, clone C92F3A-5)	Enzo Life Sciences Cat# ADI-SPA-810, RRID: AB_10616513, Lot# 05011728
Anti-Iba1 antibody (goat, polyclonal)	Abcam Cat# ab107159, RRID:AB_10972670, Lot# GR3209953-1
Anti-Iba1 antibody (rabbit, polyclonal)	Wako Cat# 019-19741, RRID: AB_839504, Lot# WDE1198
Anti-NeuN antibody (mouse, monoclonal, clone A60)	Millipore Cat# MAB377, RRID: AB_2298772, Lot# 3018822

Anti-ORP150/HSP12A antibody (rabbit, polyclonal)	Novus Cat# NBP1-32140, RRID:AB_2123515, Lot# 39785
Anti-TLR4 antibody (mouse, monoclonal, clone 25)	Santa Cruz Biotechnology Cat# sc-293072, RRID: AB_10611320, Lot# L1117
<i>Secondary antibodies:</i>	
Alexa Fluor 488 Goat anti-Mouse	Thermo Fisher Scientific Cat# A-11029, RRID: AB_2534088, Lot# 1911843
Alexa Fluor 594 Goat anti-Rabbit	Thermo Fisher Scientific Cat# A-11012, RRID: AB_2534079, Lot# 1892265
Alexa Fluor 647 Goat anti-Rabbit	Thermo Fisher Scientific Cat# A-21244, RRID: AB_2535812, Lot# 1910774
Cy2 Goat anti-Mouse	Jackson ImmunoResearch Labs Cat# 115-225-166, RRID: AB_2338746, Lot# 122679
Cy2 Donkey anti-Goat	Jackson ImmunoResearch Labs Cat# 705-225-147, RRID:AB_2307341, Lot# 133888

Biotinylated goat anti-mouse	Dako Cat# E0433, RRID: AB_2687905, Lot# 94167
Biotinylated goat anti-mouse	Vector Laboratories Cat# BA-9200, RRID: AB_2336171, Lot# ZB0324
Biotinylated goat anti-rabbit	Vector Laboratories Cat# BA-1000, RRID:AB_2313606, Lot# ZC0908
<i>Chromogens:</i>	
3,3'-diaminobenzidine tetrahydrochloride	CN75 - Carl Roth, Germany
Ammonium nickel(II) sulfate hexahydrate	A1827, Sigma Aldrich, Germany
ABC-Peroxidase Kit	Vector Laboratories Cat# PK-4003, RRID:AB_2336812
Cy3-Streptavidin	Jackson ImmunoResearch Labs Cat# 016-160-084, RRID: AB_2337244), Lot# 136321
Hoechst 33342	H3570, Thermo Fisher Scientific, Germany
Peroxidase-Streptavidin	Jackson ImmunoResearch Labs Cat# 016-030-084, RRID: AB_2337238, Lot# 126142

<i>Others:</i>	
2-propanol (for cleaning microscope slides)	9866.2 – Carl Roth, Germany
Bovine serum albumin	A9647 - Sigma-Aldrich Chemie GmbH, Germany
Casein from bovine milk	C3400 - Sigma-Aldrich Chemie GmbH, Germany
Entellan mounting medium	1 07960 - Merck KGaA, Germany
Ethanol 50%, 70%, 95% and 99.9%	AgrAlko AG, Germany
Gelatine from cold water fish skin	G7041 - Sigma-Aldrich Chemie GmbH, Germany
Hydrogen peroxide 30%	9681.4- Carl Roth, Germany
Immersionol™ 518 F immersion medium	Carl Zeiss Microscopy GmbH, Germany
Immersionol™ W 2010 immersion medium	Carl Zeiss Microscopy GmbH, Germany
Immunoselect antifading mounting medium	Dianova Cat# SCR-038447, RRID: AB_2661796, Lot# 30518
Millipore water	Merck Millipore, USA
Normal goat serum	VEC-S-1000 – Vector Labs, USA

Sodium chloride	9265.1 – Carl Roth, Germany
Sodium hydrogen phosphate	T876.3 – Carl Roth, Germany
Potassium chloride	P9541 – Sigma Aldrich, Germany
Potassium dihydrogen phosphate	26936.293P – VWR International GmbH, Germany
Tris(hydroxymethyl)aminom ethane	470302-966 - VWR International GmbH, Germany
Trisodium citrate dehydrate	3580.3 – Carl Roth, Germany
Triton X-100	X100 – Sigma Aldrich, Germany
Tween 20	P1379 – Sigma Alrich, Germany
Xylene (isomers)	9713.3 – Carl Roth, Germany

3. Protocols for immunohistochemistry

IHC in DAB

In 12 well plates with NetWells®

- 3 × 5 min wash in TBS 1X
- 1 x 30 min Heat Induced Epitope Retrieval (HIER) with sodium citrate (pH 6) in water bath pre-heated at 80 °C
- 1 x 10 min cool down
- 3 × 5 min wash in TBS 1X
- 30 min 3% H₂O₂ – TBS 1X
- 3 × 5 min wash in TBS 1X

In 24 well plates

- 1 x 60 min in blocking buffer
- Primary antibody incubation overnight in carrier at 4 °C (cold room)

In 12 well plates with NetWells®

- 3 × 5 min wash in TBST 1X

In 24 well plates

- Secondary antibody incubation 60 min 1:1000 in carrier at room temperature

In 12 well plates with NetWells®

- 3 × 5 min wash in TBST 1X

In 24 well plates

- ABC kit incubation 60 min in PBST at room temperature.

In 12 well plates with NetWells®

- 3 × 5 min wash in TBS 1X
- 5 min DAB solution
- 2 × 5 min wash in TBS 1X
- Quickly rinse with bidistilled H₂O
- Use TBST to mount brain slices on microscope slides
- Dry microscope glass overnight at room temperature
- Quickly rinse with xylene
- Coverslip with Entellan

Double immunofluorescence – parallel incubation of primary antibodies

In 12 well plates with NetWells®

- 3 x 5 min wash in PBST 1X
- 1 x 30 min Heat Induced Epitope Retrieval (HIER) with sodium citrate (pH 6) in water bath pre-heated at 80 °C
- 1 x 10 min cool down
- 3 x 5 min wash in PBST 1X

In 24 well plates

- 1 x 60 min in blocking buffer
- First primary antibody incubation overnight in carrier at 4 °C (cold room)
- Second primary antibody incubation overnight in carrier at 4 °C (cold room)

In 12 well plates with NetWells®

- 3 x 5 min wash in PBST 1X

In 24 well plates – from now on work in darkened room to preserve fluorophore

- First secondary antibody incubation 60 min (for Cy2-donkey anti-goat: 90 min) in carrier at room temperature
- Second secondary antibody incubation 60 min incubation 60 min in carrier at room temperature

Additional step for staining requiring streptavidin:

In 12 well plates with NetWells®

- 3 × 5 min wash in PBST 1X

In 24 well plates

- Streptavidin-fluorophore incubation 60 min at room temperature

In 12 well plates with NetWells®

- 3 × 5 min wash in PBS 1X
- 1 × 30 s incubation in Hoechst 33342 work solution
- 3 × 5 min wash in PBS 1X
- Use 0,1x PBST to mount brain slices on microscope slides
- 1 x 15 min dry microscope glass on heated plate at 45 °C
- Coverslip with Dianova IS Mounting Medium

Double immunofluorescence – sequential incubation of primary antibodies

In 12 well plates with NetWells®

- 3 × 5 min wash in PBST 1X
- 1 x 30 min Heat Induced Epitope Retrieval (HIER) with sodium citrate (pH 6) in water bath pre-heated at 80 °C
- 1 x 10 min cool down
- 3 × 5 min wash in PBST 1X

In 24 well plates

- 1 x 60 min in blocking buffer
- First primary antibody incubation overnight in carrier at 4 °C (cold room)

In 12 well plates with NetWells®

- 3 × 5 min wash in PBST 1X

In 24 well plates - from now on work in darkened room to preserve fluorophore

- First secondary antibody incubation 60 min in carrier at room temperature

In 12 well plates with NetWells®

- 3 × 5 min wash in PBST 1X

In 24 well plates

- Second primary antibody incubation overnight in carrier at 4 °C (cold room)

In 12 well plates with NetWells®

- 3 × 5 min wash in PBST 1X

In 24 well plates

- Second secondary antibody incubation 60 min in carrier at room temperature

Additional step for staining requiring streptavidin:

In 12 well plates with NetWells®

- 3 × 5 min wash in PBST 1X

In 24 well plates

- Streptavidin-fluorophore incubation 60 min at room temperature

In 12 well plates with NetWells®

- 3 × 5 min wash in PBS 1X
- 1 × 30 s incubation in Hoechst 33342 work solution
- 3 × 5 min wash in PBS 1X
- Use PBST 1X to mount brain slices on microscope slides
- 1 × 15 min dry microscope glass on heated plate at 45 °C
- Coverslip with Dianova IF-mounting medium

Triple immunofluorescence

The first and the second antibody come from the same host species

In 12 well plates with NetWells®

- 3 × 5 min wash in PBST 1X
- 1 x 30 min Heat Induced Epitope Retrieval (HIER) with sodium citrate (pH 6) in water bath pre-heated at 80 °C
- 1 x 10 min cool down
- 3 × 5 min wash in PBST 1XIn 24 well plates
- 1 x 60 min in blocking buffer
- First primary antibody incubation overnight in carrier at 4 °C (cold room)

In 12 well plates with NetWells®

- 3 × 5 min wash in PBST 1X

In 24 well plates - from now on work in darkened room to preserve fluorophore

- First secondary antibody incubation in carrier 60 min at room temperature

In 12 well plates with NetWells®

- 3 × 5 min wash in PBST 1X

In 24 well plates

- Second primary antibody incubation overnight in carrier at 4 °C (cold room)

- Third primary antibody incubation overnight in carrier at 4 °C (cold room)

In 12 well plates with NetWells®

- 3 × 5 min wash in PBST 1X

In 24 well plates

- Second secondary antibody incubation in carrier 60 min at room temperature
- Third secondary antibody incubation in carrier 60 min at room temperature

Additional step for staining requiring streptavidin:

In 12 well plates with NetWells®

- 3 × 5 min wash in PBST 1X

In 24 well plates

- Streptavidin-fluorophore incubation 60 min at room temperature

In 12 well plates with NetWells®

- 3 × 5 min wash in PBS 1X
- 30 s incubation in Hoechst 33342 work solution
- 3 × 5 min wash in PBS 1X
- Use PBST 1X to mount brain slices on microscope slides
- 1 x 15 min dry microscope glass on heated plate at 45 °C
- Coverslip with Dianova IF-mounting medium

XII. ACKNOWLEDGEMENT

I would like to express my gratitude and appreciation to Prof. Heidrun Potschka for the opportunity to work in her group and for her support during my whole project. Thanks to her, I was able to learn the basics of scientific work with all of its ups and downs. She allowed me to work in a multicultural team, where I could gather experience on advanced methods and equipment and participate in the neuroscientific and veterinary pathology on the national and international level. Her trust in my knowledge and abilities encouraged me many times, even in the moments of doubt, which reassured me in my goal of pursuing a career in research.

I would also like to thank Dr. Fabio Gualtieri, who was leading the HSP project and who mentored me during those two years. Thanks to willingness to share his expertise in histology and microscopy with me, I developed a deep interest in both techniques, which I would like to evolve further. He also was, and still is, a cherished friend of mine, who helped me become more open and courageous and taught to play football the Italian way.

Furthermore, I would like to acknowledge the involvement of Dr. Eva-Lotta von Rüden, who helped me several times in scientific writing, both in English and in German. She also entrusted the part of HSP project in dogs to me, which allowed me to gather experience in working with clinical samples.

Special thanks go to Dr. Roelof Maarten van Dijk, who shared with me

his in-depth knowledge of stereological cell counting, statistics as well as several recommended several very good podcasts and spent some lunch breaks playing Magic: The Gathering. I am also grateful to Nina Miljanović for her warm support and deep understanding during our years spent in the same office. I thank Claudia Siegl and Sabine Saß for their willingness to teach me the laboratory work and the technique of immunohistochemistry. I am especially grateful to my compatriots Grażyna Langer and Isabella Waclawczyk for making the Heimweh bearable. All my other colleagues I thank for creating a magnificent working atmosphere.

On the private note, I would like to thank my parents, Aleksandra and Grzegorz, for their support and trust on my educational and professional way. My friend Marta Tikhomirov I thank for the comfort of sharing our experiences as doctoral students. I am really grateful to Dr. Błażej Poźniak, my first tutor, for teaching me basics of scientific work and infecting with love for research. Last but not least, I am grateful to my love Matthieu Desplantes for his encouragement and inexhaustible patience. I would never get this far without all of them believing in me.